Characterization of the mechanical and hormonal sensitivity of glutamate receptor subtype expression on murine osteoclasts

by

Karen Melissa Black

Submitted in partial fulfillment of the requirements
for the degree of Doctor of Philosophy

at

Dalhousie University
Halifax, Nova Scotia
October, 2004

Your file Votre référence
ISBN: 0-494-00949-7
Our file Notre référence
ISBN: 0-494-00949-7

DALHOUSIE UNIVERSITY

To comply with the Canadian Privacy Act the National Library of Canada has requested that the following pages be removed from this copy of the thesis:

Preliminary Pages
- Examiners Signature Page (pii)
- Dalhousie Library Copyright Agreement (piii)

Appendices
- Copyright Releases (if applicable)

Table of Contents

For my son Mohan,

By watching you grow and explore the world around you, I too have seen through a new pair of eyes and have a renewed sense of curiosity. May we all keep and nurture that sense of curiosity throughout our lifetimes.

List of Figures

List of Tables

Abstract

Glutamate signalling, a major pathway of excitatory neurotransmission in the central nervous system, is proposed to be a mediator of mechanical stimulation in bone. Glutamate signalling in the central nervous system is involved in the processes of learning and memory: we postulate that glutamate receptors mediate mechanical stimulation in bone cells to increase bone density in a manner analogous to their role in mediating CNS synaptic plasticity. A variety of glutamate receptors (gluRs) of both the ionotropic and metabotropic subytpes are expressed in osteoblasts and osteoclasts of the long bones of rat, rabbit, and mouse. These receptors are sensitive to mechanical stimulation, the driving force for maintenance of normal bone density. We wished to examine the expression of glutamate receptor subtypes in cultured mouse osteoclasts and determine the effects of mechanical stimulation and estrogen on expression of these receptors. In mixed murine marrow-derived cultures, glutamate receptor antagonists MK801 and NBQX inhibited osteoclast differentiation and to some extent function, implying that these receptors are functional. NMDA receptors were colocalized with vinculin, placing them in a position where they could sense mechanical strain, receive glutamate signals from osteocytes, and be regulated by integrin-mediated activation of c-Src, which could produce transient increases in osteoclast activity to initiate bone remodeling in the absence of frequent mechanical stimulation. Frequent mechanical stimulation changed NMDA and AMPA receptor expression such that a shift in the balance of ionotropic receptor function from NMDA receptor-mediated pathways to AMPA receptor-mediated pathways occurred. Estrogen was shown to affect NMDA receptor subtype mRNA expression only in the absence of mechanical stimulation, while AMPA receptor subtype mRNA expression was affected by estrogen both in the presence and absence of mechanical stimulation. From these experiments, it is clear that glutamate signalling plays an important role in mediating osteoclast differentiation and function in response to mechanical stimulation and estrogen levels.

List of Abbreviations and Symbols Used

AMP	adenosine monophospate
AMPA	α-amino-3-hydroxy-5-methyl-4-isoxazolepropionic acid
BMP	bone morphogenetic protein
BMU	basic multicellular unit
cAMP	cyclic AMP
CTR	calcitonin receptor
CGRP	calcitonin gene-related peptide
CNS	central nervous system
DAB	diaminobenzidine
ERα	estrogen receptor alpha subunit
ERβ	estrogen receptor beta subunit
ECM	extracellular matrix
FGFs	fibroblast growth factors
GLAST	glutamate-aspartate transporter
IGF	insulin-like growth factor
JNK	jun N-terminal kinase
MAPK	mitogen-activated protein kinase
M-CSF	macrophage-colony stimulating factor
MK801	dizocilpine
NBQX	1,2,3,4-tetrahydo-6-nitro-2,3-dioxobenzo[f]quinoxaline-7-sulfonamide
NFkB	nuclear factor kappa-B
NMDA	N-methyl-D-aspartate
NSE	non-specific esterase
OPG	osteoprotegerin
PBS	phosphate buffered saline
PDGF	platelet-derived growth factor
PSD95	post-synaptic density protein 95
RANK	receptor activator of NFkB
RANKL	receptor activator of NFkB ligand
SDS-PAGE	sodium dodecyl sulfate-polyacrylamide gel electrophoresis
TGF-β	transforming growth factor-beta
TNF	tumor necrosis factor
TRAcP	tartrate-resistant acid phosphatase
TRAP1C	tartrate-resistant acid phosphatase isoform 1C
TRAFs	TNF receptor-associated factors
VIP	vasoactive intestinal peptide

Acknowledgements

I wish to thank my supervisor, Dr. Gail Anderson, for the support and guidance she has provided me while working on this project.

I would also like to thank Dr. Mark Nachtigal, my co-supervisor during Gail's absence, for all the assistance he has given me, particularly during the final phases of the project.

Many thanks are also due to Brigitte Thériault, technician extraordinaire, her excellent laboratory skills and fine sense of humour made the completion of this project a manageable task not to mention a truly enjoyable experience.

Thanks also to the members of Dr. Nachtigal's lab, especially Elizabeth Campbell and Yangxin Fu, for teaching and helping me so much with the northern analyses.

My unending thanks to my husband Neeraj, his support and love helped me so much in the completion of this project.

Chapter 1: Introduction

The purpose of this study was to examine glutamate signalling in cultured murine osteoclasts. In bone, glutamate signalling is proposed to be a mediator of cellular responses to mechanical stimulation which result in increased bone formation. We wished to determine which glutamate receptor subtypes were expressed on murine osteoclasts and whether signalling via these receptors affected osteoclast differentiation or bone resorptive ability. Additionally, we wished to characterize the effects of mechanical stimulation and varying estrogen levels on the expression of glutamate receptors in osteoclasts. Defining the glutamate receptor subtypes found on osteoclasts and how mechanical stimulation and estrogen levels affect their expression will lead to a better understanding of the mechanism and role of glutamate signalling in bone.

1.1 Rationale for the study of cellular mechanisms of osteoporosis

Osteoporosis is a disease that affects 1.4 million Canadians, primarily women over 50, and results in annual costs of $1.3 billion to our health care system (1). As our population ages, these numbers are expected to increase; thus, the study of osteoporosis disease mechanisms and the design of new treatment strategies is critical. Normal bone structure is maintained by regulating the balance between osteoblast activity (bone formation) and osteoclast activity (bone resorption), the driving force for which is mechanical stimulation (2-4). In

response to mechanical stimulation, osteoblast and osteoclast activities are directed to increase and decrease respectively, resulting in increased bone density. In postmenopausal women, however, the lack of estrogen has been shown to limit the sensitivity of the bone remodelling process in response to mechanical strain (5,6). Ultimately, an imbalance of catabolic versus anabolic bone remodelling can lead to substantial bone loss resulting in osteoporosis, which is characterized by enhanced bone fragility and increased fracture risk. A detailed understanding of the mechanotransductive mechanisms of bone, in particular the mechanically-regulated control of osteoclast activity, is crucial to the design of effective treatment strategies for osteoporosis.

1.2 The structure of bone

Bone is a highly specialized connective tissue that not only serves as an internal support system in higher vertebrates but also actively participates in calcium homeostasis and immune and blood cell production. Bone is a remarkably complex tissue in that its mineralized extracellular matrix lends it great rigidity and strength while still ensuring some degree of flexibility. It is this combination of strength and deformation that allow bone to withstand the many forces placed upon it during normal activity.

The organic extracellular matrix of bone is comprised of approximately 95% type I collagen: the remaining 5% consists of proteoglycans and non-collagenous proteins. Among the non-collagenous proteins in the organic extracellular matrix are ligands for cell adhesion molecules that serve as key molecules for the attachment to, and motility of cells on, the bone surface. The integrin family of receptors are adhesion molecules that bind to extracellular matrix proteins such as collagen, fibronectin, and vitronectin to allow bone cells to attach to, move along, and sense their extracellular environment (7-9). The role of these receptors in bone will be discussed in greater detail below.

From a morphological standpoint, there are two distinct forms of bone: cortical and cancellous. The primary roles of cortical bone are the structure and mechanical strength of bone: it has a compact structure where densely packed collagen fibrils are organized in concentric lamellae, referred to as Haversian systems (10). In each lamellar layer, the collagen fibrils are perpendicular to the previous layer, somewhat like plywood (11). Cortical bone has great strength and it comprises the outer layer of most bone, including the tubular structures that form the shaft of long bones such as the femur (Figure 1.1). Cancellous bone, on the other hand, primarily serves a metabolic function and has a porous matrix resembling a spongy, loosely woven mesh (10). The porous matrix formed by cancellous bone houses the bone marrow, where blood and immune precursor cells reside. Cancellous bone, also known as trabecular bone, forms the interior regions of bone while cortical bone forms the outer shell.

Bone is a vascularized and innervated tissue. Blood vessels are present throughout cortical and cancellous bone, residing within the center of each Haversian system in cortical bone. The presence of a well-developed vascular structure ensures proper oxygen and nutrient supply to bone cells, despite their existence at the surface of, or embedded within, such a highly mineralized matrix. Bone has also been shown to be densely innervated, with nerves often lying adjacent to blood vessels in small channels throughout the mineralized matrix (12). Recently, nerve fibers containing a variety of neurotransmitter substances have been identified in bone and receptors for the majority of these substances have been identified on one or more bone cell types. These neurotransmitter substances include; calcitonin gene-related peptide (CGRP) (13,14), substance P and other tachykinins (13,15), vasoactive intestinal peptide (VIP) (16), norepinephrine (17), and glutamate (18).

1.3 Cellular components of bone

Four different cell types exist in bone: osteoblasts, osteoclasts, bone lining cells, and osteocytes. Bone lining cells, osteoblasts, and osteocytes arise from the mesenchymal stem cell lineage (which can also differentiate into chondrocytes, adipocytes, myoblasts, and fibroblasts) while osteoclasts are derived from the hematopoeitic stem cell lineage (19).

1.3.1 Osteoblasts

Osteoblasts are responsible for the formation and mineralization of bone. Differentiation of mesenchymal stem cells into a committed osteoblast phenotype is not completely understood, but it is known that expression of the core binding transcription factor Cbfa1 is essential. Recently, mice that had a loss of function mutation in the Cbfa1 gene were shown to have a complete lack of cartilage ossification during development (20,21). In addition to the Cbfa1 transcription factor, other factors are required for normal osteoblast differentiation: these include fibroblast growth factors (FGFs), transforming growth factor-β (TGF-β), bone morphogenetic proteins (BMPs), glucocorticoids, and 1,25-dihydroxyvitamin D_3 (22).

Osteoblasts that are actively mineralizing bone are plump cuboidal cells with a highly basophilic membrane that contain a single nucleus and a prominent Golgi complex (23). They are found in a monolayer at the surface of newly formed but as yet unmineralized bone, known as osteoid. From this location, osteoblasts can actively synthesize and mineralize new bone matrix, and can also extend cytoplasmic processes into the bone matrix to communicate with osteocytes that are embedded within the bone. Through gap junctions composed of connexins 43 and 45, osteoblasts can communicate with adjacent cells and with more distal osteocytes via this network of cytoplasmic processes that extend through the bone matrix (24,25). Osteoblasts express a number of products that can be used

to identify their phenotype: these include type I collagen, alkaline phosphatase, osteopontin, and osteocalcin (26).

1.3.2 Bone lining cells

Bone lining cells are a quiescent form of osteoblasts. Following active mineralization of bone, osteoblasts undergo one of three fates: apoptosis, differentiation to osteocytes (as cells become embedded within the bone matrix), or quiescence (become bone lining cells). These cells are flat and elongated with a spindle-shaped nucleus and lie along the endosteal membrane that covers quiescent bone surfaces (26). Although the function of bone lining cells is not completely understood, they may play a role in the activation of bone remodelling, possibly by relaying signals received from osteocytes to osteoblasts and osteoclasts (27).

1.3.3 Osteocytes

Osteocytes are cells that differentiate from osteoblasts as they become embedded within the bone matrix. They are in contact with one another by an extensive network of cytoplasmic processes that extend through the bone matrix in fluid-filled canaliculi (28). Their location within bone matrix makes osteocytes

ideally situated to perceive the mechanical forces exerted on bone during daily activity. Their intercellular connectivity and contact with osteoblasts at the bone surface allows for effective transmission of the mechanical signal to other cells (29,30). The role of osteocytes in mechanosensation is discussed in detail in section 1.6. Osteocytes typically represent a final stage of differentiation: they may be removed from bone by undergoing apoptosis or by being phagocytosed during osteoclastic bone resorption (26).

1.3.4 Osteoclasts

Osteoclasts are large multinucleated cells responsible for bone matrix resorption. Osteoclasts are derived from hematopoeitic precursors of the monocyte/macrophage lineage that reside in hemopoietic tissues such as bone marrow and spleen (31). Multinucleated osteoclasts are terminally differentiated cells and are characterized by the presence of a prominent cytoskeleton and a ruffled border at the interface with the bone surface. They also are rich in lysosomal enzymes, including collagenase, cathepsin K, carbonic anhydrase II, and tartrate-resistant acid phosphatase (TRAcP), the latter of which is commonly used to identify the osteoclast phenotype.

Until they enter a committed osteoclast lineage at the post-mitotic stage, osteoclasts and macrophages share a common pathway of differentiation from

hematopoietic stem cells (32). The signals that cause the initiation of osteoclast differentiation come from osteoblasts, triggered by osteoblast responses to several bone resorbing agents (Figure 1.1). Osteoblasts release an osteoclast differentiation factor that causes commitment of the common macrophage/osteoclast precursor cells to the osteoclast lineage. Prior to the presence of the osteoclast differentiation factor, these cells express markers of the macrophage lineage, including non-specific esterase and antigens to Mac-1 and Mac-2 (Figure 1.1) (32). Within 12 hours of receiving the osteoclast differentiation signal from osteoblasts, differentiating osteoclast precursors begin to express osteoclast markers such as the calcitonin receptor (CTR) and TRAcP, and continue to express the macrophage markers. At 18 hours, CTR and TRAcP expression is strong, while expression of NSE and Mac-1 has ceased and the preosteoclasts begin to fuse to form multinucleated cells. Finally, about 24 hours after the initiation of osteoclast differentiation, mature multinucleated osteoclasts expressing CTR and TRAcP, but not NSE or Mac-1, are present (Figure 1.1) (33).

Figure 1.1: Factors influencing differentiation of hematopoietic precursors into mature multinucleated osteoclasts. Signalling via vitamin D_3, cAMP and gp130 induces osteoblasts to release osteoclast differentiation factor (RANKL) which induces osteoclast precursors to differentiate into mature multinucleated osteoclasts. As differentiation proceeds, osteoclast markers become expressed, while macrophage marker expression decreases. Adapted from Suda et al [33].

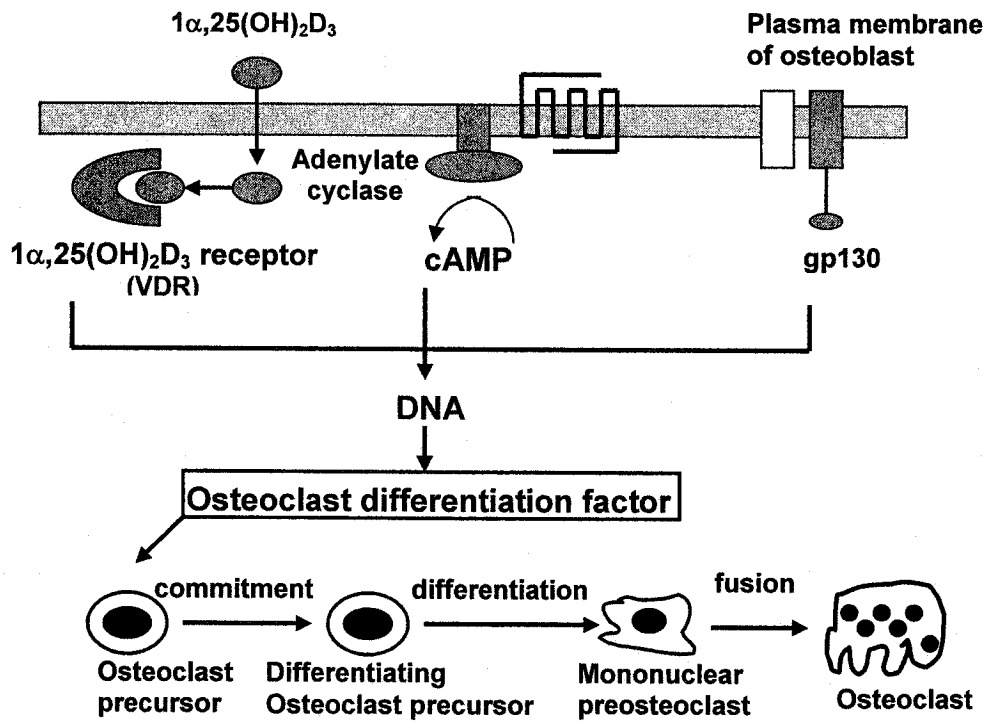

Osteclast Phenotype	CTR (-) TRAP (-)	CTR (+) TRAP (+)	CTR (+) TRAP (+)	CTR(+) TRAP (+)
Macrophage Phentotypes	NSE (+)	NSE (+)	NSE (-)	NSE (-)
	Mac-1 (+)	Mac-1 (+)	Mac-1 (-)	Mac-1 (-)
	Mac-2 (+)	Mac-2 (+)	Mac-2 (+)	Mac-2 (+)
	F4/80 (-)	F4/80 (-)	F4/80 (-)	F4/80 (-)

Three major signal transduction pathways occur in osteoblasts to trigger the release of the osteoclast differentiation factor: vitamin D_3 receptor-mediated pathways, cAMP-mediated pathways, and gp130-mediated pathways (Figure 1.1) (33). The effects of vitamin D_3 on osteoclast differentiation are known to be through osteoblasts, since osteoblasts but not osteoclasts express the vitamin D receptor (34). Parathyroid hormone, prostaglandin E2, and interleukin-1 induce intracellular cAMP-mediated signals in osteoblasts, causing the release of the osteoclast differentiation factor. Finally, other cytokines such as interleukin-6 (in conjunction with its soluble receptor), interleukin-11, oncostatin M, and leukemia inhibitory factor all stimulate osteoblasts to release the osteoclast differentiation factor through intracellular pathways mediated by gp130, a non-ligand binding signal transducing receptor.

The osteoclast differentiation factor released by osteoblasts has recently been identified as receptor activator of NFkB ligand (RANKL), and is a new member of the tumor necrosis factor (TNF) ligand family (35-37). Osteoclasts express a receptor for RANKL, known as RANK, which is a type 1 transmembrane protein. Interaction of RANKL with RANK activates intracellular cascades involving NFkB and the protein kinase JNK (jun N-terminal kinase), through interaction with TNF receptor-associated factors (TRAFs). The effect of these intracellular pathways is to increase osteoclast differentiation and the bone resorptive activity of existing osteoclasts. In addition to the osteoclast receptor RANK, a soluble decoy receptor for RANKL, named osteoprotegerin (OPG), also exists. OPG is a novel

member of the TNF receptor superfamily; it binds RANKL and prevents it from activating the RANK receptor pathway, preventing osteoclast differentiation and/or decreasing osteoclast activity (38).

Another factor that is essential to osteoclast differentiation is macrophage-colony stimulating factor (M-CSF). Released by osteoblasts, M-CSF has been shown to be essential to osteoclast differentiation by increasing the number of committed osteoclast precursors during the proliferative phases of differentiation (39,40). M-CSF also promotes osteoclast survival by inhibiting apoptosis (41), but does not appear to have direct effects on osteoclast bone resorptive activity (42).

Osteoclasts bind to the surface of bone via integrins αVβ3 and αVβ1 (vitronectin receptors) and α2β1 (collagen receptor) (43), with the αvβ3 integrin being the most important for adhesion as well as motility across bone surfaces (44). When a resorptive phase begins, major changes to the osteoclast plasma membrane occur, producing several different plasma membrane domains. Resorbing osteoclasts become polarized and form a ring-like structure of actin and other podosomal elements called the sealing zone. This occludes a region of the membrane that is in contact with bone and prevents lateral motion of proteins between the basal and ruffled border membranes (Figure 1.2). The ruffled border membrane resides within this occlusion, which is a unique membrane that is formed by rapid fusion of acidic intracellular vesicles containing proteins similar to those found in late endosomal membranes (Figure 1.2) (45). In actively

resorbing osteoclasts, the breakdown products of bone matrix resorbed at the ruffled border membrane are transported by vesicles to a fourth membrane domain at the basal (upper) surface of the cell to allow removal of bone matrix degradation products (Figure 1.2).

Osteoclasts resorb bone by the production and extracellular release of proteolytic enzymes and protons (hydrogen ions) into the subcellular compartment. To dissolve bone mineral, vacuolar ATP-driven proton pumps within the ruffled membrane acidify the subcellular compartment that has been occluded by the sealing zone. In addition to acidification of the subcellular compartment, lysosomal enzymes are released by the osteoclast. Together with tartrate-resistant acid phosphatase (TRAcP), the lysosomal enzymes and acidic environment act to degrade the organic matrix components. Material from the matrix degradation is internalized and either metabolized or transported across the cell via transcytosis and excreted at the basal membrane surface (46,47). To provide protons for the ATP-driven proton pump that acidifies the extracellular compartment, several ion exchangers, pumps and channels exist in the ruffled border and in the basal membrane of the osteoclast: these include a Na^+/H^+ antiporter, a Na^+/K^+ ATPase, a HCO_3^-/Cl^- exchanger, a Ca^{2+} ATPase, and a K^+ channel (48).

Figure 1.2: Osteoclasts undergo changes to their plasma membrane domain changes during the process of bone resorption. The nonresorbing osteoclast is polarized (1) but immediately after attachment for resorption it shows three different membrane domains (2): ruffled border (A), sealing zone (B), and basal membrane (C). Once matrix degradation has started (3) the fourth membrane domain appears in the basal membrane (D). Adapted from Suda et al [33].

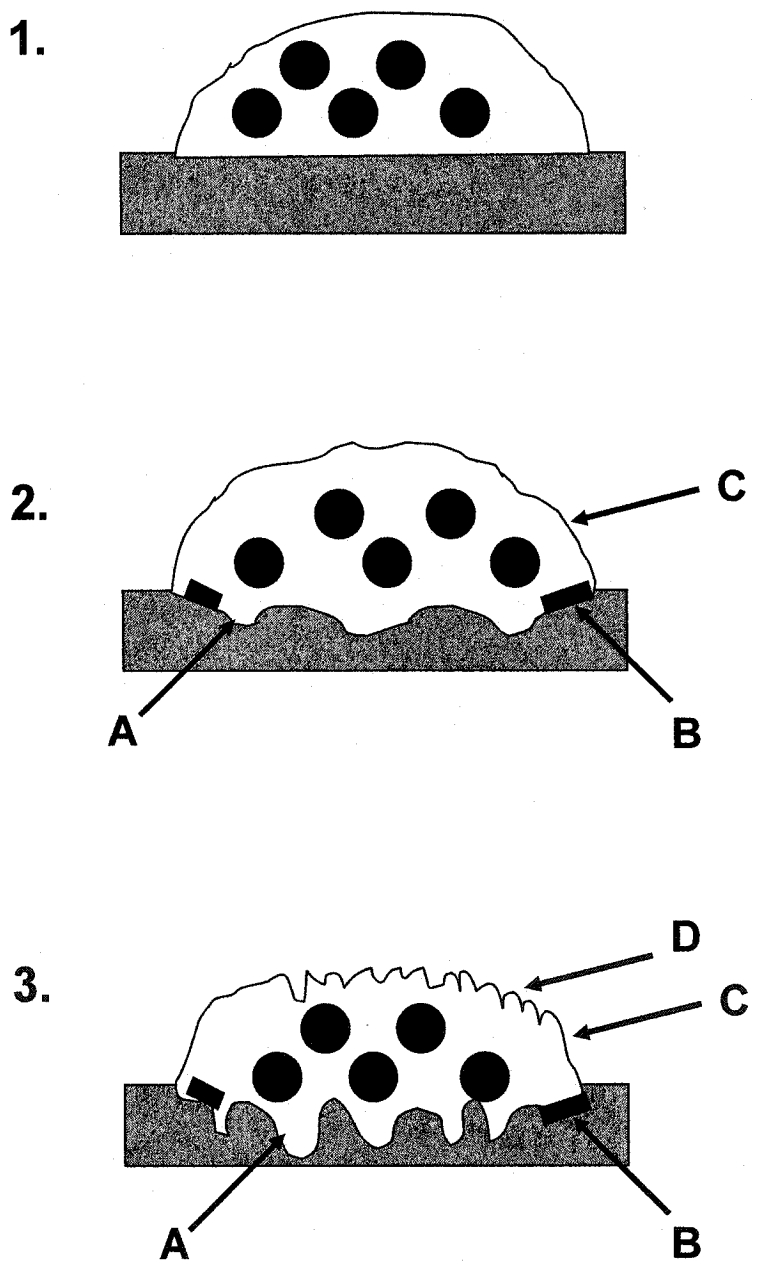

1.4 Bone remodelling

Remodelling serves two major purposes in the adult skeleton: to maintain the mechanical integrity by repair of accumulated microfractures, and as a mechanism for the regulation of calcium and phosphate ion levels. Remodelling consists of the resorption of a quantity of bone by osteoclasts, followed by the deposition of new bone by osteoblasts. In normal adult bone, resorption and formation are coupled, with the two occurring at similar rates. The sites at which bone remodelling occurs are known as basic multicellular units (BMUs) or bone remodelling units (49). A BMU in an adult human is typically active for a period of 2 to 8 months, with bone formation being the longest part of the process. Remodelling of bone is an ongoing process: at any given time about 20% of the cancellous bone surface is being remodelled such that cancellous and cortical bone are being completely remodelled every 4 and 12 years, respectively.

Figure 1.3 illustrates the steps of bone remodelling. The first step in remodelling involves retraction of the bone lining cells and degradation of the endosteal/periosteal membrane that covers the quiescent bone surface. It is hypothesized that the bone lining cells digest the endosteal membrane through the production of collagenases (27). Osteoclast precursors, attracted to the exposed bone surface, fuse to become multinucleated cells and attach themselves to the bone surface to degrade both the mineral and organic components of the extracellular matrix. As osteoclasts degrade bone, they may

release TGF-β stored within the bone matrix, which then could act as a coupling agent for resorption and formation by recruiting osteoblasts and/or inducing osteoblast differentiation and inhibiting osteoclast activity (50). Osteoblasts enter the resorption lacuna formed by the osteoclasts and form the new bone in multiple steps: first is the deposition of the proteoglycan-rich organic matrix or cement line/reversal line, followed by collagen-rich matrix or osteoid formation, and then later mineralization of this matrix to form new bone.

1.4.1 Mechanisms of regulating bone remodelling

The regulation of bone remodelling involves the interaction of a host of different factors, including mechanical stimuli, systemic hormones, and local mediators such as growth factors and cytokines. When normal physiological strains are placed upon bone, the resulting tissue deformation causes fluid to flow through the canaliculi that house the osteocyte network. This fluid flow generates shear stresses, activating mechanosensors on the osteocytes such as stretch-activated calcium channels, and leading to calcium influx and the production of local mediators such as prostaglandins and nitric oxide (51). The mechanisms by which osteocytes sense mechanical stimulation are described in section 1.6.

Figure 1.3: Schematic representation of bone remodeling. Adapted from Compston [22].

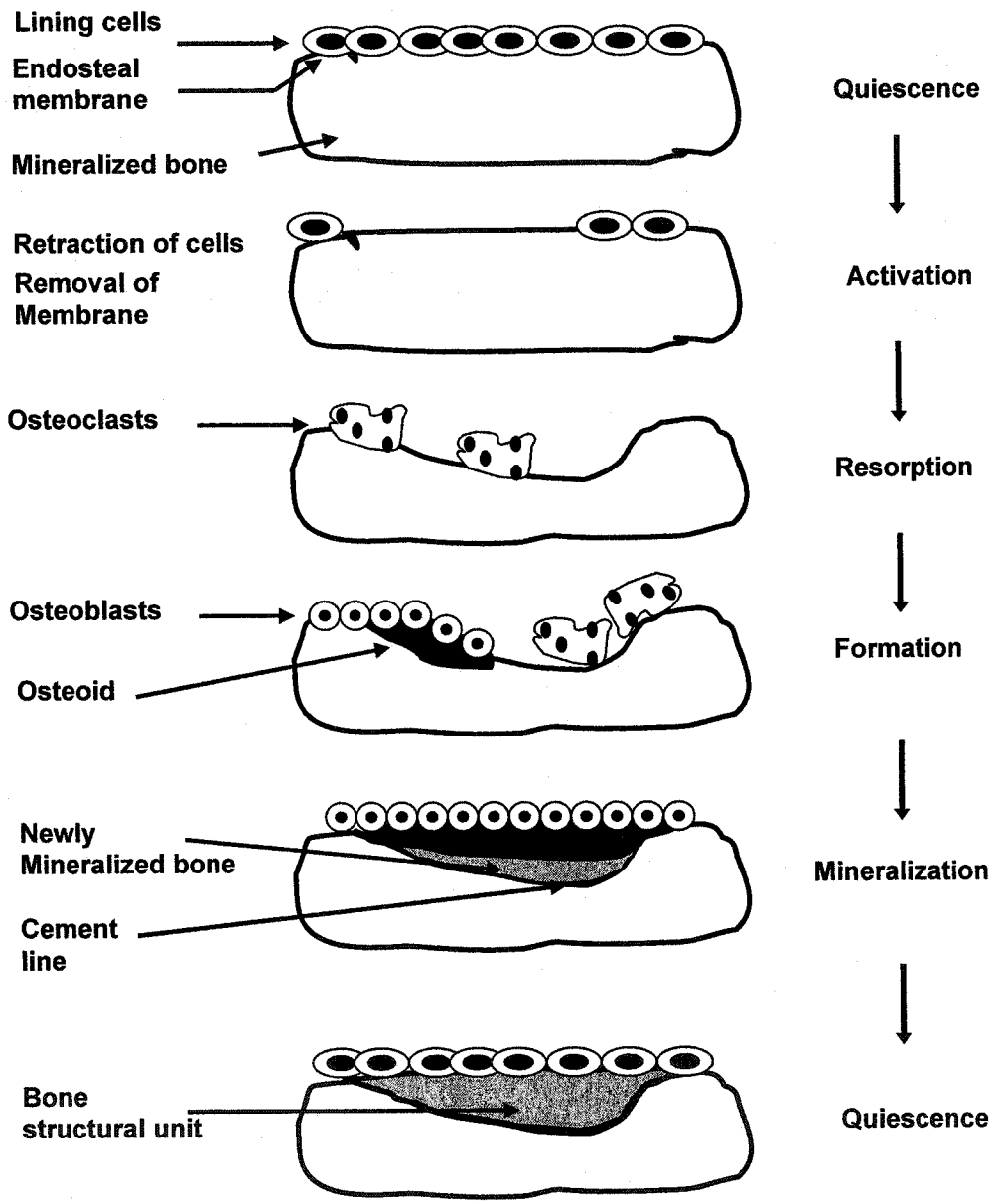

Systemic hormones also influence bone remodelling. The actions of hormones such as parathyroid hormone and vitamin D_3 are mediated through receptors on osteoblasts: they increase osteoclast activity by stimulating osteoblasts to release RANKL. Estrogen can also influence bone remodelling: its actions are described in section 1.4.4.

The cells in the bone microenvironment play an important role in the regulation of bone remodelling. Table 1.1 lists the numerous cytokines and growth factors that are local mediators of bone remodelling (22). Bone resorption is stimulated by factors such as interleukins-1, -6, -8, and -11, which act to increase the proliferation and differentiation of osteoclast precursors and to increase osteoclast activity (52). Bone formation is stimulated by growth factors such as insulin-like growth factor (IGFs), transforming growth factor-β (TGF-β), fibroblast growth factors (FGFs), platelet-derived growth factors (PDGFs), as well as several of the bone morphogenetic proteins (BMPs) (53). The wide variety of cytokines and growth factors that influence bone cells through paracrine signalling demonstrate that cellular activity within the bone microenvironment is regulated by many different pathways.

Table 1.1: Cytokines and growth factors affecting bone.

Effect on bone	Cytokine/Growth Factor
Stimulators of bone resorption	Interleukins-1, -6, -8, -11
	Tumor necrosis factors
	Epidermal growth factor
	Platelet-derived growth factor
	Fibroblast growth factors
	Leukemia inhibitory factor
	Macrophage-colony stimulating factor
	Granulocyte/macrophage-colony stimulating factor
Inhibitors of bone resorption	Interferon-γ
	Interleukin-4
Stimulators of bone formation	Insulin-like growth factors
	Transforming growth factor-β
	Fibroblast growth factors
	Platelet-derived growth factor
	Bone morphogenetic proteins

1.4.2 Effects of mechanical stimulation at the tissue level

The mass and architecture of bone is dependent to a large extent on adaptive mechanisms that respond to mechanical loading. In 1892, the anatomist Julius Wolff proposed that mechanical stress is responsible for determining the architecture of bone and that bone tissue is able to adapt its mass and three-dimensional structure to the prevailing loading conditions (54). Wolff's proposal that mechanical loading (exercise) affects the form and health of bone has gained general acceptance. Little doubt exists that removal of mechanical load permits an imbalance in bone remodelling, as seen by the rapid loss of bone that accompanies bed rest, immobilization or space flight (55,56). Conversely, increased loading of bone by exercise increases bone mass, and retards bone loss caused by post-menopausal osteoporosis (57,58).

Mechanical loading can be characterized by several parameters that include load magnitude, number of cycles, and the rate at which strain occurs. The magnitude of mechanical load is described using the term strain, which is defined as the change in length divided by the original length of an object (i.e. a bone): strain is dimensionless and is often described as percentage deformation (59). Deformation can also be described in microstrain (μstrain), where 1000 microstrain would be equal to 0.1% deformation. For example, the mechanical load applied to cells in this study deformed the cells by 0.5%: this magnitude of deformation could also be denoted as 5000 μstrain. The application of load to

bone during movement produces a number of stimuli for bone cells *in situ*, including hydrostatic pressure, direct cell strain, and fluid flow-induced shear stresses (60).

The effect of mechanical loading on whole bones has been studied in a number of models *in vivo* (61-64), which have confirmed that application of cyclical loads rather than static loads stimulate bone formation. Bone formation in response to mechanical stimulation includes thickening of cortical bone and strengthening of the trabecular (cancellous) meshwork to produce stronger bones. However, whether it is the magnitude or the rate of application of strain that determines the response of bone is debatable. High strain magnitudes clearly increase bone formation (2), but high rates of application of lower strain magnitudes were also shown to increase bone formation (65,66). Normal healthy bones are typically subjected to strain magnitudes ranging from 800 μstrain (walking) to 4000 μstrain (running to catch a bus, high impact aerobics) (67). It is thought that a threshold exists near 1000 μstrain for the formation of bone in response to mechanical load: if bones are not routinely subjected to at least this load, bone loss may occur (67). Bone has an ultimate strength of 25,000 μstrain (2.5% deformation), which when reached or surpassed will cause fractures (68). In this study, our cells were subjected to peak strain magnitudes of 5000 μstrain. This strain magnitude is somewhat supra-physiologic, resembling the strain a gymnast's bones might see during an apparatus dismount; but was chosen so that

measurable responses to mechanical stimulation would be produced within the culture period.

1.4.3 Effects of mechanical stimulation at the cellular level

In bone, the process of mechanotransduction is postulated to involve four distinct steps: mechanocoupling, biochemical coupling, transmission of signal, and effector cell response (60). In mechanocoupling, deformation of bone cells occurs in response to fluid flow or mechanical strain. Mechanical loading of the bone matrix induces flow of extracellular fluid along the endosteal surface as well as through the canaliculi, creating shear stresses on osteoblasts and osteocytes in these regions. The shear stress produces intracellular effects and leads to paracrine signalling between osteoblasts, osteocytes, and possibly osteoclasts (69); the mechanisms by which shear stress may mediate mechanotransduction are discussed in detail in section 1.6.

The coupling of mechanical signals with intracellular biochemical signals is suggested to involve several mechanisms including integrin signalling (section 1.6.2), stretch-activated cation channels within the cell membrane, and G protein-dependent pathways (70). Cells possess an intricate cytoskeletal structure that links the nucleus and other organelles together, and, via integrin receptors, connects to the extracellular matrix. Mechanical deformation, via integrin

receptors, can alter cytoskeletal arrangement and its attachments to the nucleus, possibly altering gene expression, increasing intracellular second messengers, or increasing tyrosine phosphorylation (71-73). The integrin-mediated attachment of bone cells to the extracellular matrix may also modulate ion channel activity. Specifically, stretch-activated, non-selective cation (SA-cat) channels were identified on osteoblast-like cells and were shown to interact with the cytoskeleton (74). Mechanical strain increased SA-cat channel activity and single channel conductance in rat osteoblasts (75).

Within bone cells, several modes of transmission of the mechanical stimulation signal have been identified. In osteoblasts, mechanical strain has been shown to elevate levels of second messengers, including cAMP (cyclic adenosine monophosphate), inositol trisphosphate, and protein kinase C (76). Upon sensing of mechanical strain, bone cells may communicate with each other in a paracrine fashion via agents such as insulin-like growth factor (IGF), prostaglandins, and nitric oxide. For example, loading produced increases in IGF expression in osteocytes that led to increased production of type I collagen and osteocalcin on the bone surface (77). Also, prostaglandin E_2, which stimulates osteoblast differentiation and function (78), is released by osteoblasts in response to mechanical stimulation (79,80). Finally, transient increases in the production and release of nitric oxide occur almost immediately upon application of physiological levels of mechanical strain in both osteoclasts and osteoblasts *in vitro* (81). The signalling mechanisms outlined above vary according to the

magnitude, duration, and rate of applied load to produce cellular responses that produce changes to skeletal mass and architecture (82).

1.4.4 Effects of estrogen on bone remodelling

Though the bone-preserving actions of estrogen are exerted by limiting osteoclast number and activity, these effects are mediated primarily through the control of cytokines released by local osteoblasts and osteocytes that impact upon osteoclast differentiation and activity, rather than through the direct actions of estrogen on osteoclasts (22). Among the actions of estrogen on osteoblasts are increased TGF-β and OPG production and decreased IL-6 production, which serve to limit osteoclast differentiation and bone resorptive ability (83). In addition to the indirect effects of estrogen on osteoclast activity, direct effects on cultured osteoclasts have been observed: estrogen produced decreases in bone resorption, lysozyme, and TRAcP, while increasing expression of transcription factors fos and jun and apoptosis (83). The actions of estrogen are perceived through at least two receptor subtypes, ERα and ERβ: ERα expression has been reported in osteoblasts (84), osteocytes (85), and osteoclasts (86), while ERβ expression has only been identified in osteoblasts (87).

A rat ovariectomy model has been used to assess skeletal effects of estrogen withdrawal. Ovariectomy of rats leads to the development of increases in

osteoclast and osteoblast numbers, along with increases in osteoclast size, to produce bone loss (88,89). Changes to bone turnover rates persist for at least one year after ovariectomy, causing loss of cancellous bone as well as resorption of cortical bone such that the medullary canals of long bones widen (90,91). Similar observations have been made about the bones of post-menopausal women, where increased bone turnover leads to increased osteoclast numbers and activity, disrupting cancellous bone architecture (92) and often causing cortical wall thinning (93). Hormone replacement therapy reduces bone turnover rates in post-menopausal women (94); also, decreased resorption cavity sizes were observed, indicating that osteoclast activity was inhibited (95). Hormone replacement, however, appears to merely preserve the existing bone microarchitecture rather than reversing previously incurred structural disruptions (96). Thus, estrogen levels are important for the maintenance of bone mass and quality: exogenous estrogen supplementation after menopause will not reverse existing bone damage, but can prevent bone quality and mass from becoming further compromised.

1.5 Osteoporosis – the loss of normal bone remodelling balance

When bone resorption and bone formation remain coupled, bone mass and quality remain constant. When these processes become uncoupled, both the quality and the quantity of bone become compromised. Osteoporosis is

characterized by a reduction in bone mass and a change in bone microarchitecture due to accelerated bone resorption relative to bone formation. In postmenopausal osteoporosis, estrogen deficiency leads to increased bone turnover and an elevation in the number of osteoclasts. These effects could be mediated by direct effects of estrogen on bone cells or via estrogen regulation of cytokine, prostaglandin, and growth factor production and activity.

Trabecular bone contains a high concentration of osteoblasts and osteoclasts on its surface and is in a constant state of turnover throughout life. Trabecular bone, because of its high rate of turnover, is more susceptible to the perturbations in bone remodelling balance seen at menopause as a result of decreased estrogen levels. Sites rich in trabecular bone such as the vertebrae, the ends of long bones, the wrist, and the ankle, are the most common sites of osteoporotic fractures (97).

1.6 Mechanotransduction in bone – what do bone cells "see"?

Osteocytes differentiate from osteoblasts as they are embedded within extracellular matrix (ECM). Osteocytes are central to mechanosensation of bone tissue: they extend long cellular processes through fluid-filled canaliculi in the ECM to interact with other cells via gap junctions and extracellular signalling (98). Osteocytes possess mechanoreceptors such as integrins and stretch-activated

cation channels (99). When compressive forces on the bone push fluid through the canaliculi in which osteocyte cellular processes reside, shear forces are generated and are sensed by these mechanoreceptors and converted to intracellular signals. The magnitude of the shear forces generated by fluid flow is related to the diameter of the canaliculi: widened canaliculi produce lower shear forces, whereas narrowed canaliculi produce greater shear forces (100).

Both the magnitude (100) and rate of application (101) of shear forces determines the cellular response of the osteocytes: this can be best illustrated by examining osteocyte responses to different levels of mechanical stimulation (load). Burger et al. proposed that, under normal loading conditions, osteocytes signal to the osteoblasts at the bone surface to become bone-lining cells, a 'quiescent' form of osteoblast (100). Inhibitory signals are sent to osteoclasts to prevent them from resorbing bone, and hence bone density is maintained. Under conditions of low load or disuse (sedentary, microgravity), fluid flow, and thus shear forces, are decreased: the osteocytes no longer sense adequate shear forces, and can be damaged due to decreased nutrient exchange via fluid flow. This results in decreased inhibitory signals being transmitted to osteoclasts: the disinhibited osteoclasts begin to resorb bone, hence decreasing its density (100). Fatigue failure of the bone structure occurs both as a part of normal wear and tear or from overuse (high load). Microcracks damage some osteocyte processes, thus decreasing communication with the bone surface; and may also widen the canaliculi resulting in decreased shear forces acting upon the

osteocytes and likely leading to osteocytes apoptosis. Osteoclasts no longer receive inhibitory signals from osteocytes and may even be activated by osteocyte apoptosis signals and thus begin to resorb the bone ECM (100). As the damaged bone is resorbed, undamaged bone containing intact osteocytes is uncovered, restoring the inhibitory signal to the osteoclasts. Now, however, the shear forces being sensed by the osteocytes are too high (because bone density has been decreased) so osteoblasts are recruited to the surface to produce new ECM and become part of the osteocyte network (100). When the correct level of shear force is perceived by the osteocytes, the osteoblasts at the surface become bone-lining cells and the remodelling is complete.

1.6.1 Current methods to study the effects of mechanical perturbation of bone cells

The examination of cellular responses to mechanical stimulation has involved a variety of culture systems with controlled delivery of mechanical input such as hydrostatic pressure, fluid shear stress, or substrate strain (102). A variety of laboratory apparatuses to exert these mechanical inputs have been designed, with each having their respective advantages and disadvantages. Early efforts to provide mechanical stimulation to cell cultures included surface tension distraction of cells grown in hanging drop cultures (103,104), hydrostatic pressurization of suspensions of isolated cartilage or bone cells (105), and

tensile straining of rat calvarial cells grown on collagen ribbons (106). Advances have since been made on the ease of use and quantification of strains applied in mechanical loading systems.

Hydrostatic pressurization has been frequently used for compression of cell, tissue, and explant cultures (107-109). This method involves culturing cells in a reservoir to which positive or negative pressurization can be applied. The advantages of this system include the simplicity of the equipment, homogeneity of the mechanical stimulus, and ease of delivering static or transient loading inputs, all without impeding nutrient flow. The main disadvantage of this system is that delivery of physiologically relevant pressures results in high partial pressures of CO_2 being generated, which can adversely affect cultures (80). Also, this method of strain application reflects only a small part of the normal physiological stresses that cells would experience.

Fluid shear stress has also been applied to cell cultures as a means of providing mechanical stimulation. A wide range of intracellular phenomena have been associated with fluid shear perception, including activation of plasma membrane receptors, ion channels, integrin signalling, and cytoskeletal rearrangement (110). Two widely used configurations for the generation of shear stress are a cone and plate flow chamber, where a broad cone is placed in close proximity to a flat culture surface and rotated to generate shear stress (111); and a pressure gradient flow chamber, where fluid shear is generated by fluid flow through

between inlet and outlet manifolds at opposite ends of the chamber (112). These systems can be used to provide information of the responses of cells to shear flow, but are of limited use in bone, where cells experience a combination of shear stress and deformation of the bone matrix.

Systems that apply mechanical load by means of longitudinal stretch of the culture substrate have also been used widely due to their simple design and range of strain amplitudes that can be applied. By using motor-driven actuators or spring systems, controlled longitudinal stretch can be applied to deformable culture substrates (e.g. elastin from bovine aortic tissue, silicone membranes) in an oscillatory fashion to produce the dynamic strains known to induce bone turnover (113-115). However, many of these systems produce deformations that are too high to be physiologically relevant for bone (102). To produce the low strains that are relevant to bone, systems of substrate flexure were developed, where four-point bending was applied to plastic strips upon which osteoblast-like cells and osteocytes were cultured (81).

Mechanical load can also be applied to cells by deforming circular culture substrates. Early devices used convex platens to deform standard plastic culture dishes (116), but newer models have used vacuum pressures to deform specially designed silicone culture surfaces (117). The latter of these systems, developed by Banes's group, involved the placement of flexible bottomed cell culture plates on a vacuum manifold system that was controlled by a PC-based programmable

loading device (117). Application of vacuum to the undersurface of the culture plates caused a downward deformation of the membranes, imparting strain to the culture layer. A broad range of parameters could be adjusted in this system, including vacuum magnitude, waveform, frequency, and number of cycles. These characteristics made the system applicable to a broad range of culture conditions and thus it was commercialized in 1987 under the name of Flexercell. However, subsequent studies to characterize the strain on the substrate culture surface revealed that although radial strains were uniform, the circumferential strain was heterogeneous (118). To circumvent this problem, a retrofit for the Flexercell system was devised in which a central platen was placed under each flexible culture membrane. As vacuum was applied, the membrane was stretched over the platen such that the membrane atop the platen experienced equibiaxial strain.

In this project, we used a system constructed in-house that is similar to the Flexercell system, but that is capable of exerting the low magnitudes of mechanical strain that are physiologically relevant for bone. This system applies strain in a sinusoidal waveform, and was demonstrated to produce the same uniform biaxial strains over the platen area as the Flexercell system (119). We applied mechanical strain to our cultures on days 4, 5, and 6 of an 8-day culture period: each period of mechanical strain involved 900 cycles of strain at a peak magnitude of 5000 μstrain at a rate of 1 Hz. To further ensure uniform strains are perceived by the cells, plating of cultures is restricted to the surface area over

the platens by means of inserting plastic rings into the culture wells prior to cell plating.

1.6.2 The role of integrins in mechanotransduction

Integrin signalling has been established as an important mechanosensory mechanism in a variety of cell types including endothelial cells, chondrocytes, and bone cells (osteocytes, osteoblasts, osteoclasts) (120-122). Signalling via integrins involves several intracellular pathways, resulting in transcriptional initiation, cytoskeletal rearrangement, and modulation of intracellular signals via phosphorylation (122,123).

Osteoclasts possess the integrin receptors $\alpha V\beta 3$ and $\alpha V\beta 1$ (vitronectin receptors), and $\alpha 2\beta 1$ (collagen receptor) (43). Recently, the $\alpha V\beta 3$ integrin has been shown to be central to mechanotransduction of shear stress in endothelial cells (122). As shear stress is applied to cells, the cells shift and the $\alpha V\beta 3$ integrins bind 'new' vitronectin sites, which activates Shc (adapter for Fyn, Grb2 and Sos) and RhoA (activator of FAK and c-Src), and in turn initiates the cascades of integrin signalling (122). Since osteoclasts experience compressive, tensile, and shear stresses; and $\alpha V\beta 3$ is their principal integrin, it is highly likely that this integrin plays a similar role in osteoclast mechanotransduction.

The complex intracellular pathways of integrin signalling permit many avenues by which receptors, such as glutamate receptors, might be regulated. Activation of the mitogen-activated protein kinase (MAPK) pathway can cause phosphorylation of transcription factors and induce transcription of genes including transcriptional activators or repressors that may affect receptor expression. Other molecules phosphorylated by integrin signalling, such as Fyn and c-Src, may in turn regulate receptor function by phosphorylation. Since mechanical stimulation activates integrin signalling and modulates glutamate receptor expression and/or function (64), perhaps the former regulates the latter.

1.7 Glutamate receptors and glutamate signalling in the CNS

Glutamate receptors are the primary mediators of excitatory neurotransmission in the mammalian central nervous system (CNS). Additionally, signal transduction by the actions of glutamate on post-synaptic ionotropic glutamate receptors figures prominently in neuronal development and elicits the long-term cellular effects necessary for the synaptic plasticity that underlies the processes of learning and memory. However, glutamate signalling pathways are also hypothesized to be responsible for the excitotoxic cell death that occurs in a variety of neurologic disorders including ischemic brain damage (i.e. following stroke), epilepsy, as well as neurodegenerative conditions such as Parkinson's and Alzheimer's diseases (124,125). Many glutamate receptor subtypes are

expressed in the CNS and serve to mediate the effects of glutamate through a variety of intracellular mechanisms. Glutamate receptors are divided into two distinct groups: ionotropic receptors, or glutamate-gated ion channels and G protein-coupled metabotropic receptors (126,127).

1.7.1 Ionotropic glutamate receptors

Three classes of ionotropic glutamate receptors exist: categorized by their respective selective agonists, they are the NMDA (N-methyl-D-aspartate) receptors, AMPA (α-amino-3-hydroxy-5-methyl-4-isoxazolepropionic acid) receptors, and kainate receptors. Each of these classes of ionotropic receptors contains several different subunits, yielding a total of fifteen different ionotropic receptor subunits identified to date. Specifically, there are six NMDA receptor subunits (NMDAR1, NMDAR2A, NMDAR2B, NMDAR2C, NMDAR2D, NMDAR3), four AMPA receptor subunits (AMPAR1, AMPAR2, AMPAR3, AMPAR4, also known as GluRs 1-4), and 5 kainate receptor subunits (GluR5, GluR6, GluR7, KA1, KA2) (126-128).

The NMDA receptors are involved in excitatory neurotransmission and are widespread throughout the brain with the highest density found in the forebrain. NMDA receptors are characterized by a high permeability to Ca^{2+}, a voltage-dependent block by Mg^{2+}, and slow gating kinetics (127,129). Additionally, to

achieve maximum activation of the NMDA receptor channel, glycine is required as a co-agonist (130). The NMDA receptor subunits cluster in groups of four (or possibly five) with the presence of the NMDAR1 subunit required for a functional ion channel (127). The subunit composition of the ion channel can influence its function by altering the number of phosphorylation sites on subunit cytoplasmic tails and by modulating the clustering of the ion channels into post-synaptic densities (127).

AMPA receptors are found ubiquitously throughout the CNS, although their highest concentrations are in the postsynaptic densities of the hippocampus (131). AMPA receptors potentiate the rapid excitatory neurotransmission initiated by NMDA receptors to produce long-term changes to synaptic architecture. AMPA receptor ion channels are assembled from four subunits and can be homomeric or heteromeric. The subunit composition of the AMPA receptor channel dictates its permeability to Na^+, K^+, and Ca^{2+}. Calcium permeability is regulated in this manner, with receptors containing no AMPAR2 having high Ca^{2+} permeability, receptors containing AMPAR2 having low Ca^{2+} permeability, and homomeric AMPAR2 receptors having very little Ca^{2+} permeability (131). Each of the AMPA receptor subunits has two splice variants, known as "flip" and "flop": the "flip" forms are expressed predominantly during embryonic development, while adult brains predominantly express the "flop" forms. These splice variants are associated with different electrophysiological

characteristics with channels of the "flop" form showing a faster desensitization rate than those assembled from the "flip" form (132).

Kainate receptors are also abundant throughout the CNS, although their physiological significance is less well understood (131). Homomeric receptors of GluR5 and GluR6 are functional (133), while homomeric channels of GluR7, KA1, or KA2 are not (134). Finally, homomeric receptors comprised of GluR6 are highly permeable to calcium ions (131).

1.7.2 Metabotropic glutamate receptors

The metabotropic glutamate receptors are typical G protein-coupled receptors (135). Their structure contains seven transmembrane domains, a large hydrophilic N-terminal region, and a cytoplasmic C-terminal domain. Eight subtypes of metabotropic glutamate receptors have been identified and are denoted as mGluR1-mGluR8. These receptors are structurally related, but they vary greatly in their agonist selectivity, signal transduction mechanism, and distribution in the brain (135). The metabotropic glutamate receptors are pharmacologically distinct and have been divided into three classes based on their responsiveness to glutamate analogs such as quisqualate (group I), (2S,1'R,2'R,3'R)-2-(2,3-dicarboxycyclopropyl) glycine (group II), and 1-AP4 (L-2-amino-4-phosphonobutyrate, group III). Group I receptors (mGluR1, mGluR5)

are coupled to the activation to the phospholipase C pathway (128). Group II receptors (mGluR2, mGluR3) are activated by and are negatively coupled to the adenylate cyclase pathway (136). Group III receptors (mGluRs 4, 6, 7, and 8) are also negatively coupled to the adenylate cyclase pathway (136).

Metabotropic glutamate receptors exert both direct and indirect actions on neurotransmission. These receptors play an important role in synaptic plasticity, including long-term potentiation in the hippocampus (137). Additionally, metabotropic glutamate receptors can enhance NMDA receptor-mediated responses to regulate excitatory neurotransmission (135,137).

1.8 The role of glutamate in bone

The above description of mechanotransduction in bone states that osteocytes send inhibitory signals to osteoclasts so that bone resorption is inhibited except when required for bone repair processes. These signals may be directly sent from osteocytes, or osteoblasts can be solicited by osteocyte signalling or by local mediators to send signals to osteoclasts (100). The signalling molecules responsible for osteoclast inhibition are often growth factors, cytokines such as prostaglandins and TGF-β, hormones, and calcitonin. These molecules inhibit either osteoclast differentiation or function, or promote osteoclast apoptosis.

Recently, signalling via glutamate, the chief excitatory neurotransmitter in the mammalian CNS, has been demonstrated in bone (18,138-144). Both osteocytes and osteoblasts have been shown to possess glutamate uptake transporters and the machinery required for regulated exocytosis of glutamate (Figure 1.4) (140,145). Additionally, both osteoblasts and osteoclasts have been shown to express glutamate receptors of ionotropic and metabotropic subtypes and the expression and/or function of these receptors is sensitive to mechanical stimulation (144,146,147). This evidence has led to the proposal that glutamate signalling forms part of the mechanotransduction circuitry necessary for the maintenance of bone density. Much like learning and memory in the CNS, glutamate signalling in bone is hypothesized to induce the long-term changes to the ECM in response to intermittent mechanical stimuli.

The presence of glutamate receptors on osteoclasts is of particular interest. Glutamate signals received from osteocytes and osteoblasts are likely to be inhibitory since osteoclasts are recruited to resorb bone in the absence of inhibition (100). Indeed, mechanical stimulation that causes inhibition of osteoclasts also produces apparent decreases in glutamate receptor levels, suggestive of high levels of glutamate signalling from osteocytes and/or osteoblasts (144,148). These apparent changes in glutamate receptor levels may be partially attributed to feedback inhibition due to high levels of glutamate signalling. However, we postulate that osteoclasts possess an independent mechanism of regulating glutamate receptor levels and/or activity in response to

mechanical stimulation, the driving force for bone density maintenance. Such a regulatory mechanism in osteoclasts could explain why even during high levels of mechanical stimulation, a minimal level of osteoclast activity is still observed. Complete inhibition of osteoclast function is undesirable since bone resorption is an essential step for repair of matrix damaged by fatigue. This regulatory mechanism may be found to be sensitive to hormone levels and provide an explanation as to why osteoclasts appear to become less sensitive to mechanical stimulation after menopause. However, it is not yet known how glutamate receptor expression and/or activity are regulated in response to mechanical stimulation.

1.8.1 Glutamate receptors on osteoblasts

Following the discovery that osteoblasts expressed a glutamate transporter, GLAST (145), researchers identified several glutamate receptor subtypes on osteoblasts. Ionotropic NMDA receptor subtypes NMDAR1 (138,143,149), NMDAR2A (64,150), and NMDAR2B (64,150) were identified on osteoblasts and shown to produce functional ion channels (146). Other ionotropic receptor subtypes identified in osteoblasts were AMPA receptor subtypes AMPAR1 (138), AMPAR2 (138), and AMPAR3 (149) and kainate receptor subtypes KA1 (149) and KA2 (149). Functional metabotropic receptors were also identified on

osteoblasts: these included the group I receptor mGluR1b (147), and two group III receptors, mGluR4 and mGluR8 (151).

1.8.2 Glutamate receptors on osteoclasts

Establishment of osteoclast culture conditions proved more difficult because osteoclasts require factors secreted from other cells in order to survive. The knowledge of osteoclast glutamate receptor expression therefore lagged behind what was already known in osteoblasts. Osteoclast cell lines such as RAW264.7 cells were used in addition to marrow cultures and osteoclast cultures to elucidate which glutamate receptor subtypes were expressed on osteoclasts (152). The ionotropic NMDA receptor subtypes NMDAR1 (152), NMDAR2A and NMDAR2B (141,143,152) were identified in both RAW264.7 cells and in osteoclasts cultured from bone marrow. Our laboratory has identified the NMDAR2A and NMDAR2B subtypes on osteoclasts *in vivo* (64). The ion channels formed by these NMDA receptors were shown to be functional on osteoclasts through electrophysiological studies (139). Previous work in our laboratory has also identified the presence of AMPA and kainate receptors via immunostaining of osteoclasts within longitudinal sections of rat long bones. These experiments showed that osteoclasts were immunopositive for AMPA receptors AMPAR2/3 and AMPAR4 and kainate receptor(s) gluR5/6/7 (64).

Figure 1.4: Glutamate signalling pathways in bone.

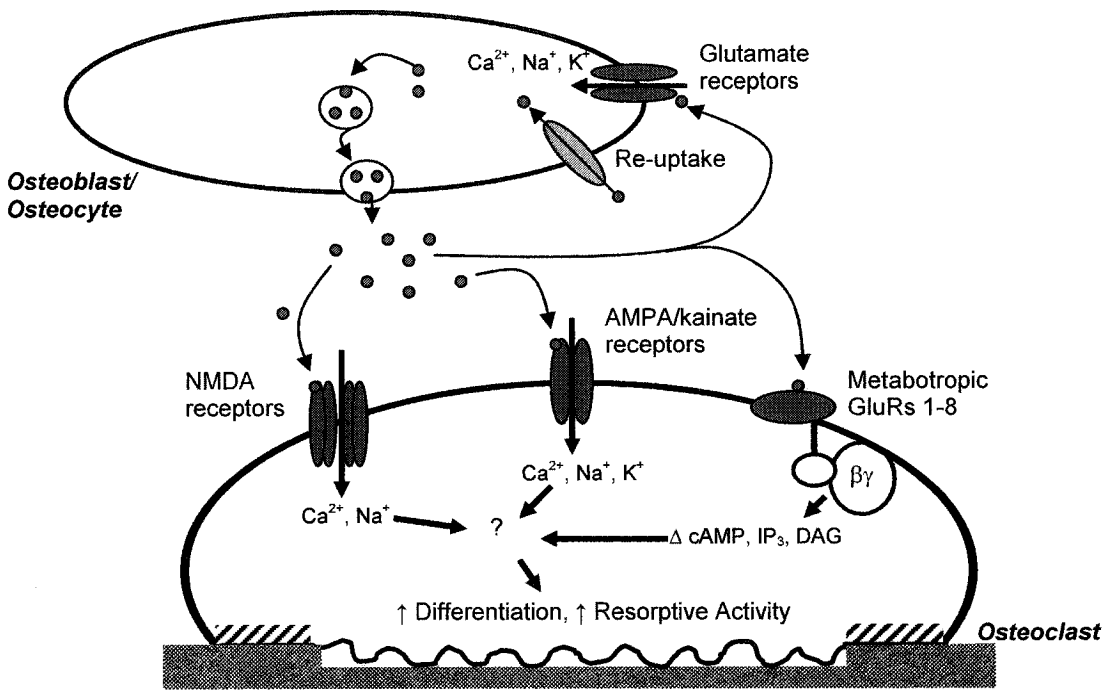

1.8.3 Glutamate signalling in bone

The pathways of glutamate signalling in bone resemble closely those found in the CNS (Figure 1.4). Glutamate is released from osteoblasts via exocytosis that is regulated by voltage-dependent calcium entry (140,153). Alternatively, mechanically-induced opening of stretch-activated calcium channels might lead to glutamate release from osteocytes (154). Glutamate released by osteoblasts and/or osteocytes binds to glutamate receptors on osteoblasts, osteocytes, or osteoclasts. Glutamate binding to G protein-coupled receptors activates either cAMP, inositol trisphosphate (IP3), or diacylglycerol pathways. Ionotropic glutamate receptor activation leads to opening of cation channels: NMDA receptors admit calcium, while AMPA and kainate receptors admit calcium, sodium, and potassium, with ion selectivity depending on subunit composition. Activation of ionotropic glutamate receptors on osteoblasts causes membrane depolarization and calcium influx, leading to glutamate release and activation of intracellular signalling pathways (146). Although these intracellular pathways have not been characterized in osteoblasts, ionotropic glutamate receptor activity has been shown to induce nuclear translocation of the transcription factor AP-1 (155).

The effects of NMDA receptor activation on osteoblasts (inferred from *in vitro* antagonist studies) are increases in differentiation, expression of bone matrix proteins, and bone formation (155-157); these effects may be mediated by

increases in the transcription factor Cbfa1 (downregulated by NMDA receptor antagonists) (157). Osteoblast phenotype can also be affected though AMPA and kainate receptor-mediated signalling; non-NMDA receptor antagonists increase bone formation at low doses but inhibit bone formation at high doses, with these concentration-dependent differences likely due to different responses of AMPA and kainate receptors to the antagonists (155,156). Osteoclasts also exhibit phenotypic effects when glutamate binds to NMDA receptors. Osteoclast bone resorptive ability and sealing zone formation (158,159), and differentiation (152,160), all appear to require NMDA receptor-mediated signals since NMDA receptor antagonists inhibit these processes. Finally, the glutamate signal is terminated by uptake through two high-affinity sodium-dependent glutamate transporters: GLAST-1 (EAAT1), expressed by osteoblasts and osteocytes, and GLT-1 (EAAT2), expressed by mononuclear (osteoclast-lineage) cells (145).

1.9 Hypothesis: Glutamate receptors act as mechanotransducers in bone

We hypothesize that glutamate receptors on osteoclasts receive glutamate signals from osteoblasts and/or osteocytes, which, in addition to a host of other signals from these cells, serve to regulate osteoclast differentiation and function. We speculate that the expression and activity of glutamate receptors is regulated by mechanical stimulation and represent a way in which osteoclasts can

modulate their intracellular responses to incoming glutamate signals from osteoblasts and/or osteocytes. Although at this time, a mechanism for the control of glutamate receptor expression and function in osteoclasts is not known, it is possible integrin signalling may be involved given that integrins are known to sense mechanical stimulation. In addition, we hypothesize that estrogen levels modulate mechanically-regulated glutamate receptor subtype expression in osteoclasts, thus affecting osteoclast functional responses to mechanical stimulation.

1.10 Research objectives

The objective of this project was to increase the understanding of glutamate signalling in bone, in particular in osteoclasts, so as to further elucidate the role that glutamate signalling may play in how bones perceive mechanical strain and how they respond to it by increasing bone formation. A better understanding of mechanotransductive mechanisms in bone will reveal potential therapeutic targets for diseases such as osteoporosis where accelerated bone resorption results in bone loss rather than a balanced bone turnover.

Previous *in vivo* experiments conducted in our laboratory showed (by immunohistochemistry) that osteoclasts in rat long bones expressed many glutamate receptor subtypes and that the expression of these receptors was

altered in response to mechanical stimulation (64). In this project, we wished to develop a mouse marrow-derived mixed culture system which produced mature multinucleated osteoclasts that could be used for more detailed molecular analyses of glutamate receptor subtype expression. A mouse cell culture model was chosen because genomic information and molecular tools are more readily available for mice than for other species. A mixed culture system was chosen so that the *in vitro* environment reflected as closely as possible the heterogeneity of cell types observed *in vivo*. To study the effects of mechanical stimulation, cultures were grown on flexible collagen-I coated plates and subjected to periods of cyclically applied strain.

In the first phase of the project, cultures were grown in the presence of glutamate receptor agonists or antagonists and assayed for osteoclast differentiation and bone resorptive ability to demonstrate the presence of functional glutamate receptors on the cultured osteoclasts. The second phase of the project involved immunocytochemical identification of glutamate receptor subtypes on the cultured osteoclasts and a gross assessment of the effects of mechanical stimulation on glutamate receptor subtype expression. We also examined whether several of the glutamate receptor subtypes observed colocalized with cytoskeletal elements F-actin and vinculin. In the third phase, osteoclast-enriched cell fractions from mixed cultures grown in the presence or absence of mechanical stimulation were prepared by an immunomagnetic bead-based method and RNA and protein isolated for molecular analyses. Western blots,

RT-PCR and Northern analyses were used to determine which glutamate receptor subtypes were expressed in our cultured osteoclasts and whether the expression of these receptors changed with mechanical stimulation. Finally, in the fourth phase of the project, mixed cultures grown in the presence or absence of mechanical stimulation were given doses of 17β-estradiol throughout the culture period; phenotypic effects were observed through osteoclast differentiation and bone resorption assays, and RNA and protein were isolated from osteoclast-enriched fractions and subjected to the same analyses as described above. Glutamate receptor subtype expression and mechanical sensitivity in osteoclasts grown in the presence of varying levels of estrogen were examined. The aim of the studies was to provide information about the importance of hormonal status in osteoclast responses to mechanical stimulation and thus shed light on the cellular mechanisms that lead to osteoporosis.

Chapter 2: Materials and Methods

2.1 Cell culture

Mice were chosen as the species from which to harvest cells for primary culture because of the ready availability of genomic sequence information and molecular tools. Adolescent (7 week old) mice were chosen since their bones contain many osteoclast precursor cells required for the bone remodelling necessary to achieve skeletal maturity. All mice used were female so that the osteoclasts cultured from their marrow would respond in a homogeneous manner to estrogen. Femora and tibiae were harvested from 7 week old female CD1 mice (Charles River Laboratories), and the marrow flushed using α-minimal essential medium (Invitrogen) supplemented with 20% fetal bovine serum (Sigma, Canadian source), 28 mM vitamin C (Invitrogen), 10^{-8} M vitamin D_3 (Sigma), 100 µg/mL penicillin (ICN Inc. Ohio, USA), 0.3 µg/mL amphotericin B (Invitrogen), and 50 µg/mL gentamicin (Invitrogen). Unless noted below, cells were seeded onto type I collagen-coated flexible silastic membranes in 6-well plates (FlexCell International) at a density of 8×10^6 cells per 35 mm well and cultured at 37°C, 5% CO_2 for a total of 8 days. The high cell seeding density was necessary to ensure sufficient bone cell precursors adhered to the plate: many of the marrow cells that were plated were non-adherent blood cell precursors and were removed by a media change after 24 hours of culture. After 8 days, cultures had not yet reached confluence and consisted mostly of osteoclast-lineage cells (pre-

osteoclasts, mononuclear osteoclasts, multinucleated osteoclasts), osteoblast-lineage cells (mostly pre-osteoclasts), stromal cells, and fibroblasts. For TRAcP staining, cells were seeded at the same density on 35 mm plastic dishes and cultured for 8 days. For osteoclastic bone resorption assays, cells were seeded at a density of 4×10^6 cells per 8 mm diameter bovine cortical bone slice and cultured for 8 days. For confocal microscopy of immunostained osteoclasts, cells were seeded at a density of 4×10^6 cells per 18 mm diameter glass coverslip (contained in the wells of a 24-well plate). Complete media changes were carried out on days 1, 4, and 6 of culture.

2.2 Mechanical stimulation of osteoclast cultures

To assess the effects of mechanical stimulation on osteoclast glutamate receptor subtype expression, cultures were grown in 6-well dishes with collagen-I coated flexible silastic membrane culture surfaces (Bioflex Col-I plates, FlexCell International). Type I collagen-coated plates were chosen because type I collagen is one of the chief extracellular matrix proteins in bone (10). Additionally, previous experiments in our laboratory showed that bone cell cultures adhered and grew best on silastic membranes coated with collagen I relative to laminin- or fibronectin-coated plates available from FlexCell International (data not shown). On days 4, 5, and 6 of culture, cell cultures were mechanically-stimulated using an apparatus manufactured and

characterized in-house that applied uniform biaxial load in a sinusoidal waveform controlled by LabView software (119) (Figure 2.1). The cells received 900 cycles of strain at a rate of 1 Hz and peak strain magnitude of 5000 μstrain, which is representative of the upper end of normal physiological levels.

2.3 Treatment of osteoclast cultures with glutamate receptor agonists, antagonists or estrogen

Glutamate receptor agonists or antagonists (all purchased from Sigma) were added to cultures destined for TRAcP staining or bone resorption assays. Agonists NMDA (N-methyl-D-aspartate) or AMPA ((±)-α-amino-3-hydroxy-5-methylisoxazole-4-propionic acid hydrate) or antagonists MK801 (dizocilpine) or NBQX (1,2,3,4-tetrahydro-6-nitro-2,3-dioxobenzo[f]quinoxaline-7-sulfonamide) were added at doses of 0-100 μM to cultures during media changes on days 1, 4, and 6.

The effect of 17β-estradiol (Sigma) on osteoclast differentiation and bone resorptive activity was tested. Concentrations of 0, 0.0001, 0.001, 0.01, 0.1, and 1.0 μM of 17β-estradiol were added to cultures destined for TRAcP staining or bone resorption assays on days 1, 4, and 6 of culture during media changes. To test the effects of estrogen on glutamate receptor subtype mRNA expression, the same concentrations of 17β-estradiol were added to mechanically-stimulated and

non-stimulated cultures destined for RNA isolation. For western blot analysis of the effects of estrogen on glutamate receptor expression, concentrations of 1 μM 17β-estradiol were added to mechanically-stimulated and non-stimulated cultures destined for protein isolation.

2.4 Tartrate-resistant acid phosphatase staining for the assessment of osteoclast numbers

To assess osteoclast differentiation, mouse marrow cultures were stained for TRAcP, an enzyme that is a marker of osteoclast differentiation, expressed by osteoclasts shortly before fusion into multinucleated cells (161). Cultured cells were washed with phosphate-buffered saline (PBS), fixed with 10% formalin (10 % v/v formaldehyde in PBS, Fisher) for 30 minutes, and stained for TRAcP according to established protocols (161). The final concentrations of components of the stain solution were 1.34 mM naphthol AS-BI phosphate (Sigma), 28.6 mM N,N-dimethyl formamide (Fisher), 47.6 mM sodium acetate (Sigma), 65.4 mM sodium barbiturate (Sigma), 33.8 mM $NaNO_2$ (Fisher), 4.4 mM pararosaniline HCl, and 34.4 mM L-tartaric acid. The mixture was filtered using Whatman fast filter paper, and the pH adjusted to 5.0. To each 35 mm well, 2 mL of stain solution was added and incubated at room temperature for 20-30 minutes until red staining of the cells was apparent. The cells were rinsed with PBS, and then rinsed and stored in sterile dH_2O.

Figure 2.1: Picture of the Cell Stimulation System (CSS) used for mechanical stimulation of osteoclast cultures. The apparatus applies mechanical stimulation to six Bioflex culture plates (6 x 35 mm wells). In the picture below, three plates on the left have been removed to illustrate the central platens that permit the system to produce uniform biaxial strain on the flexible silastic culture surfaces.

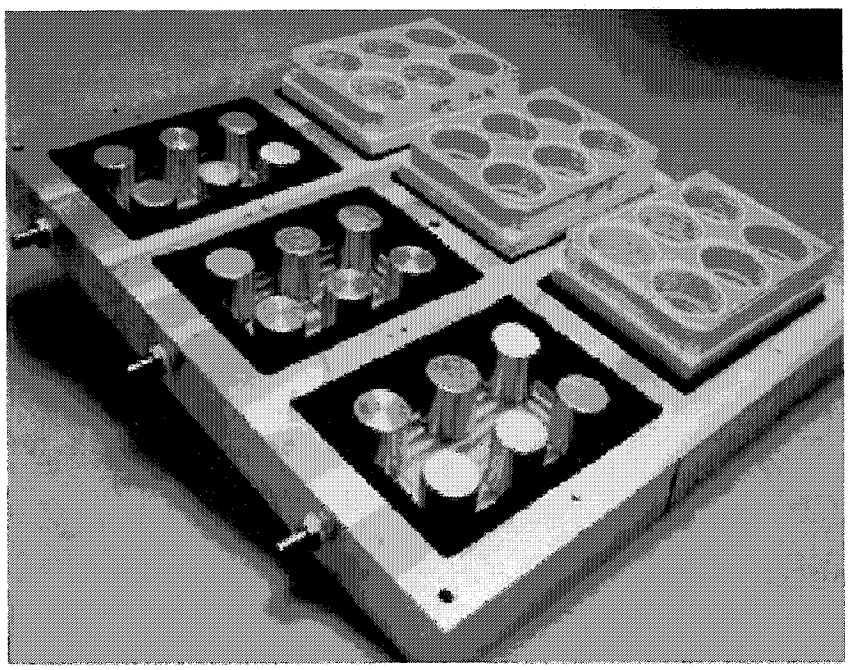

Figure 2.2: Photomicrographs of (A) Osteoclasts stained for TRAcP and (B) Resorption pits formed by osteoclasts on bovine cortical bone slices. A, Mature multinucleated osteoclasts were stained red to indicate TRAcP expression. B, Bovine cortical bone slices were immunostained (brown) for collagen-I fibrils that were exposed when osteoclasts cultured on the bone slices resorbed the mineralized bone matrix.

A

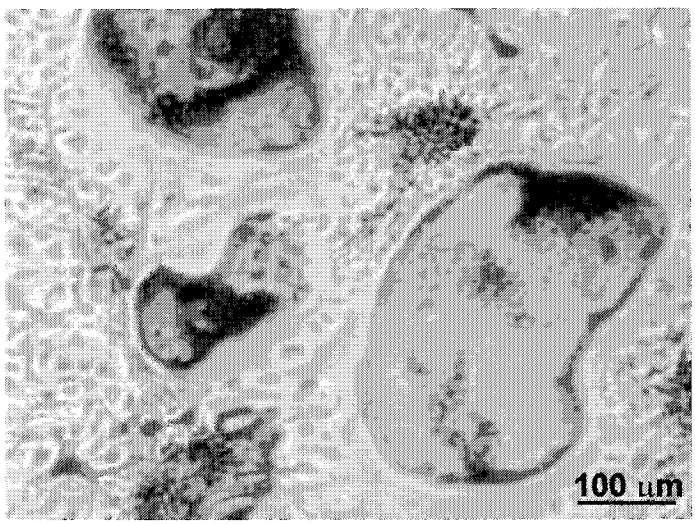

B

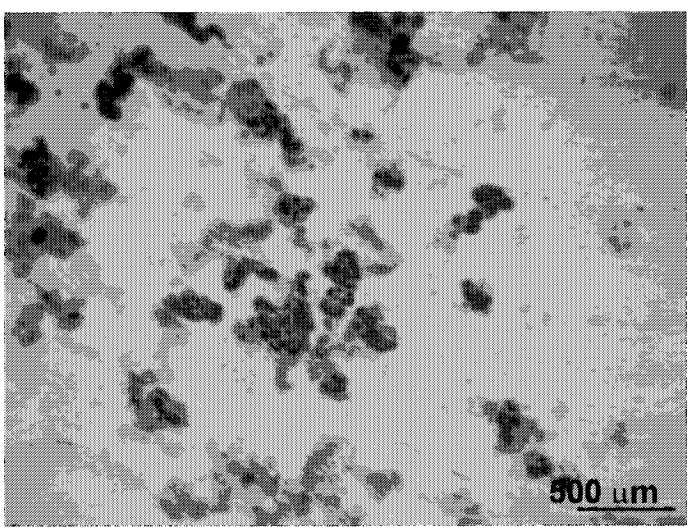

Both mononuclear TRAcP-positive cells and large multinucleated (>3 nuclei) TRAcP-positive cells (Figure 2.2A) were counted using a grid system that sampled 180 mm^2 of the center of the culture surface of each well (162). This area represented 18.5% of the total dish area, and 47% of the central 22 mm diameter area upon which cells were cultured. Results were expressed as the mean number (+/- SEM) of mononuclear or multinucleated TRAcP-positive cells per mm^2.

2.5 Assessment of osteoclastic bone resorption by resorption pit staining and area measurement

To quantify bone resorption by cultured murine osteoclasts, bovine cortical bone slices upon which cells were grown were immunostained for collagen-I fibrils that became exposed as bone mineral was resorbed. The percent area per bone slice covered in resorption pits (stained for exposed collagen-I) was then quantified. To allow assessment of bone resorption, cells were removed from the bovine cortical bone slices upon which they had been cultured by wiping with cotton-tipped applicators dipped in 0.25 N NH_4OH (Fisher). The bone slices were rinsed twice with PBS, and incubated 30 minutes at room temperature in 3% H_2O_2 (Sigma) in CH_3OH (Fisher). Non-specific binding sites were blocked by incubating the bone slices in blocking buffer (0.045 M Tris, 0.1% BSA, 0.05% Tween, pH 7.2) for 30 minutes at room temperature. The blocking solution was

removed and a 1:2000 dilution of monoclonal anti-collagen type I antibody (Sigma) in PBS was added to the bone slices and incubated for 30 minutes at room temperature. Unbound primary antibody was removed by washing twice with PBS, and a 1:250 dilution in PBS of the secondary antibody, sheep anti-mouse IgG conjugated to horseradish peroxidase (Chemicon), was added to the slices and incubated for 30 minutes at room temperature. The slices were washed twice with PBS to remove unbound secondary antibody. A diaminobenzidine (DAB)-based stain (Roche Diagnostics) was used to stain the antibody-bound regions: the DAB substrate was mixed in a 1:11 ratio with peroxide buffer, added to the slices and incubated for 2 hours. Ten fields per slice were photographed at 100 x magnification (10x objective, 10x ocular) and the percentage of the field covered by stained resorption pits (Figure 2.2B) was quantitated using either a LECO semi-automated image analysis system or by analysis of digital photographs using Image-J software. To determine the percentage of resorbed bone per slice, the mean percentage of the ten fields was determined. At least four bone slices per condition were quantified in each experiment and the mean percentage area of bone slice resorbed of four slices was compared between experiments. Results were expressed as the mean (+/- SEM) percentage of bone area resorbed.

2.6 Assessment of glutamate receptor subtypes using immunofluorescence staining

After 7 days in culture, cells were washed with PBS and fixed with 4% paraformaldehyde (Sigma) in PBS. One of a selection of rabbit anti-mouse glutamate receptor subunit primary antibodies (1:100 dilutions, Sigma) was added to the cells [in PBS containing 10% donkey serum (Jackson ImmunoResearch) as a blocking agent] and incubated at 4°C overnight. A Cy3-conjugated (Jackson Immunosresearch) or Alexa Fluor 594-conjugated (Molecular Probes Inc.) goat anti-rabbit IgG secondary antibody diluted in PBS containing 10% donkey serum was applied to the cells for 2-3 h and incubated at 37°C in the dark. The flexible membranes upon which the cells were grown were removed from their plastic housing, mounted onto glass slides with Gel/Mount aqueous mounting medium (Biomeda Corp.) and coverslipped. Mature multinucleated osteoclasts were identified in the cultures using DIC (differential interference contrast) light microscopy. The presence of glutamate receptors on these cells was then visualized using fluorescence microscopy with a 40 x objective lens. Preparations in which the primary antibody incubation had been omitted were used as a negative control.

2.6.1 Fluorescent staining of actin to assess the association of glutamate receptor subtypes with the cytoskeleton

To stain cells for both glutamate receptors and filamentous actin, cells grown on glass coverslips were fixed and then permeabilized by incubation in lysis buffer (0.2% Triton X-100 in PBS) for 5 minutes prior to staining for glutamate receptor subtypes as outlined in section 2.6. After removal of the secondary antibody for glutamate receptor detection, a 1:40 dilution of Alexa Fluor 488 conjugated phalloidin (Molecular Probes Inc.) in dilution buffer (0.1% BSA, 0.05% Tween in PBS) was added to the cells for 30 minutes in the dark. Unbound phalloidin was removed by three washes with PBS. The coverslips containing stained cells were mounted onto glass slides as described in section 2.6 and stored in the dark until viewed by microscopy.

2.6.2 Immunofluorescence staining of vinculin to assess the association of glutamate receptor subtypes with focal adhesion complexes

To stain cells for both glutamate receptors and vinculin, fixed cells grown on glass coverslips were permeabilized by incubation in 0.2% Triton X-100 in PBS for 5 minutes prior to staining for glutamate receptor subtypes as outlined in section 2.6. After removal of the secondary antibody for glutamate receptor detection, a 1:100 dilution of monoclonal anti-human (hVin1) vinculin (Sigma) in

dilution buffer (0.1% BSA, 0.05% Tween in PBS) was added to the cells and incubated in the dark for 1 hour at 37°C. Unbound primary antibody was removed by washing 3 times with PBS. A 1:500 dilution of Alexa Fluor 488 conjugated goat anti-mouse IgG secondary antibody (Molecular Probes Inc.) in dilution buffer was added to the cells and incubated for 2 hours at 37°C in the dark. Unbound secondary antibody was removed by washing three times with PBS and the membranes or coverslips mounted as outlined in section 2.6.

2.6.3 Colocalization of glutamate receptor subtypes with cytoskeletal elements using confocal microscopy

Cells stained for glutamate receptor subtypes and actin or vinculin were examined using a Zeiss LSM 510 Laser Scanning confocal microscope. Multinucleated osteoclasts were identified under brightfield, and then 0.1 μm thick planes were scanned for fluorescence using an Argon 458/488 nm laser to detect green fluorescence (Alexa Fluor 488-phalloidin, Alexa Fluor 488- or Cy5-conjugated goat anti-mouse IgG) and a HeNe 543 nm laser to detect red fluorescence (Alexa Fluor 594- or Cy3-conjugated goat anti-rabbit IgG). Images of the 0.1 μm thick planes were examined for overlap of red (glutamate receptor subtype) and green (actin or vinculin) fluorescence: regions of yellow colour (combined red and green fluorescence) present in the image indicated colocalization of glutamate receptor subtypes with actin or vinculin.

2.7 Immunomagnetic bead-based enrichment of osteoclast populations for protein and RNA isolation

Magacell goat anti-rat IgG-coated immunomagnetic beads (available as a suspension of 3 x 10^8 beads/mL, Cortex Biochem) were coated with rat anti-mouse RANK (receptor activator of NF-kappa B) (Serotec). An aliquot of beads (1 x 10^7 beads per mL of cell suspension to be separated) was placed in a 1.5 mL microcentrifuge tube and the volume made to 1 mL with PBS. The beads were washed twice with cold sterile PBS by placing in a magnetic field for 2 minutes and then removing the supernatant PBS. The beads were resuspended after washing in 1 mL of PBS and mixed with antibody at a ratio of 1 µg of antibody per 1 x 10^7 beads. The antibody was bound to the beads by incubation overnight at 4°C with gentle inversion. To remove unbound antibody, the beads were washed twice with cold sterile PBS and stored at 4°C until needed.

Cells were removed from 6-well plates by incubation with 0.5% trypsin-EDTA in Hanks balanced salt solution (Invitrogen) for 3 minutes at 37°C and gentle scraping with a rubber cell scraper. The cells were pelleted and resuspended in 1 mL of ice-cold PBS. To each 1 mL of cell suspension, 1 x 10^7 anti-RANK-coated immunomagnetic beads were added and the mixture incubated 20 minutes at 4°C with gentle inversion. The mixture was placed in a magnetic field for 2 minutes and unbound non-osteoclasts were removed by pipetting and pelleted by centrifugation while bead-bound osteoclasts were retained.

2.8 Glutamate receptor subtype protein expression assessment using western blot analysis

2.8.1 Membrane and cytosolic protein isolation and quantification method

Membrane and cytosolic proteins were isolated from both osteoclast-enriched and osteoclast-depleted fractions by incubation on ice for 45 minutes with a 0.5% Triton X-100 lysis buffer (30 mM NaCl, 50 mM Tris.Cl pH 7.6, 0.5% Triton X-100, 10 mg/mL leupeptin, 10 mg/mL aprotinin, 1 mM phenylmethylsulfonyl fluoride, 1.8 mg/mL iodoacetimide (all reagents from Sigma)), followed by centrifugation at 4°C for 10 minutes at 15,000 g to pellet nuclei. The supernatant containing membrane and cytosolic proteins was stored at -20°C.

Protein samples were quantitated using the Bradford method (163). Protein samples were diluted to 100 μL with 150 mM NaCl and placed into disposable plastic spectrophotometer cuvettes. To each sample 1 mL of Coomassie brilliant blue solution (1.17 mM Coomassie Brilliant blue G-250, 5% ethanol, 8.5% phosphoric acid) was added, the mixture vortexed, and allowed to incubate at room temperature for 10 minutes. The absorbance at 595 nm was measured using a spectrophotometer and the concentration of protein in the sample determined by extrapolation from a standard curve constructed by measuring the A_{595} of known concentrations of bovine albumin (Sigma) that were prepared in the same way as the unknown protein samples (163).

2.8.2 Electrophoresis of protein samples and transfer to PVDF membranes for immunoblotting

Protein samples were electrophoresed on SDS-PAGE (sodium dodecyl sulfate - polyacrylamide gel electrophoresis) gels, following the Laemmli gel method of denaturing discontinuous gel electrophoresis (164,165). Briefly, a 10 cm x 10 cm polyacrylamide gel was cast with a 6% final acrylamide concentration in the separating gel and 3.9% acrylamide in the stacking gel. Forty micrograms of protein sample were loaded in each lane and prepared by mixing 6:1 with 6x SDS sample buffer (0.35 M Tris.Cl, 30% v/v glycerol, 10% w/v SDS, 0.6 M dithiothreitol, 0.012% w/v bromophenol blue (all reagents from Pharmacia), pH 6.8) and heated 3-5 minutes at 100°C in a screw-cap microcentrifuge tube. Prestained molecular marker (Pharmacia) was included in each gel. The samples were electrophoresed in 1X SDS electrophoresis buffer (0.05 M Tris base, 0.192 M glycine, 0.1% SDS (Pharmacia), pH 8.3) for 30 minutes at 10 mA, then 1 – 1.5 hours at 15 mA.

Following electrophoresis, the protein samples were transferred to PVDF membranes (polyvinylidine fluoride, Pharmacia) using a tank transfer system (164). Briefly, the polyacrylamide gel was equilibrated for 30 minutes at room temperature in transfer buffer (0.025 M Tris base (Pharmacia), 0.19 M glycine (Pharmacia), 15% v/v methanol (Fisher), pH 8.3 – 8.4), assembled with a PVDF membrane (equilibrated in transfer buffer for 15 minutes) in a transfer sandwich,

and placed in a transfer tank full of transfer buffer with the gel side oriented toward the cathode (negative electrode). The proteins were electrophoretically transferred onto the PVDF membrane for 90 minutes at 100 V, during which time the transfer buffer was kept cool by placement of the transfer tank in a container of ice and by constant stirring of the transfer buffer.

To optimize blotting techniques in our lab, the PVDF membranes were reversibly stained with Ponceau S (Sigma) to assess transfer efficiency (164). Membranes were immersed in Ponceau S solution (0.5 g Ponceau S, 1 mL glacial acetic acid in 100 mL H_2O) for 5 minutes at room temperature, followed by destaining for 2 minutes in distilled water. The stained proteins of the molecular weight ladder were marked using pencil. To completely remove the stain, membranes were soaked for an additional 10 minutes in distilled water.

2.8.3 Application of antibodies and development of Western blots

Non-specific binding sites on the PVDF membranes were blocked by incubation in 5% non-fat dried milk (Carnation) in TTBS [0.1% v/v Tween 20 (Sigma) in 100 mM Tris-Cl (Pharmacia), 150 mM NaCl (EM Science), pH 7.5] at 4°C overnight or for 1 hour at room temperature. Excess blocking solution was removed by 2 x 5 minute washes in TTBS at room temperature on an orbital shaker.

The primary antibody was diluted in TTBS according to Table 3.1, and incubated on an orbital shaker. Excess primary antibody was removed from the membrane by washing 3 x 10 minutes in TTBS at room temperature on an orbital shaker. The secondary antibody, goat anti-rabbit IgG horseradish peroxidase conjugate (Jackson Immunoresearch), was diluted 1:15,000 in TTBS. A volume of 5 mL was placed with a 5 cm x 10 cm membrane in a resealable plastic bag and incubated at room temperature on an orbital shaker for 2 hours. Excess secondary antibody was removed by washing 3 x 10 minutes in TTBS at room temperature on an orbital shaker.

The presence of glutamate receptor subunits was detected using the ECL Plus Western Blot Kit (Pharmacia) and exposed to Hyperfilm ECL x-ray film (Pharmacia). The resulting developed film was placed on a light box and digitally photographed for densitometric analysis of the band intensities using Image-J software.

Table 2.1: Primary antibody dilutions and incubation conditions used for Western blots.

Glutamate receptor subtype	Dilution	Incubation time and temperature
NMDAR1	1:250	Overnight, 4°C
NMDAR2A	1:1000	Overnight, 4°C
NMDAR2B	1:500	Overnight, 4°C
NMDAR2C	1:500	Overnight, 4°C
AMPAR1	1:100	1 hour, room temperature
AMPAR4	1:100	1 hour, room temperature

2.9 RT-PCR analysis of the mRNA expression of glutamate receptor subtypes, estrogen receptor subtypes, PSD95, and osteoclast marker genes

2.9.1 Isolation of total RNA from cell samples

Total RNA was isolated from both the osteoclast and non-osteoclast populations using the GenElute Mammalian Total RNA kit (Sigma). Samples were lysed and homogenized in lysis buffer containing guanidine thiocyanate and 2-mercaptoethanol to release RNA and inactivate RNases. The lysates were applied to filtration columns and centrifuged to remove cellular debris and to shear DNA. The filtrate was then mixed with an equal volume of ethanol and applied to a high capacity silica column to bind total RNA. The bound RNA was washed with high and low salt buffers included in the kit and finally eluted with sterile DEPC-treated dH_2O and stored at -20°C.

To isolate RNA from mouse brain tissue (used for positive controls), the RNeasy Lipid Tissue Mini kit (Qiagen) was used. Brain tissues were harvested from euthanized mice, immediately frozen by immersion in liquid nitrogen and stored at -70°C until needed. Frozen brain tissue (100 mg) was homogenized in 1 mL of Qiazol lysis reagent (containing phenol and guanidine thiocyanate) using a mini tissue homogenizer (Sigma) equipped with a sterile pestle. The homogenized mixture was incubated at room temperature for 5 minutes to

disrupt nucleoprotein complexes. A chloroform extraction was performed using 200 μL of chloroform and centrifugation for 10-15 minutes to separate the phases. The aqueous phase was retained, mixed with an equal volume of 70% ethanol, and applied to an RNeasy spin column to bind RNA to the column membrane. The RNA was washed on the column with high and low salt buffers and then eluted with RNase-free sterile distilled water and stored at -20°C until needed.

2.9.2 Removal of DNA from RNA samples and RNA quantitation

A DNase digestion of the RNA was carried out using the DNA-free kit (Ambion). To 50 μL of RNA, 5 μL of 10x DNase I buffer and 1 μL of rDNase I were added and the mixture incubated at 37°C for 30 minutes. 5 μL of resuspended DNase I inactivation reagent was added, mixed well, and incubated for 2 minutes at room temperature with occasional mixing. The mixture was then centrifuged at 10,000 x g for 1.5 minutes and the supernatant containing RNA removed and stored at -20°C until needed. The RNA was then quantitated by measuring its absorbance at 260 nm.

2.9.3 Electrophoresis of RNA samples to assess RNA quality

RNA samples were electrophoresed in formaldehyde gels to ensure that no degradation had taken place during the isolation process. A 1% agarose gel containing 2.2 M formaldehyde (Fisher), 18 mM MOPS (Sigma), 7.12 mM sodium acetate (Sigma), and 0.89 mM EDTA (USB) was cast in a fume hood and immersed in formaldehyde running buffer (20 mM MOPS, 8 mM sodium acetate, 1 mM EDTA). RNA samples were prepared by diluting 0.5 μg of RNA sample to 20 μL in a buffer containing 2 mM formaldehyde, 12.5 mM formamide, 10 mM MOPS, 4 mM sodium acetate, and 0.5 mM EDTA. The mixture was incubated at 65°C for 15 minutes to denature the secondary structural elements in the RNA and then quenched on ice for 2 minutes. Two to three microlitres of acridine orange 6x loading buffer [0.25% Orange G (Sigma), 15% Ficoll (Sigma)] and 1 μL of 1 mg/mL ethidium bromide (Invitrogen) were added to each sample. The samples were mixed, loaded onto the gel and electrophoresed for 55 minutes at 100 V. Good quality RNA samples produced distinct bands on the gel of 1.9 kb and 4.7 kb, corresponding to the 18S and 28S ribosomal RNAs, respectively.

2.9.4 Reverse transcription of mRNA samples for cDNA synthesis

The mRNA was reverse transcribed into cDNA using the Omniscript RT kit (Qiagen). A 20 μL reaction volume contained 2 μg of RNA, 0.5 mM each dNTP,

1 μM Oligo $dT_{(12-18)}$ (Pharmacia), 10 units RNase inhibitor (Fermentas), and 4 units of Omniscript Reverse Transcriptase (Qiagen) in RT buffer (Qiagen). The reaction was incubated at 37°C for 1 hour and then stored at -20°C.

2.9.5 PCR amplification of cDNA transcripts

PCR reactions were carried out with 1.25 U of Taq DNA polymerase (Fermentas) according to manufacturer's directions, using buffer containing $(NH_4)_2SO_4$, 1.5-2.0 mM $MgCl_2$, 10 mM dNTP mix, 1 pmol of each oligonucleotide primer (sequences, melting temperatures, and expected fragment sizes shown in Table m2), and 1 μL of cDNA template per 25 μL reaction. Thermocycle programs used an initial 2-minute denaturation step at 94°C; then 94°C/30 sec, annealing/30 sec, 72°C/30 sec; followed by a final extension step at 72°C for 10 min. Annealing was typically carried out at 0.5°C below the lowest primer Tm (Tables 3.2 and 3.3), 40 cycles were used for all reactions except GAPDH, for which 20 cycles were used. The PCR products were electrophoresed in TBE buffer [0.44 M Tris base, 0.44 M boric acid, 10 mM EDTA (all reagents from USB)] on 2% agarose-TBE gels containing 40 ng/mL ethidium bromide, and photographed under UV illumination. The size of the amplified PCR products was estimated by comparison with a 100 bp DNA ladder (Fermentas) and the relative intensities of the bands were compared via densitometric analysis using Image-J software.

Table 2.2: Primer sequences used for RT-PCR, primer pair melting temperatures (Tm), and expected fragment sizes

Gene	Primer Sequence	Tm (°C)	Fragment size (bp)
NMDAR1	F: 5'-gctgtacctgctggaccgct-3'	63.5	219 bp
	R: 5'-gcagtgtaggaagccactatgatc-3'	62.7	
NMDAR2A	F: 5'-gctacgggcagacagagaag-3'	61.4	257 bp
	R: 5'-gtggttgtcatctggctcac-3'	59.4	
NMDAR2B	F: 5'-gctacaacacccacgagaagag-3'	62.1	314 bp
	R: 5'-gagagggtccacgctttcc-3'	61.0	
NMDAR2C	F: 5'-aaccacaccttcagcagcg-3'	58.8	464 bp
	R: 5'-gacttcttgcccttggtgag-3'	59.4	
AMPAR1	F: 5'-ggaccacagaggaaggcatgatc-3'	64.2	365 bp
	R: 5'-cagtcccagccctccaatc-3'	61.0	
AMPAR2	F: 5'-tgtgtttgtgaggactacggca-3'	60.3	453 bp
	R: 5'-ggattctttgccaccttcattc-3'	58.4	
AMPAR3	F: 5'-gcagagccatctgtgtttaccaa-3'	60.6	472 bp
	R: 5'-agttttgggtgttctttgtgagtt-3'	57.6	
TRAP1-C	F: 5'-gcctctctgaccacctgtgct-3'	63.7	311 bp
	R: 5'-cgaagggcacggtctgtgcagagacgttgccaa-3'	74.5	
OCN	F: 5'-aggaccctctctctgctcac-3'	55.9	371 bp
	R: 5'-accggtggtgccatagatgc-3'	56.1	
CALCP1	F: 5'-agcccgtccttggaagcaactt-3'	62.1	560 bp
	R: 5'-cggagtcagtgagattggtaggag-3'	64.4	430 bp
CALCP3	F: 5'-ccctgaagcccaaaggaaactgtg-3'	64.4	185 bp
	R: 5'-cggagtcagtgagattggtaggag-3'	64.4	
	R: 5'-ctcagctctccctatgacgg-3'	61.4	
PSD95	F: 5'-ctcaggtctgggcttcagcat-3'	61.8	629 bp
	R: 5'-ggtagtcggtgcccaagtag-3'	61.4	
ERα	F: 5'-aattctgacaatcgacgccag-3'	57.9	344 bp
	R: 5'-gtgcttcaacattctccctcctc-3'	62.4	
ERβ	F: 5'-ttcccagcagcaccggtaacc-3'	63.7	300 bp
	R: 5'-tccctcttagagcttggacta-3'	57.9	
GAPDH	F: 5'-tggaaatcccatcaccatct-3'	55.3	426 bp
	R: 5'-gtcttctgggtggcagtgat-3'	59.4	

Table 2.3: Annealing temperatures and number of cycles for PCR

Gene	Annealing temperature (°C)	Number of cycles
NMDAR1	61	40
NMDAR2A	58.5	45
NMDAR2B	60.5	45
NMDAR2C	58	45
AMPAR1	60.5	45
AMPAR2	58	45
AMPAR3	57	45
TRAP-1C	63.2	26
OCN	55	25
CALCP1	60	35
CALCP3	61	40
PSD-95	61	40
ERα	57.4	45
ERβ	57.4	45
GAPDH	59	25

2.9.6 Subcloning of PCR products to confirm sequence and for Northern analysis probe synthesis

PCR products of the expected fragment sizes were subcloned using the TOPO TA cloning kit (Invitrogen) with pCRII-TOPO vector and *E. coli* TOP10 chemically competent cells. Two microlitres of fresh PCR product were mixed with 1 μL of salt solution (1.2 M NaCl, 0.06 M $MgCl_2$), 1 μL of pCRII-TOPO vector solution (10 ng/μL plasmid DNA in 50% glycerol, 50 mM Tris.Cl pH 7.4, 1 mM EDTA, 1 mM DTT, 0.1% Triton X-100, 100 μg/mL BSA, and phenol red), and 2 μL of sterile distilled water. The mixture was incubated for 5 minutes at room temperature to allow ligation to occur. Five microlitres of the ligation mixture were added to 1 vial of *E. coli* TOP10 chemically competent cells that had been thawed on ice. The mixture was incubated on ice for 30 minutes, heat-shocked at 42°C for 30 seconds, and placed on ice while 250 μL of SOC medium were added. The mixture was then incubated at 37°C for 30 minutes and centrifuged to pellet the cells. Media (125 μL) were removed, the cells resuspended in the remaining media, and plated onto LB-Amp plates (1% w/v tryptone, 0.5% w/v yeast extract, 170 mM NaCl, 1% v/v glycerol, 1.5% agar, 0.1 mg/mL ampicillin) to which 40 μL of x-gal (Sigma) had been added for blue-white selection.

After overnight culture at 37°C, colonies containing plasmid (white-coloured colonies) were isolated and grown in 3 mL volumes of LB-Amp broth overnight. Plasmid DNA was purified from the overnight cultures using a QIAprep Miniprep

kit (Qiagen), which is a modified version of the alkali lysis method (166,167). Briefly, the bacterial cells were pelleted by centrifugation, resuspended in buffer containing RNase A and lysed by the addition of a buffer containing NaOH and SDS. The mixture was neutralized in a buffer containing guanidine hydrochloride and acetic acid causing denatured proteins, chromosomal DNA, cellular debris, and SDS to precipitate. The supernatant was applied to a QIAprep column to allow the plasmid DNA to bind to the column. The column was washed with high and low salt buffers and the purified plasmid DNA eluted with sterile distilled water. The plasmid was quantitated by measuring A_{260}. To check that the plasmid contained the expected insert size, 1 µg of plasmid was digested with EcoRI for 30 minutes at 37°C and electrophoresed on a 2% agarose gel with TBE buffer. Inserts were verified by sequencing (Cortec DNA Laboratories).

2.10 Northern analysis of glutamate receptor subtype mRNA expression

2.10.1 Electrophoresis of the RNA samples

To verify the glutamate receptor subtype mRNA changes observed with RT-PCR, northern analysis was performed. RNA samples (10 µg aliquots) were prepared according to section 2.9.3, loaded onto the formaldehyde gel, and electrophoresed at 35 V overnight (15-18 hours) until the 18S and 28S ribosomal RNA bands were separated by at least 4 cm. The gel was photographed under

UV illumination so that the intensities of the 18S and 28S ribosomal RNA bands could be used as a control for loading differences.

2.10.2 Transfer of the electrophoresed RNA samples to nylon membranes

The electrophoresed RNA samples were transferred from the gel to a Brightstar Plus nylon membrane (Ambion) via capillary action, as depicted in Figure 2.2. Transfer was allowed to occur for about 20 hours. Upon completion of transfer, the wells from the gel were marked onto the membrane using pencil and the gel discarded. The RNA was crosslinked to the nylon membrane using a UV crosslinker (Stratagene) and under UV light the molecular weight marker bands were marked with pencil. The moist membrane was sealed into a plastic bag and stored at room temperature.

Figure 2.3: A schematic of the apparatus for transfer of RNA from an agarose gel to nylon membranes for northern analysis.

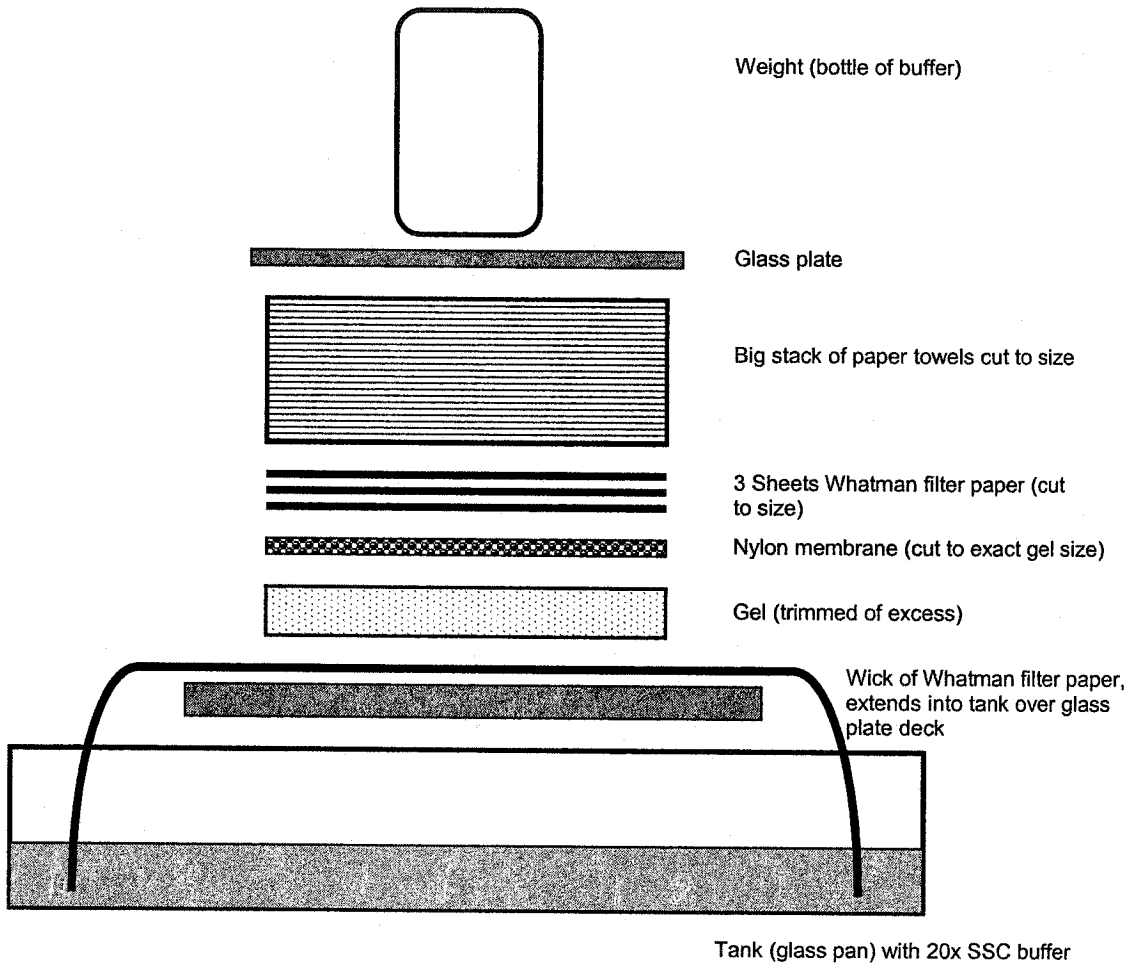

2.10.3 Synthesis of labelled DNA probes

The NMDAR1, NMDAR2A, NMDAR2B, AMPAR1, and AMPAR3 cDNA fragments produced through RT-PCR were used to make probes for northern analysis. The Strip-EZ DNA StripAble DNA probe synthesis and removal kit (Ambion) was used to make the cDNA probes. 25 ng of DNA template was diluted to 8 µL with dH_2O in a 1.5 mL screw-capped tube and heated to 95-100°C for 5 minutes. The tube was immediately placed on ice, briefly centrifuged to bring down any condensation, and the following were added while the tube was kept on ice: 2.5 µL 10x decamer solution, 5.0 µL buffer -dATP/-dCTP, 2.5 µL 10 x dCTP, and 1.0 µL of 1 pmol/µL of specific 3' primer. 5.0 µL [α-^{32}P]dATP and 1.0 µL exonuclease-free Klenow reagent were added and the reaction allowed to proceed for 1 hour at 37°C. The reaction was stopped by adding 1 µL of 0.5 M EDTA. Unincorporated nucleotides were removed from the reaction mixtures by filtration through spin columns containing Sephadex G-50 (Roche Molecular Biochemicals) according to the manufacturer's specifications. Specific activity of the probe was determined by quantifying1 µL of probe with a scintillation counter.

2.10.4 Probing the RNA blots with labeled DNA probes

Northern blots were pre-hybridized in 8 mL of ULTRAhyb hybridization buffer (Ambion) for 2 hours at 42°C with constant rotation. Labeled probe (1 x 10^6 cpm

per mL of hybridization buffer) was prepared by 10-fold dilution in 10 mM EDTA and incubation at 90°C for 10 minutes. The diluted probe was added directly to the buffer in the hybridization tube. The membrane was incubated with the probe overnight (16-18 hours) at 42°C with constant rotation. The hybridization buffer was then removed and the blot washed 2 x 5 minutes with 2x SSC/0.1% SDS, followed by one or two 15 minute washes with 0.1xSSC/0.1% SDS. Blots were heat-sealed into plastic bags for exposure for 16-20 hours at room temperature in a cassette with a PhosphorImaging screen. Following scanning of the phosphorimage, the blots were placed in a cassette with x-ray film at -80°C for 7 days. Four blots in total were made, allowing three different blots to be probed for each of NMDAR1, NMDAR2B, AMPAR1, and AMPAR3, and two different blots to be probed for NMDAR2A. Each blot was also probed for cyclophilin, which was used to normalize the data for any differences in loading between samples on the same blot. The PhosphorImage data for each probe was normalized against the GAPDH data and the differences between treatment conditions determined.

2.10.5 Removal of labeled DNA probes from membranes

The removal of old probe from the blots was facilitated by the use of Ambion's StripEZ DNA StripAble DNA probe synthesis and removal kit. The probes synthesized using this kit contain modified dCTP nucleotides which allow specific

degradation of the probes when blots are incubated with the proprietary probe degradation buffer included in the kit. To remove DNA probe, the blot was incubated in 40 mL of probe degradation buffer (200 µL of 200x probe degradation buffer, 400 µL of 100x degradation dilution buffer, 40 mL dH_2O) for 2 minutes at room temperature and then 10 minutes at 68°C. The degradation buffer was removed and 40 mL of blot reconstitution buffer (400 µL of 100x blot reconstitution buffer, 200 µL 20% SDS, 40 mL dH_2O) was added to the blot and incubated for 10 minutes at 68°C. Following removal of the reconstitution buffer, blots were ready to be hybridized with fresh probe as outlined in section 2.10.4.

2.11 Statistical analysis methods

Statistical analyses were performed on the data collected from the assays for osteoclast differentiation and bone resorptive ability and for the northern analyses. Using Microsoft Excel, analysis of variance (ANOVA) was performed to assess whether experimental conditions (e.g. drug concentration, mechanical stimulation) produced statistically significant results relative to control conditions (e.g. no drug, no mechanical stimulation). Unpaired t-tests were then used to compare the results of each experimental condition with the control condition to determine the actual p-value. P-values of less than 0.05 were considered significant.

Chapter 3: Results

3.1 Effect of glutamate on osteoclast differentiation and resorptive activity

Since glutamate receptor subtype expression was the subject of study, we wished to know the effect, if any, of the presence of glutamate in the culture media, especially on osteoclast differentiation and bone resorptive activity. The cell culture medium that was typically used (α-MEM) had a glutamate concentration of 75 µg/mL, and the fetal bovine serum added to the medium contained glutamate in an unknown concentration. It is known, however, that glutamate has a short half-life in media, and therefore its presence in the medium may not be affecting cell cultures through glutamate receptor-mediated pathways. To determine whether glutamate had an effect on osteoclast differentiation, mixed cultures were grown on six-well plastic plates in glutamate-free medium with concentrations of 0, 10, 25, 50, 75, and 100 µg/mL glutamate added to cultures during media changes. Cultures were stained for TRAcP and the number of mononuclear and multinucleated TRAcP- positive osteoclasts per square millimeter of dish area was determined. In the concentration range tested, glutamate did not have an effect on osteoclast differentiation (Figure 3.1). The effect of glutamate on osteoclast-mediated bone resorption was also tested by adding the same doses of glutamate as above to mixed cultures grown on bovine cortical bone slices. The percentage of each bone slice that was covered by resorption pits was determined by analysis of digital photographs of the bone

slices. As with the observations of glutamate effects on osteoclast differentiation, a no changes in the percentage area of bone resorbed were noted at the glutamate concentrations tested (Figure 3.2).

3.2 Effect of glutamate receptor agonists NMDA and AMPA on osteoclast differentiation

The effect of 0, 0.1, 1, 10, 25, 50, and 100 μM concentrations of agonists NMDA or AMPA in standard media on osteoclast differentiation were tested. Cultures were stained for TRAcP and the number of mononuclear and multinucleated TRAcP-positive osteoclasts per square millimeter of dish area was determined. Only when cultures were treated with 100 μM NMDA did the number of multinucleated TRAcP-positive osteoclasts decrease (Figure 3.3A). At 50 and 100 μM concentrations of AMPA, a decrease in numbers of mononuclear and multinucleated TRAcP+ osteoclasts was observed (Figure 3.3B). Comparison of the 100 μM AMPA concentration with the DMSO vehicle control suggests that the decrease in osteoclast differentiation may be partly attributed to toxicity of the DMSO in which the AMPA was dissolved (Figure 3.3B). However, the inhibitory effect of AMPA at 100 μM is still significantly greater than that of DMSO alone. Since neither of the agonists inhibited osteoclast differentiation across a wide range of doses and the number of mature osteoclasts is an important factor in

bone resorptive ability, the effects of these agonists on osteoclastic bone resorption were not tested.

3.3 Effect of glutamate receptor antagonists MK801 and NBQX on osteoclast differentiation and resorptive activity

The effect of 0, 0.01, 0.1, 1, 10, 25, 50, and 100 μM concentrations of the NMDA receptor antagonist, MK801, and the AMPA receptor antagonist, NBQX, on osteoclast differentiation and bone resorptive activity were tested (Figure 3.4). At concentrations of 10 μM and above, MK801 significantly decreased the numbers of both mononuclear and multinucleated TRAcP-positive osteoclasts (Figure 3.4A); the number of TRAcP+ mononuclear osteoclasts observed at an MK801 dose of 100 μM was reduced to the level of TRAcP+ multinucleated osteoclasts observed in the control (0 μM MK801). The effects of NBQX on osteoclast differentiation were similar, with concentrations of 10 μM and above decreasing multinucleated TRAcP-positive cell numbers, but mononuclear TRAcP-positive cell numbers decreased only in the presence of 100 μM NBQX (Figure 3.4B).

When the same concentrations of MK801 or NBQX were added to osteoclast cultures grown on bovine cortical bone slices, inhibition of bone resorptive ability was observed for both drugs. At concentrations of 50 and 100 μM, MK801 decreased osteoclast bone resorptive ability to less than one-third of its control

value (Figure 3.5A). Treatment of cultures with 25 μM and higher concentrations of NBQX also decreased osteoclast bone resorptive ability to about one-half the control value at 25 μM NBQX to about one-third the control value at 100 μM NBQX (Figure 3.5B).

Figure 3.1: The effect of glutamate on murine osteoclast differentiation. Doses of 10 – 100 µg/mL glutamate were added to cells grown in glutamate-free media on days 1, 4, and 6 of the culture period. The 'creg' (control-regular: contained regular α-MEM and regular FBS) cultures contained greater than 75 µg/mL glutamate (75 µg/mL from α-MEM, plus an unknown concentration of glutamate in the FBS), while the 'cbFBS' cultures contained exactly 75 µg/mL glutamate (75 µg/mL from α-MEM, no glutamate from the FBS since it was dialyzed against a MW = 10 kDa membrane). The numbers of TRAP-positive cells contained within a specified grid encompassing 180 mm^2 of the center of the culture surface were counted in the following categories: multinucleated TRAP+ (> 3 nuclei, black bars), and mononuclear TRAP+ (open bars). Each bar represents the mean +/- SEM of six replicates in three independent experiments (n=3).

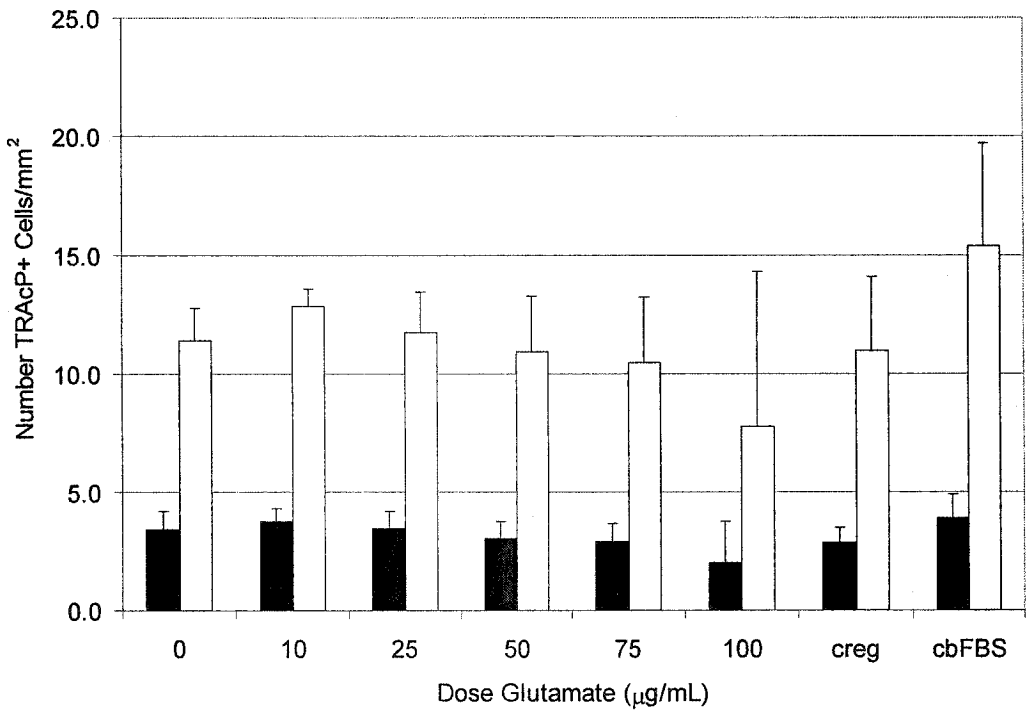

Figure 3.2: The effect of glutamate on murine osteoclast-mediated bone resorption pit area. Doses of 10 – 100 µg/mL glutamate were added to cells grown in glutamate-free media on days 1, 4, and 6 of the culture period. The percentage of each bone slice surface covered by resorption pits (immunostained for exposed collagen-I fibrils) was determined by analyzing digital photomicrographs of bone slices using Image-J software. Each bar represents the mean +/- SEM of quadruplicate determinations of three independent experiments (n=3).

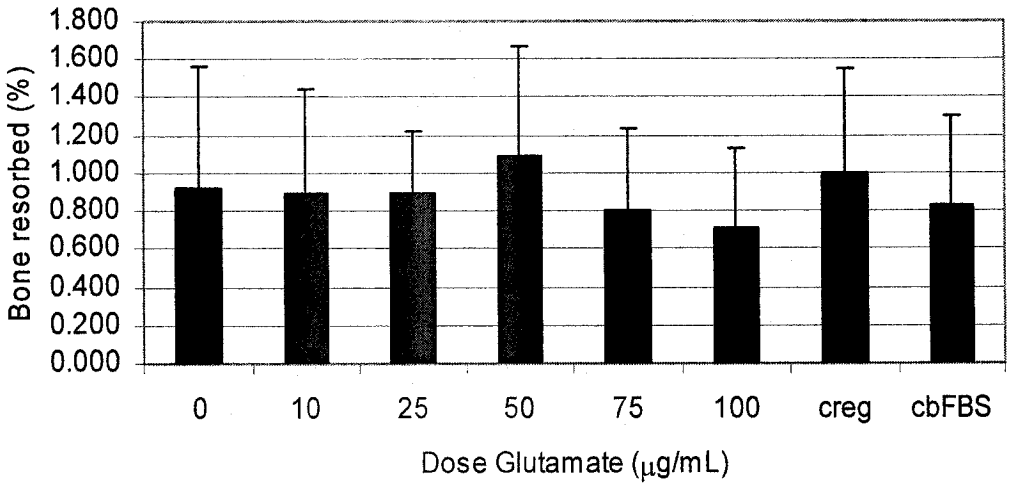

Figure 3.3: Effect of glutamate receptor agonists NMDA and AMPA on osteoclast differentiation. Doses of 0.1-100 µM NMDA (A) or AMPA (B) were added to cells on days 1, 4, and 6 of the culture period. The AMPA graph includes the DMSO vehicle control (30 µL per mL of medium). Numbers of TRAcP-positive cells contained within a specified grid encompassing 180 mm^2 of the center of the culture surface were counted in the following categories: multinucleated TRAP+ (>3 nuclei, black bars), and mononuclear TRAP+ (open bars). Each bar represents the mean +/- SEM of four determinations in two independent experiments. * = $p<0.05$ compared to multinucleated control, # = $p<0.05$ compared to mononuclear control.

A

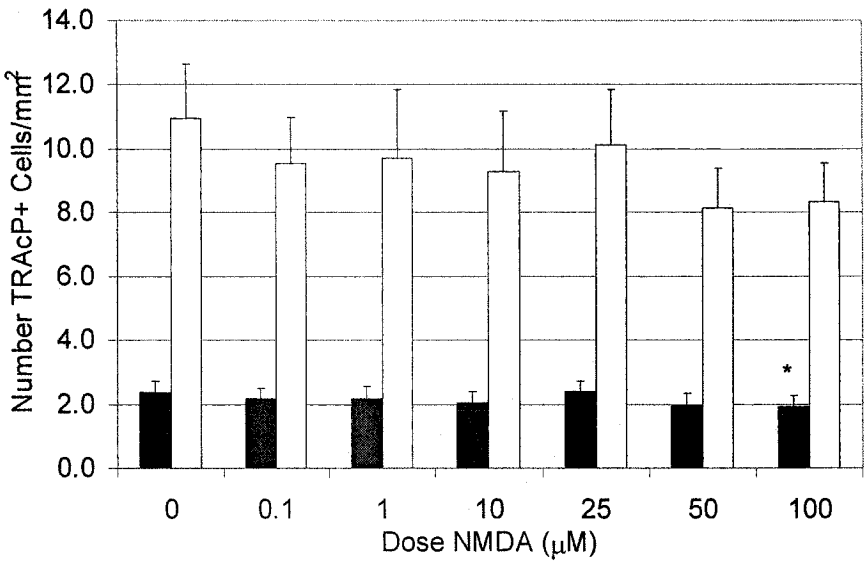

B

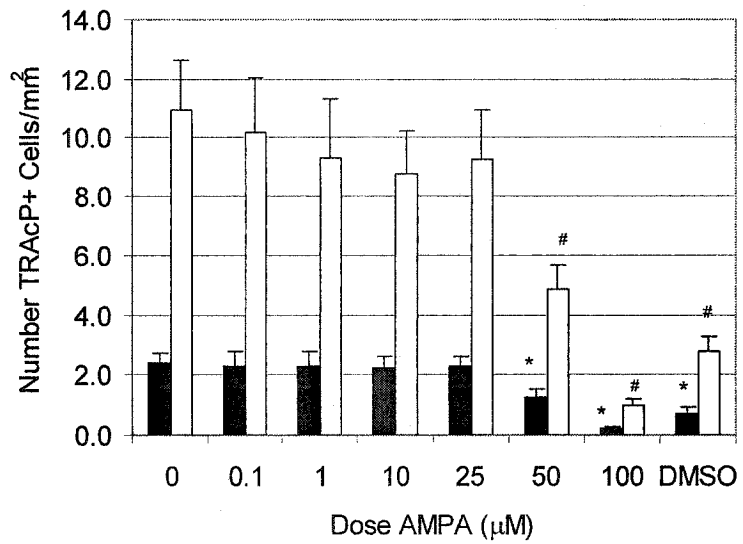

Figure 3.4: The effect of glutamate receptor antagonists MK801 and NBQX on osteoclast differentiation. Doses of 0.01 – 100 μM MK801 (A) or NBQX (B) were added to cells on days 1, 4, and 6 of the culture period. The numbers of multinucleated (>3 nuclei, black bars) and mononuclear (open bars) TRAP-positive cells contained within a specified grid encompassing 180 mm^2 of the center of the culture surface were counted. Each bar represents the mean +/- SEM of quadruplicate determinations in four independent experiments (n=4). *, # = $p<0.05$ when compared to multinucleated and mononuclear controls, respectively.

A

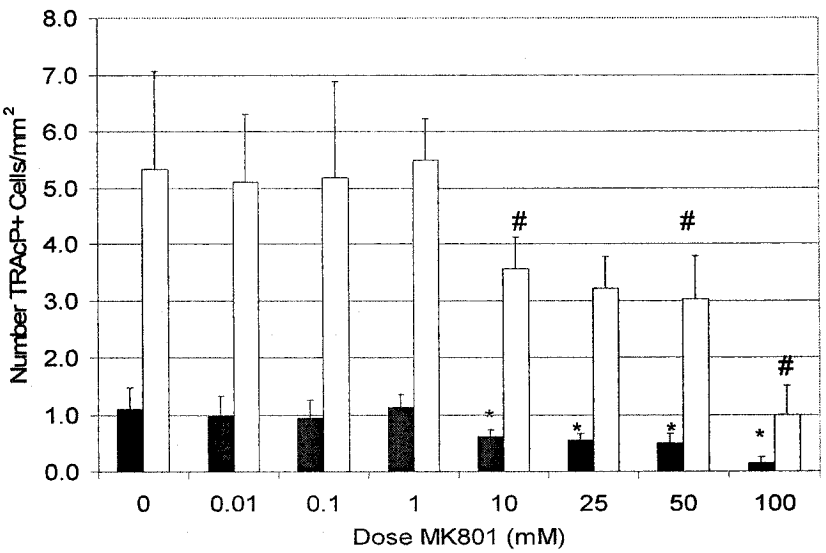

B

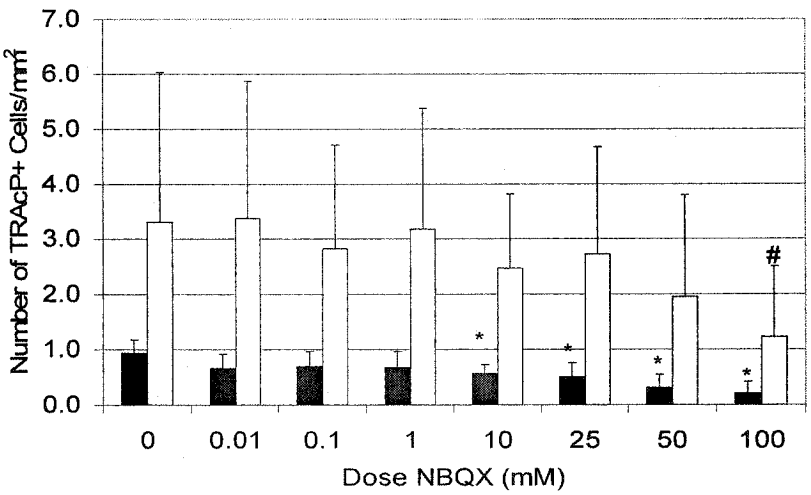

Figure 3.5: The effect of glutamate receptor antagonists MK801 and NBQX on osteoclast-mediated bone resorption pit area. Doses of 0.01 – 100 μM MK801 (A) or NBQX (B) were added to the cells on days 1, 4, and 6 of the culture period. The percentage of each bone slice surface covered by resorption pits (immunostained for exposed collagen-I fibrils) was determined using a LECO semi-automated image analysis system. Each bar represents the mean +/- SEM of quadruplicate determinations of four independent experiments (n=4). * = $p<0.05$.

A

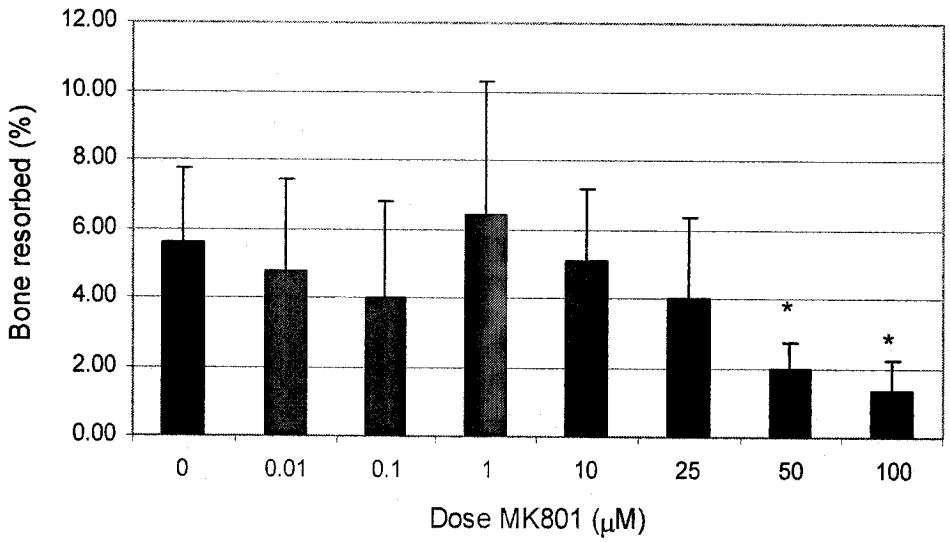

B

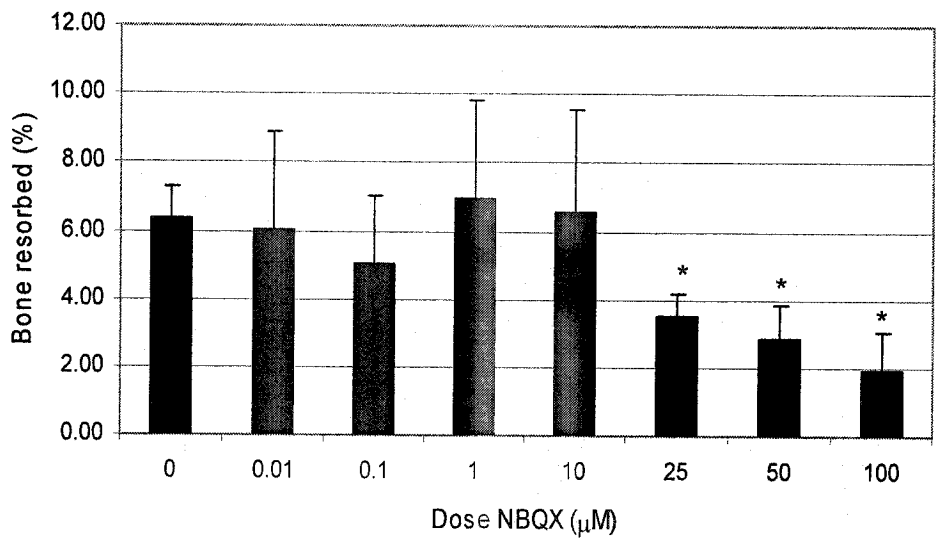

3.4 Effect of estrogen on osteoclast differentiation and function

The effect of 0, 0.0001, 0.001, 0.01, 0.1, and 1 μM concentrations of 17β-estradiol on osteoclast differentiation was tested (Figure 3.6). Estrogen appeared to have a biphasic effect on osteoclast differentiation as the numbers of TRAcP-positive mononuclear osteoclasts were significantly increased at a concentration of 0.0001 μM 17β-estradiol, while higher concentrations of 0.1 and 1 μM decreased mononuclear TRAcP-positive osteoclast numbers (Figure 3.6). The effect of estrogen on differentiation to multinucleated TRAcP-positive osteoclasts was less clear but appeared to be biphasic also: doses of 0.0001 and 0.01 μM 17β-estradiol significantly increased multinucleated osteoclast numbers (the increase produced by the 0.001 μM dose was not significant), while higher estrogen concentrations appeared to decrease multinucleated osteoclast numbers, with the 1 μM 17β-estradiol concentration having a statistically significant inhibitory effect. The same concentrations of 17β-estradiol used above were added to osteoclasts cultured on bovine cortical bone slices to study the effect of estrogen on osteoclast bone resorptive ability (Figure 3.7). No changes in osteoclastic bone resorption were noted at any of the concentrations used.

3.5 Immunocytochemical identification of glutamate receptors on murine osteoclasts

Numerous glutamate receptor subunits were identified on mature multinucleated murine osteoclasts using immunocytochemistry (Figure 3.8). Seven ionotropic receptor subunits were identified: NMDA receptor subunits NMDAR1, NMDAR2A, NMDAR2B, and NMDAR2C, and AMPA receptor subunits AMPAR1, AMPAR2/3, and AMPAR4. Two group I metabotropic receptors, mGluR1a and mGluR5 were identified; but the group II metabotropic receptors, mGluR2 and mGluR3, were not detected. When the cultures were mechanically-stimulated, the expression of all of these receptors appeared to decrease, with the exception of NMDAR2B and AMPAR4, for which no change was noted. Table 3.1 outlines each of the receptor subtypes examined and whether (by gross changes in fluorescent staining) their expression appeared to be altered in response to mechanical stimulation.

Figure 3.6: The effect of estrogen on osteoclast differentiation. Doses of 10^{-4} – 1 μM 17β-estradiol were added to cells on days 1, 4, and 6 of the culture period. The numbers of multinucleated (>3 nuclei, black bars) and mononuclear (open bars) TRAP-positive cells contained within a specified grid encompassing 180 mm^2 of the center of the culture surface were counted. Each bar represents the mean +/- SEM of sextuplicate determinations in four independent experiments (n=4). *, # = $p<0.05$ when compared with multinucleated and mononuclear controls, respectively.

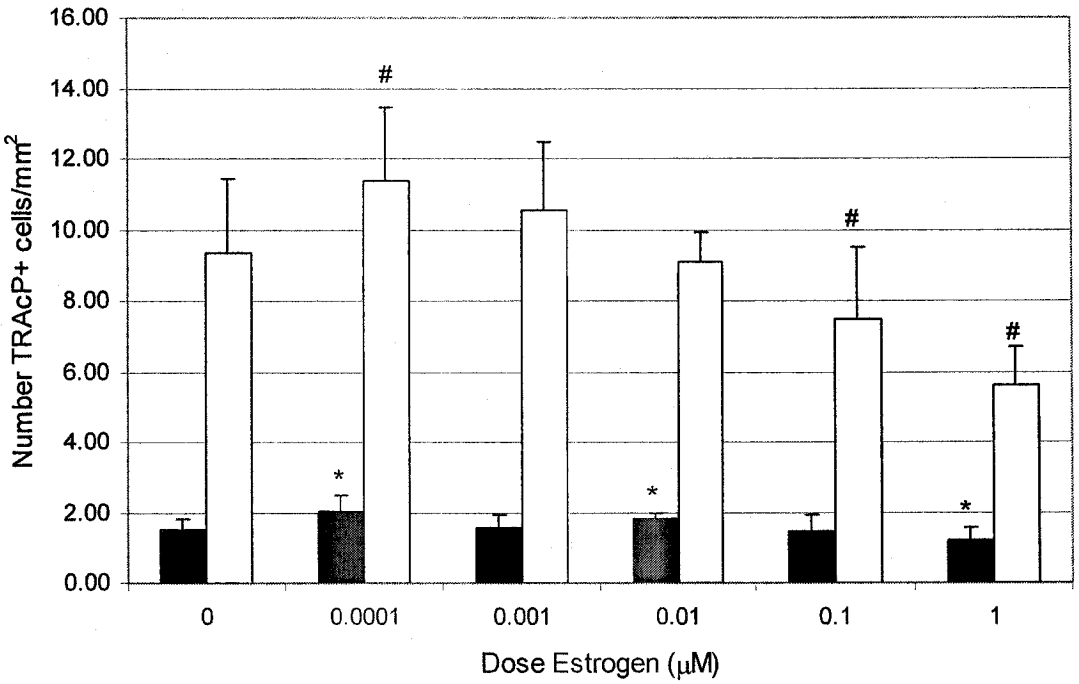

Figure 3.7: The effect of estrogen on osteoclast-mediated bone resorption pit area. Doses of 0.01 – 100 μM 17β-estradiol were added to the cells on days 1, 4, and 6 of the culture period. The percentage of each bone slice surface covered by resorption pits (immunostained for exposed collagen-I fibrils) was determined by analyzing digital photomicrographs using Image-J software. Each bar represents the mean +/- SEM of quadruplicate determinations of four independent experiments (n=4).

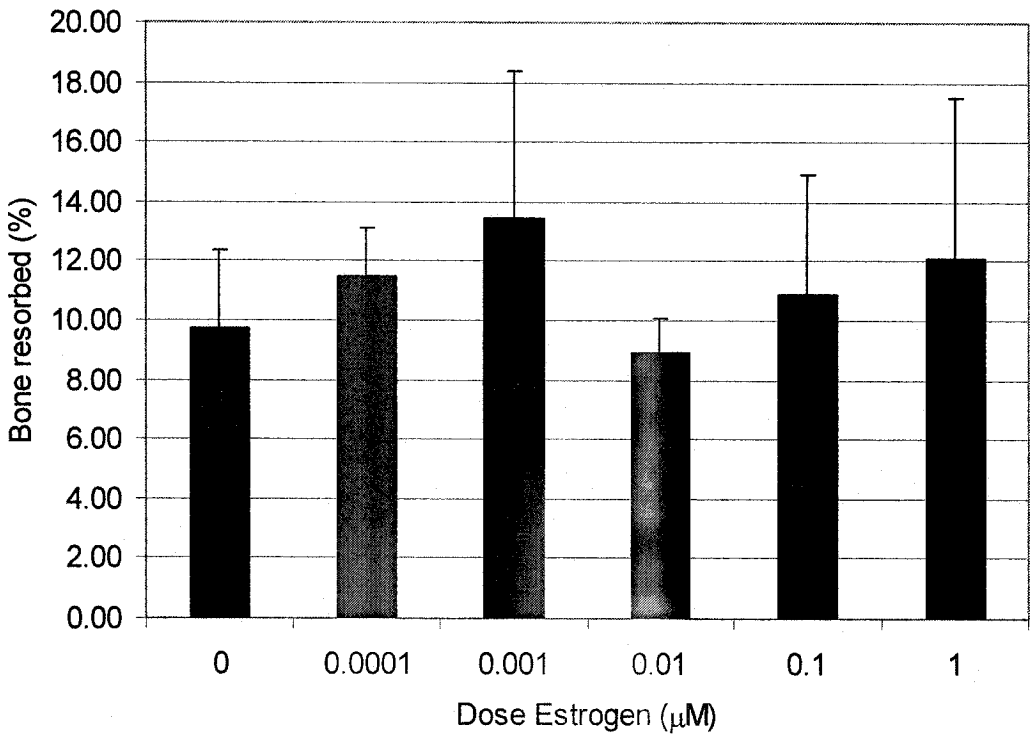

Figure 3.8: Immunocytochemical staining of glutamate receptors on murine osteoclasts. Murine mixed marrow cultures grown on collagen-I coated flexible membranes with or without mechanical stimulation were immunostained for glutamate receptor subtypes (red). Osteoclasts in these cultures were morphologically identified using DIC light microscopy and the glutamate receptor immunostaining viewed by fluorescent microscopy at an original magnification of 40x. Photographs are representative of four osteoclasts viewed per condition in each of three independent experiments, scale bars represent 50 μm.

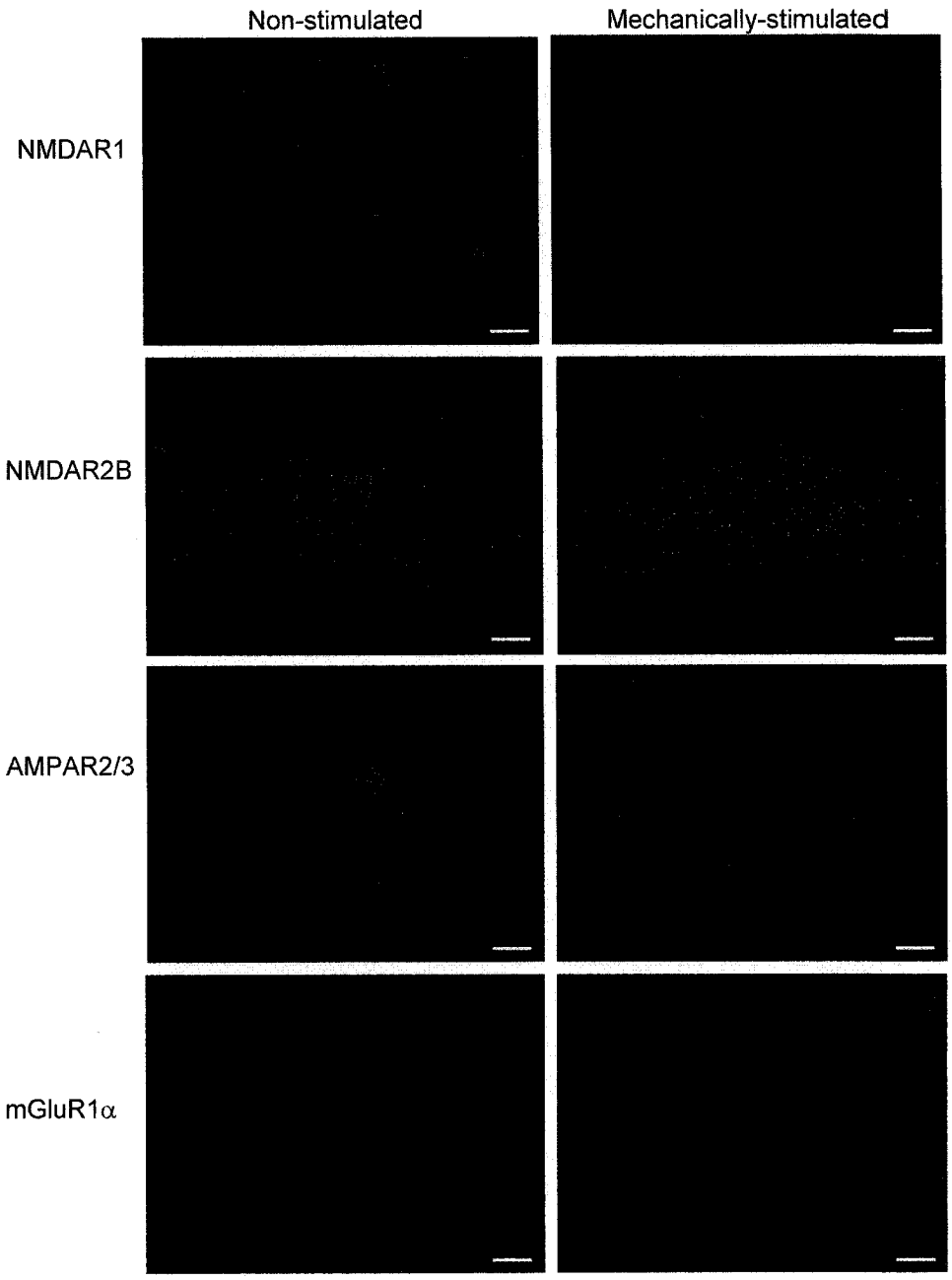

Table 3.1: Immunocytochemical determination of the mechanical sensitivity of glutamate receptor subtype expression on murine osteoclasts. Mature multinucleated osteoclasts that were immunostained for glutamate receptor subtypes were examined for the presence (Y) or absence (N) of glutamate receptor subtype expression in non-stimulated osteoclasts. The effect of mechanical stimulation on glutamate receptor subtype expression in osteoclasts was also assessed by the gross changes in fluorescent staining observed between non-stimulated and mechanically-stimulated osteoclasts. Four osteoclasts were viewed per condition in each of three independent experiments.

Receptor	Non-stimulated	Stimulated
NMDAR1	Y	↓
NMDAR2A	Y	↓
NMDAR2B	Y	No change
NMDAR2C	Y	↓
AMPAR1	Y	↓ (not detected)
AMPAR2/3	Y	↓
AMPAR4	Y	No change
mGluR1α	Y	↓
mGluR2/3	N	N
mGluR5	Y	↓

3.5.1 Colocalization of glutamate receptors with actin

The examination of glutamate receptor subunits on osteoclasts via immunocytochemistry showed that their expression was sensitive to mechanical stimulation. Since mechanical stimulation of cells is known to be sensed through the cytoskeleton, we wished to determine whether any of the glutamate receptor subunits were associated with one or more cytoskeletal elements. Osteoclasts were therefore stained for both glutamate receptor subunits and either filamentous actin or vinculin and examined using confocal microscopy to determine whether glutamate receptors could be colocalized with cytoskeletal elements and therefore infer possible interactions.

Initially, cells were grown on collagen-I coated flexible silastic membranes and subjected to mechanical stimulation prior to fixing and staining, as was previously done for the glutamate receptor identification experiments (Section 3.1). Growth on the flexible membranes would have allowed the examination of glutamate receptor cytoskeletal association under both non-stimulated and mechanically-stimulated conditions. Unfortunately, the thickness and optical nature of these flexible membranes prevented clear images from being obtained using the confocal microscope. Therefore, cultures destined for confocal microscopy were grown on 22 mm round glass coverslips; this permitted clear images to be obtained but prevented the examination of glutamate receptor cytoskeletal association under conditions of mechanical stimulation.

When osteoclasts stained for both NMDAR1 and actin were examined using confocal microscopy, red fluorescence, indicating NMDAR1 expression, was primarily observed in the nucleus, while green fluorescence, indicating actin expression, was primarily found in the periphery of the cell and resembled a characteristic osteoclast sealing zone (Figure 3.9). In the nuclear region, a yellow colour was also observed in the images, suggesting that NMDAR1 colocalizes with actin in this region. No colocalization of NMDAR1 and actin was observed in the filopodia.

Osteoclasts stained for both NMDAR2B and actin expression in the same sealing zone pattern as described above, whereas NMDAR2B expression was uniformly distributed throughout the same region of the cell as actin and was not associated with the nucleus (Figure 3.10). Despite NMDAR2B and actin staining both being present in the sealing zone, no yellow colour was observed suggesting that these molecules do not colocalize in this region when osteoclasts are grown on glass coverslips. A yellow colour indicating colocalization was however observed in several filopodia protruding from the edge of the osteoclast, suggesting that colocalization of NMDAR2B and actin occurs in these structures.

Staining of osteoclasts for both AMPAR1 and actin showed both molecules were present in the region where a sealing zone would form (Figure 3.11). However,

no yellow colour was observed in the images, suggesting that AMPAR1 and actin do not colocalize in osteoclasts grown on glass coverslips.

3.5.2 Colocalization of glutamate receptors with vinculin

To further assess the association of glutamate receptors with the osteoclast cytoskeleton, osteoclasts were stained for both glutamate receptor subunits and vinculin. Vinculin is found in focal adhesion complexes, which are important for mechanosensation, and functions to tether integrins in the cell membrane to intracellular actin filament structures (168). In osteoclasts, focal adhesion complexes containing vinculin are associated with the sealing zone that is formed during bone resorption (169).

When osteoclasts stained for both NMDAR1 and vinculin were examined, NMDAR1 expression was observed primarily in the nucleus, while vinculin expression was observed near the basal periphery where a sealing zone might typically form (Figure 3.9). Colocalization was observed in the images in both the perinuclear region and as a punctate staining pattern in the sealing zone region.

When osteoclasts were stained for both NMDAR2B and vinculin, both molecules were observed in the sealing zone region (Figure 3.10). Additionally, punctate

regions of yellow colour were observed in the images suggesting that NMDAR2B and vinculin were colocalized in the sealing zone.

Staining of osteoclasts for both AMPAR1 and vinculin indicated that both molecules were found in this region (Figure 3.11). However, no punctate or diffuse regions of yellow colour were observed in the images, suggesting that AMPAR1 and vinculin do not colocalize in osteoclasts grown on glass coverslips.

Figure 3.9: Colocalization of NMDAR1 with actin and vinculin on mature multinucleated osteoclasts. Cultures were grown on glass coverslips and thus were not mechanically-stimulated. Images represent 0.1 μM thick slices of osteoclasts immunostained for NMDAR1 (red) and actin or vinculin (green) taken at an original magnification of 63x. On the left, the top image shows the edge of an osteoclast stained for NMDAR1 and actin, while the bottom image shows the edge of an osteoclast stained for NMDAR1 and vinculin. The smaller images represent secondary antibody controls to demonstrate the lack of fluorescence in the absence of anti-NMDAR1 antibody (red control) or in the absence of anti-vinculin antibody (greed control). White arrows point to regions where a yellow colour appears, indicating colocalization of NMDAR1 with actin (top image) or vinculin (middle image).

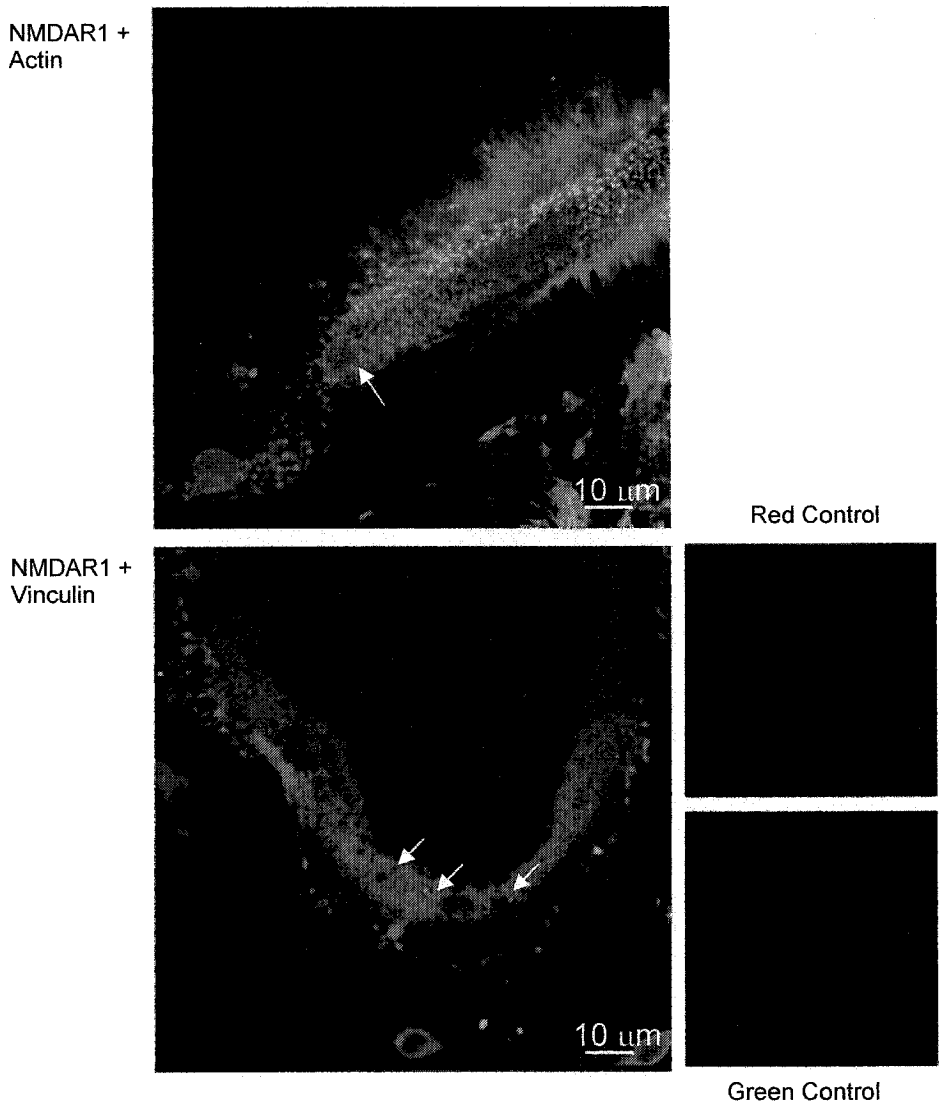

Figure 3.10: Colocalization of NMDAR2B with actin and vinculin on mature multinucleated osteoclasts. Cultures were grown on glass coverslips and thus were not mechanically-stimulated. Images represent 0.1 μM thick slices of osteoclasts immunostained for NMDAR2B (red) and actin or vinculin (green) taken at an original magnification of 63x. The top image shows the edge of an osteoclast stained for NMDAR2B and actin, while the bottom image shows the edge of an osteoclast stained for NMDAR1 and vinculin. White arrows point to regions where a yellow colour appears, indicating colocalization of NMDAR2B with actin (top image) or vinculin (bottom image).

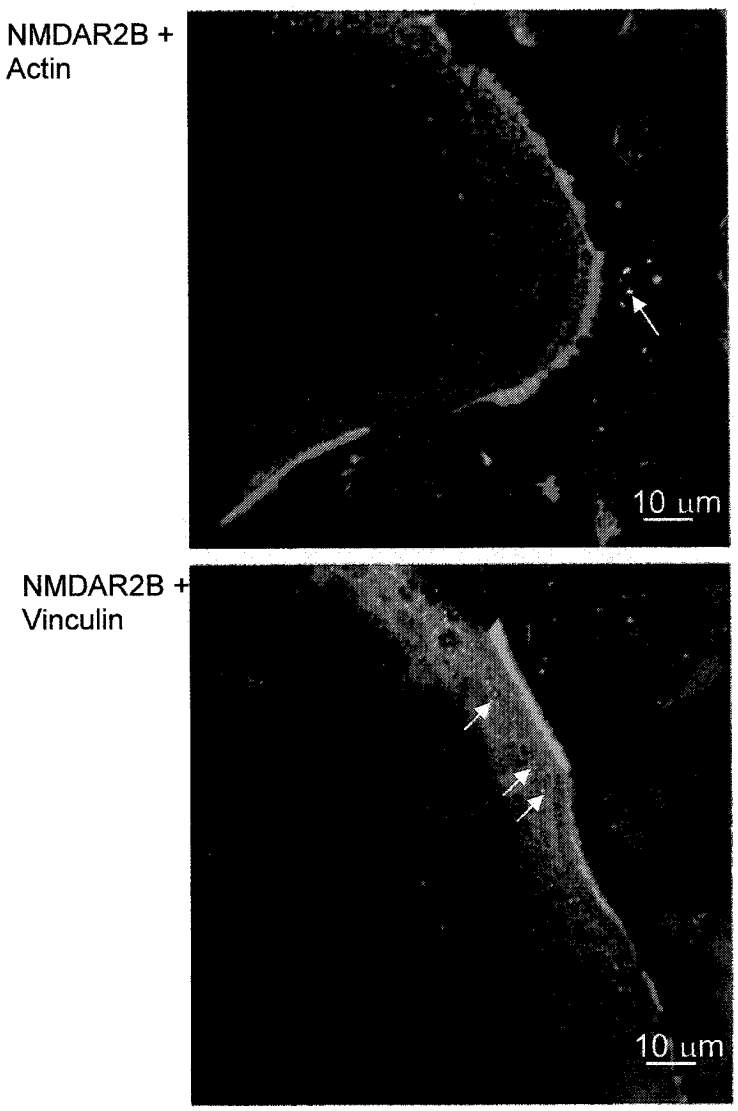

Figure 3.11: Colocalization of AMPAR1 with actin and vinculin on mature multinucleated osteoclasts. Cultures were grown on glass coverslips and thus were not mechanically-stimulated. Images represent 0.1 μM thick slices of osteoclasts immunostained for AMPAR1 (red) and actin or vinculin (green) taken at an original magnification of 63x. The top image shows the edge of an osteoclast stained for AMPAR1 and actin, while the bottom image shows the edge of an osteoclast stained for AMPAR1 and vinculin. Note the absence of yellow colour in both images, indicating that AMPAR1 does not appear to colocalize with actin or vinculin in osteoclasts when grown under these conditions.

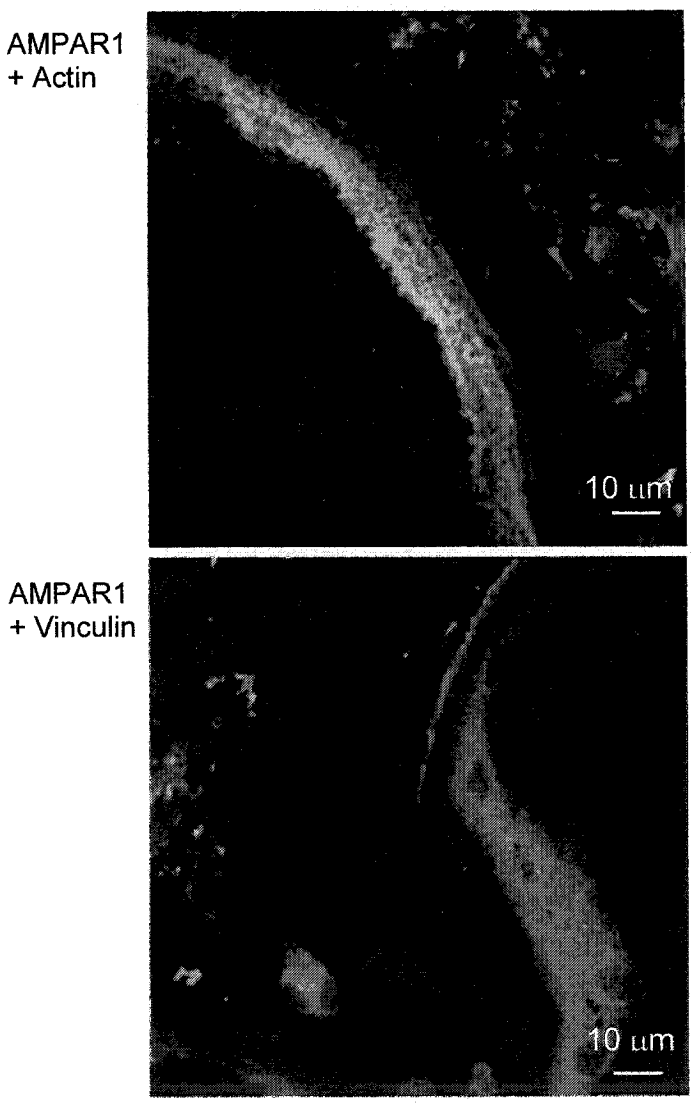

3.6 Analysis of the immunomagnetic bead-based preparation of osteoclast-enriched cell fractions for RNA and protein isolation

In this culture system, bone marrow, containing precursor cells of both osteoclast and osteoblast lineages, was seeded onto culture dishes and grown under conditions which favoured osteoclast differentiation. These mixed culture conditions were necessary because osteoclast differentiation is dependent on the presence of signals from osteoblast-lineage cells (33). Although many mature multinucleated osteoclasts were observed at the end of the culture period, other cell types such as osteoblast-lineage and fibroblast cells also were present. This mixed culture system did not pose challenges for immunocytochemical methods as mature osteoclasts were always identified morphologically via microscopy prior to examination of staining patterns. However, molecular analysis of glutamate receptor subtype expression by osteoclasts required that these cells be at least partially purified from their mixed cultures prior to RNA or protein isolation to ensure that the major contribution to a gene expression signal came from mononuclear or multinucleated osteoclasts rather than other cell types.

To produce osteoclast-enriched fractions from cells harvested at the end of the mixed culture period, immunomagnetic beads were used. The beads were coated with anti-RANK (receptor activator of NF-κB, an osteoclast surface marker) and incubated with the mixed cell populations harvested from culture plates. Mature multinucleated osteoclasts, which expressed RANK, were bound

by the beads and separated from non-bound cells by incubation in a magnetic field. Although not expected to produce pure osteoclast fractions, this method would enrich osteoclast numbers.

To follow the enrichment of osteoclast numbers produced by immunomagnetic bead-based separation, RT-PCR was used to monitor the expression of osteoclast and osteoblast marker genes in RNA samples isolated from osteoclast-enriched (OC) and osteoclast-depleted (UN) cell fractions. Figure 3.12 shows representative photographs of electrophoresed RT-PCR products of TRAP1C and osteocalcin amplification from four independent experiments. High levels of TRAP1C (osteoclast-specific tartrate-resistant acid phosphatase 1C) expression were observed in both OC and UN fractions, indicating that many mature multinucleated osteoclasts were produced in the mixed culture system (Figure 3.12). Conversely, low levels of osteoblast-specific OCN (osteocalcin) expression were observed, indicating that the mixed culture system produced few mature osteoblasts (Figure 3.12). Although a positive control for the osteocalcin RT-PCR was not shown, identical oligonucleotide primers and reaction conditions were used routinely in our laboratory to amplify OCN from osteoblast cultures.

Figure 3.12: Evidence of immunomagnetic bead-based enrichment of osteoclasts in cell fractions for protein and RNA isolation. Marker genes for mature osteoclasts (TRAP1C, a bone-specific tartrate-resistant acid phosphatase) and mature osteoblasts (OCN, osteocalcin), along with a GAPDH reaction control, were amplified by RT-PCR from RNA isolated from osteoclast cultures fractionated by binding to immunomagnetic beads coated with RANK (receptor activator of NF-KB, an osteoclast surface marker). Cultures were grown in the absence (NS) or presence (S) of mechanical stimulation and separated into osteoclast-enriched (OC) and osteoclast-depleted (UN) cell fractions. Gel pictures of electrophoresed PCR products shown below are representative of two RT-PCR reactions per gene performed on each of three independent experiments.

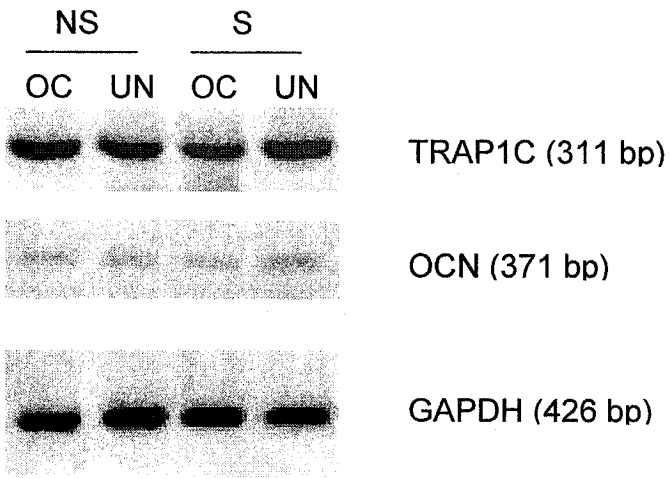

3.7 Detection of glutamate receptor subtypes on osteoclasts using western blots

The anti-glutamate receptor antibodies used for immunocytochemistry were used in western blot analysis to examine the expression and mechanosensitivity of glutamate receptor subunit proteins on osteoclasts. When blots containing protein samples isolated from osteoclast-enriched cell fractions were probed for the presence of glutamate receptor subunits, bands corresponding to NMDAR1, NMDAR2A, NMDAR2B, and AMPAR1, but not NMDAR2C were identified (Figure 3.13). In the NMDAR1 blot, two bands were identified: the 116 kDa band corresponds to the fully glycosylated form of NMDAR1 while the 100 kDa band is likely the non-glycosylated form. Expression of NMDAR1 in mouse osteoclasts appeared to be considerably less than in the mouse brain positive control. In the NMDAR2A blot, multiple proteins ranging from 130 to 180 kDa were observed in the mouse brain positive control, while the level of expression in osteoclasts appeared to be much less with a faint band being identified at 170 kDa. In the NMDAR2B blot, a protein of 180 kDa was observed in both non-stimulated and mechanically-stimulated osteoclast samples as well as being present in abundance in the brain positive control. Although not detected in osteoclast samples, a faint band at 140 kDa corresponding to NMDAR2C was identified in the mouse brain positive control showing that the antibody did in fact recognize NMDAR2C. A band at 170 kDa was also observed in all samples on the NMDAR2C blot: this most likely represents NMDAR2A and/or NMDAR2B as the

antibody used was known to have some cross-reactivity with these proteins. Finally, blotting for AMPAR1 showed two proteins in each sample of 110 kDa and 105 kDa, likely corresponding to two different isoforms of the receptor (170).

3.7.1 Western blot analysis of the mechanosensitivity of glutamate receptor subtype expression

The western blot analysis was useful in confirming the expression of glutamate receptor subunits observed through immunocytochemistry. However, the levels of expression observed in osteoclasts were very low and thus the western blots could not be used as a means for determining potential changes in glutamate receptor subtype expression produced by mechanical stimulation of cell cultures.

Figure 3.13: Western blot analysis of the presence and mechanical sensitivity of glutamate receptor subtype expression on murine osteoclasts. The presence of glutamate receptor subtype protein expression was assessed in protein samples derived from osteoclast-enriched fractions of cells that had been grown in the absence (NS) or presence (S) of mechanical stimulation, as well as the positive brain tissue control (Brain). Pictures shown below are representative of two blots performed per receptor subtype in each of three independent experiments.

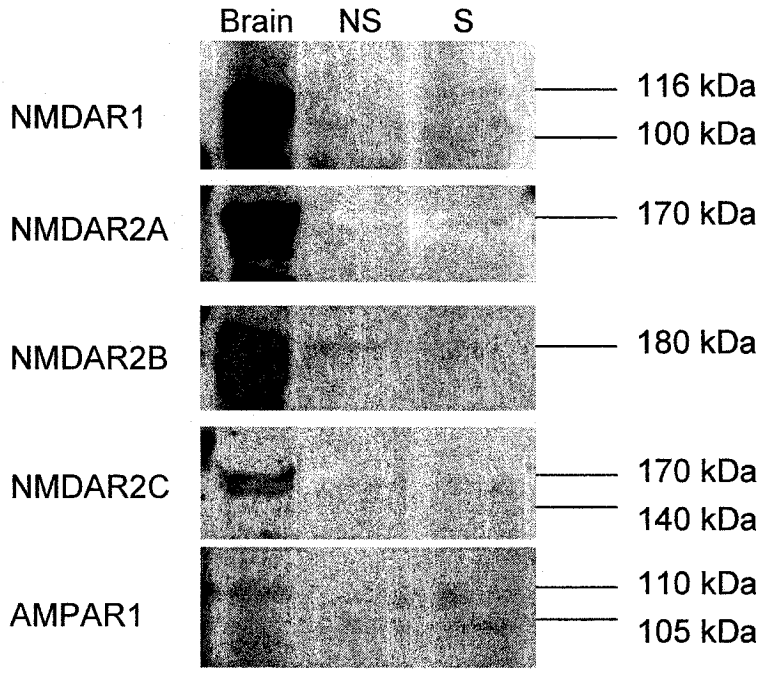

3.8 Detection of glutamate receptor subtypes on osteoclasts using RT-PCR

RT-PCR was used to detect glutamate receptor subtype mRNA expression in mouse osteoclasts. We detected changes in mRNA expression of the glutamate receptor subunits elicited by mechanical stimulation or estrogen. Using this method to analyze RNA samples isolated from osteoclast-enriched (OC) and osteoclast-depleted cell fractions (UN), mRNA was detected for NMDAR1, NMDAR2A, NMDAR2B, AMPAR1, and AMPAR3, but not NMDAR2C or AMPAR2 (Figure 3.14). RNA isolated from mouse brain homogenate was used as a positive control: all seven glutamate receptor subtypes examined were detected in the mouse brain RNA (Figure 3.14).

3.8.1 Assessing the mechanosensitivity of glutamate receptor subtype expression using RT-PCR

When RT-PCR was used to amplify glutamate receptor subunit mRNAs from RNA samples isolated from non-stimulated (NS) and mechanically-stimulated (S) cell populations, the mRNA levels of all five glutamate receptor subunits detected changed in response to mechanical stimulation. Messenger RNA levels for NMDAR2A, AMPAR1 and AMPAR3 increased when osteoclasts were mechanically-stimulated, while mRNA levels for NMDAR1 and NMDAR2B decreased with mechanical stimulation (Figure 3.14). Although this was not a

quantitative PCR analysis, gross changes in mRNA expression were assessed by densitometric analysis of photographs of the electrophoresed glutamate receptor subunit PCR products normalized to GAPDH expression. The fold change in gene expression of each subunit elicited by mechanical stimulation compared to non-stimulated conditions was determined through analysis of four independent experiments (Figure 3.15). Mechanical stimulation during culture increased osteoclast mRNA expression of NMDAR2A by 4.5-fold, AMPAR1 by 7-fold, and AMPAR3 by 7.2-fold, while decreasing expression of NMDAR1 by 7.5-fold and NMDAR2B by 7-fold.

Figure 3.14: Assessment of the presence and mechanical sensitivity of glutamate receptor subtype expression on murine osteoclasts using RT-PCR. The presence of glutamate receptor subtype mRNA expression was assessed in RNA samples derived from osteoclast-enriched (OC) and osteoclast-depleted (UN) cell fractions from cultures that were non-stimulated (NS) or mechanically-stimulated (S). RNA isolated from mouse brain was used as a positive tissue control and the GAPDH gene was amplified as a reaction control. Pictures shown below are representative of three reactions performed per receptor subtype in each of three independent experiments.

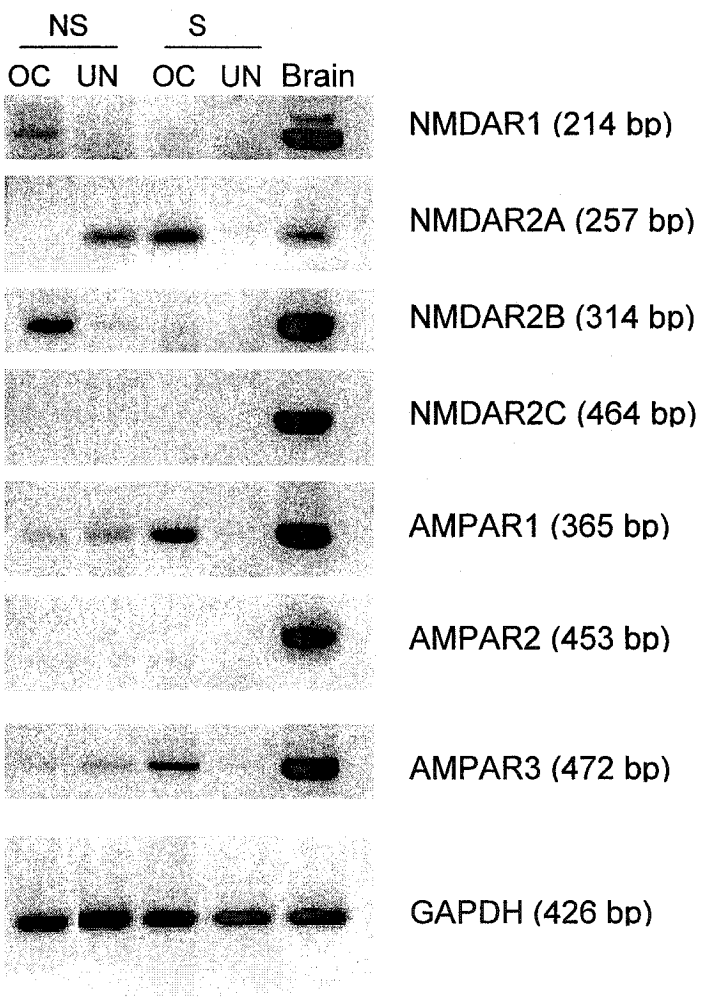

Figure 3.15: RT-PCR: Densitometric analysis of electrophoresed PCR products demonstrates the magnitude of glutamate receptor subunit expression changes when osteoclasts were mechanically stimulated during culture. Photographs of the electrophoresed PCR products (as represented in Figure r15) were normalized against the GAPDH control and the fold change in gene expression determined for mechanically-stimulated osteoclasts relative to non-stimulated osteoclasts. Bars represent the mean +/- SEM of the fold change in glutamate receptor subtype expression observed in six RT-PCR reactions.

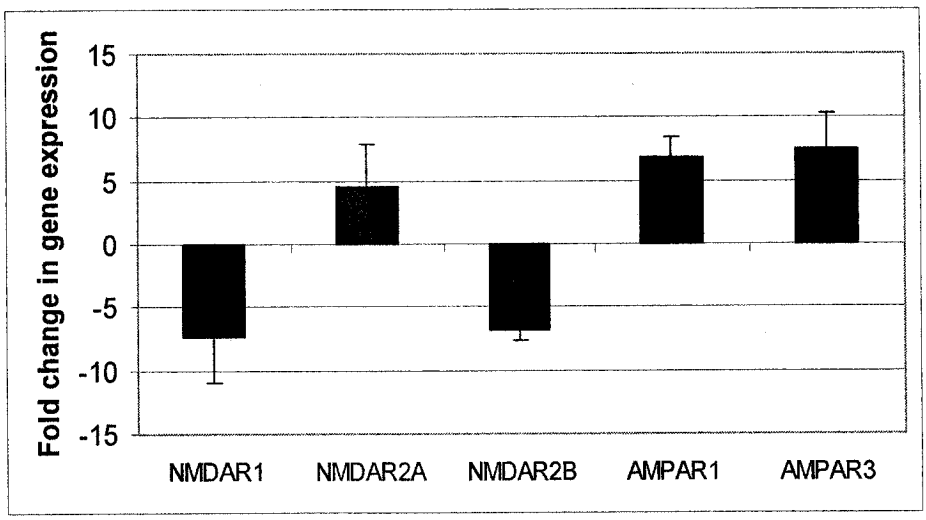

3.8.2 Assessing the effects of estrogen on glutamate receptor subtype expression and mechanosensitivity using RT-PCR

In previous experiments, cells had been cultured in phenol red-containing media. Phenol red is known to bind to estrogen receptors and produce estrogenic effects – therefore it may have provided some level of estrogenic stimulus to the cultured osteoclasts. To assess the effects of estrogen on glutamate receptor subtype expression in osteoclasts, cultures were grown in phenol red-free media and concentrations of 0, 0.0001, 0.001, 0.01, 0.1, or 1.0 μM 17β-estradiol added with media changes. RNA was isolated from osteoclast-enriched fractions of these cultures and RT-PCR performed to examine the effects of estrogen levels on glutamate receptor subtype expression and its sensitivity to mechanical stimulation.

Figure 3.16 shows representative photographs from four independent experiments of the electrophoresed PCR products of amplified glutamate receptor subtype fragments. Increasing concentrations of estrogen appeared to increase NMDAR1 expression in non-stimulated osteoclasts, while NMDAR1 expression decreased to below detectable levels mechanically-stimulated osteoclasts at all concentrations of estrogen. NMDAR2A expression also appeared to increase in non-stimulated osteoclasts with increasing concentrations of estrogen, but an inconsistent effect was noted in mechanically-stimulated osteoclasts where, at varying concentrations, estrogen increased or

decreased NMDAR2A mRNA expression. In these samples, NMDAR2B expression was only detected in the non-stimulated 0.001 μM estrogen and mechanically-stimulated 0.1 μM estrogen samples; the effect of estrogen on the expression of this subunit did not appear to be linear or biphasic as observed for the other receptor subtypes examined. Estrogen appeared to have a biphasic effect on AMPAR1 mRNA expression in non-stimulated osteoclasts with mid-range concentrations of 0.001 μM and 0.01 μM suppressing expression. In the mechanically-stimulated cells, estrogen had the opposite effect on AMPAR1 expression, with the mid-range concentrations of 0.001 μM and 0.01 μM increasing mRNA expression. Finally, AMPAR3 mRNA levels in non-stimulated osteoclasts were increased uniformly with 0.0001 μM to 1.0 μM concentrations of estrogen above the levels observed in the absence of estrogen. In the mechanically-stimulated cells, AMPAR3 mRNA levels were lower than in non-stimulated cells and appeared to decrease substantially with estrogen concentrations of 0.01 μM and greater.

Figure 3.16: Effects of estrogen on glutamate receptor subtype mRNA expression in non-stimulated and mechanically-stimulated cells. RT-PCR was performed on RNA samples prepared from osteoclast-enriched cell fractions grown in non-stimulated or mechanically-stimulated conditions and treated with the doses of 17β-estradiol (E_2) shown below (in molarity). RNA isolated from mouse brain homogenate was used as a positive tissue control and GAPDH was amplified as a reaction control. Pictures shown below are representative of four RT-PCR reactions performed for each glutamate receptor subunit in each of two independent experiments.

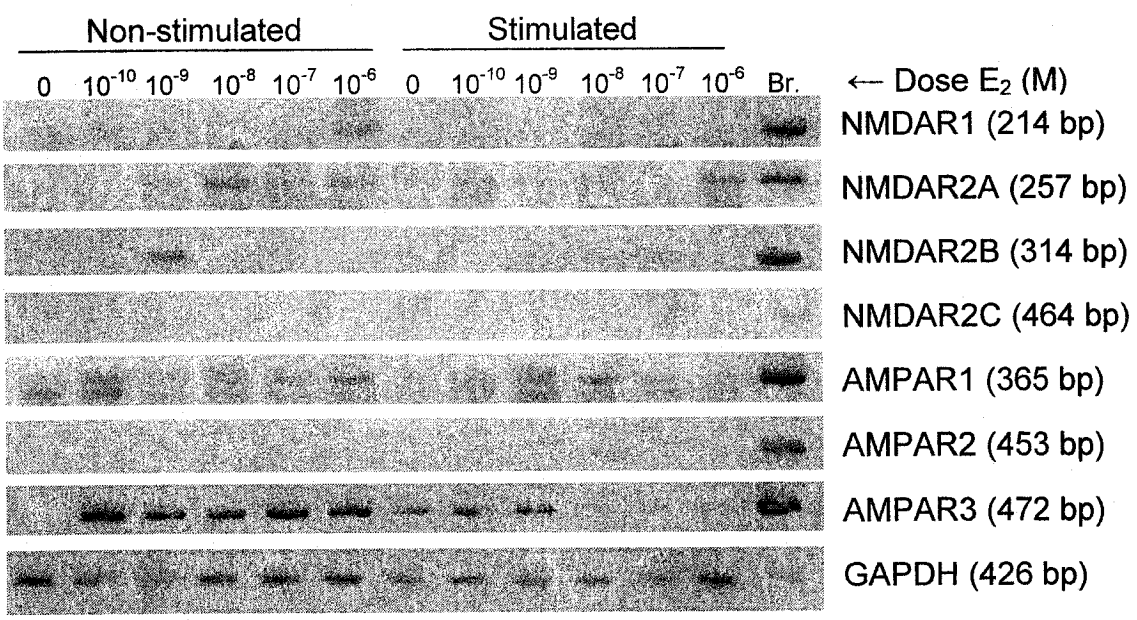

3.9 Northern analysis of the effects of estrogen and mechanical stimulation on osteoclast glutamate receptor subtype expression

RNA samples isolated from osteoclast-enriched and osteoclast-depleted fractions of cells grown with or without estrogen and/or mechanical stimulation were analyzed by northern blotting to confirm the expression of glutamate receptor subtype mRNA in osteoclasts. Figure 3.17A shows pictures of representative blots of the five glutamate receptor subtypes examined: NMDAR1, NMDAR2A, NMDAR2B, AMPAR1, and AMPAR3, along with cyclophilin, which was used as a control. Each blot also contained RNA isolated from mouse brain as a positive control. In all treatment conditions, expression of NMDAR1, NMDAR2B, AMPAR1, and AMPAR3 mRNA was detected. PhosphorImage data from the samples derived from osteoclast-enriched cell fractions were normalized against the cyclophilin control and plotted as a percentage mRNA expression relative to non-stimulated 0 μM estrogen samples for each glutamate receptor subtype examined (Figure 3.17B). Neither estrogen nor mechanical stimulation appeared to have an effect on NMDAR1 or AMPAR3 mRNA expression. Both estrogen and mechanical stimulation appeared to increase mRNA expression of NMDAR2B and AMPAR1, but only the increase noted for NMDAR2B mRNA expression in the presence of estrogen and mechanical stimulation was found to be statistically significant.

Figure 3.17: Northern analysis of glutamate receptor subtype expression responsiveness to mechanical stimulation and estrogen. A: Representative images of northern blots of RNA samples isolated from osteoclast-enriched and osteoclast-depleted fractions of cells that were non-stimulated (NS), non-stimulated + 1 μM estrogen (NSE), mechanically-stimulated (S), and mechanically-stimulated + 1 μM estrogen (SE). A positive control of RNA isolated from mouse brain homogenate was included (Brain). B: Graph of the percentage change in mRNA expression with mechanical stimulation relative to non-stimulated samples for each glutamate receptor subtype examined by northern analysis. Each bar represents the mean +/- SEM of the three blots per receptor subtype that were normalized against a cyclophilin control. * = $p<0.05$.

A

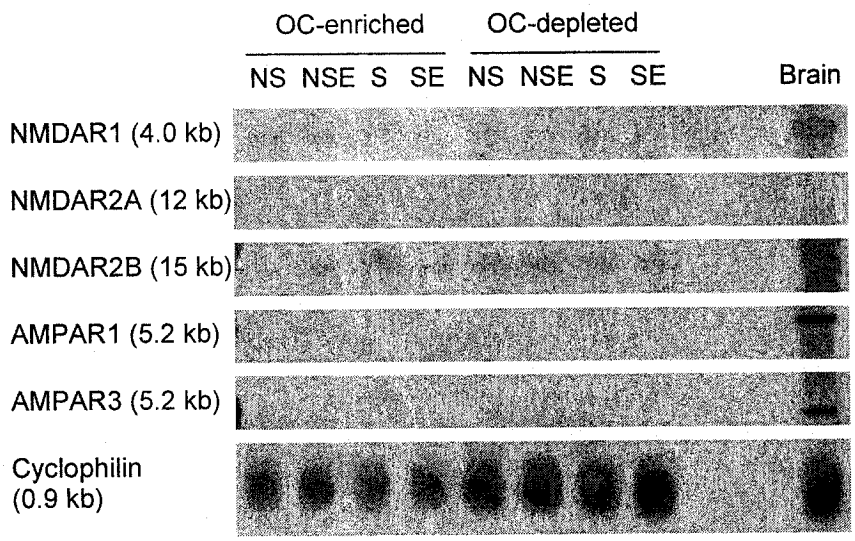

B

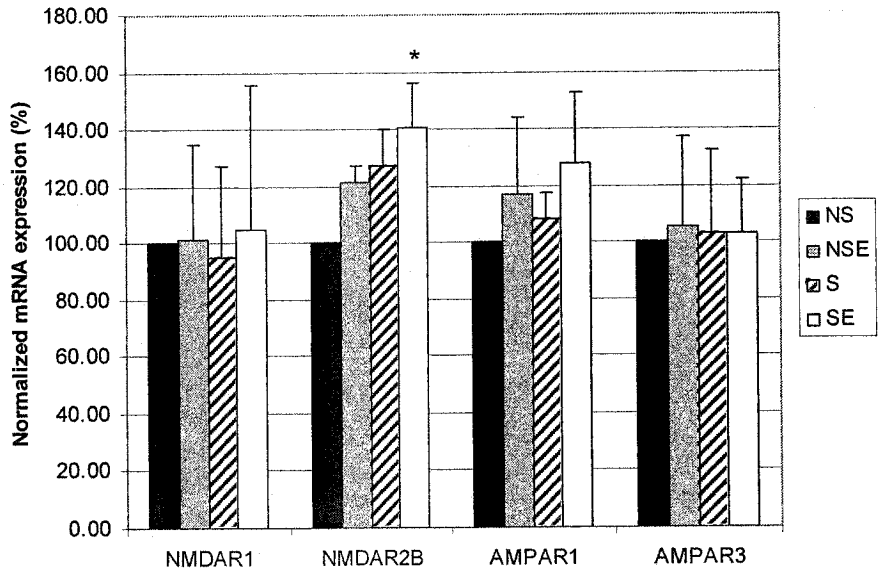

3.10 Analysis of the presence and sensitivity to mechanical stimulation and estrogen of ER-α and PSD95 mRNA using RT-PCR

Since the cellular effects of estrogen are typically mediated through its nuclear hormone receptor, the effects of estrogen and mechanical stimulation on the expression of the estrogen receptor alpha subunit (ER-α) mRNA were examined by RT-PCR of RNA samples derived from three independent experiments. RNA was isolated from osteoclast-enriched fractions derived from cultures that had been non-stimulated or mechanically-stimulated in the presence of 0, 0.0001, 0.001, 0.01, 0.1, and 1 μM 17β-estradiol (Figure 3.18). In non-stimulated osteoclasts, estrogen appears to increase the expression of ER-α in a concentration-dependent manner from 0 to 0.01 μM, but then inhibit its expression at higher concentrations such that no ER-α mRNA was detected at an estrogen concentration of 1.0 μM. In mechanically-stimulated osteoclasts, the effects of estrogen on ER-α mRNA expression were less clear. The highest levels of ER-α mRNA expression were observed in the 0 μM estrogen sample. Decreases of its expression were observed in the 0.001, 0.01, and 0.1 μM doses, but no ER-α mRNA expression was observed in the samples that had been treated with 0.0001 μM estrogen concentrations. Finally, only very low levels of ER-α mRNA expression were observed in samples treated with 1 μM estrogen concentrations. Overall, doses of 0 to 0.01 μM estrogen appear to increase ER-α mRNA expression in a concentration-dependent manner in non-stimulated

osteoclasts, while decreasing ER-α mRNA expression in mechanically-stimulated osteoclasts.

In the brain, the post-synaptic density protein, PSD95, has been shown to be important for NMDA receptor function as it clusters and retains NMDA receptors at the post-synaptic terminus of neurons (171). The effects of estrogen and mechanical stimulation on PSD95 mRNA expression were therefore examined using RT-PCR (Figure 3.18). RNA samples were derived from the same culture treatment conditions as used in the ER-α RT-PCR as outlined above. In non-stimulated osteoclasts, the highest levels of PSD95 expression were observed at estrogen concentrations of 0.0001 to 0.01 μM – the same concentrations for which the highest levels of ER-α expression were observed. In mechanically-stimulated osteoclasts, PSD95 expression was barely detectable, except in the sample that was treated with 0.0001 μM estrogen – the concentration at which ER-α expression was not detected. These results suggest that estrogen concentrations of 0.1 μM and higher inhibit PSD95 expression in non-stimulated osteoclasts, while mechanical stimulation appears to increase the estrogen-induced inhibition of PSD-95 expression in osteoclasts such that estrogen concentrations as low as 0.001 μM will inhibit PSD95 expression.

Figure 3.18: The effects of estrogen and mechanical stimulation on mRNA expression of estrogen receptor alpha (ER-α) and PSD95 genes. Amplification of the desired mRNA fragments was carried out on RNA samples prepared from osteoclast-enriched cell fractions grown in non-stimulated (NS) or mechanically-stimulated (S) conditions and treated with the doses of 17β-estradiol shown below (in molarity). RNA isolated from mouse brain homogenate (Br) was used as a positive tissue control and GAPDH was amplified as a reaction control. Pictures shown below are representative of three RT-PCR reactions performed per gene in each of two independent experiments.

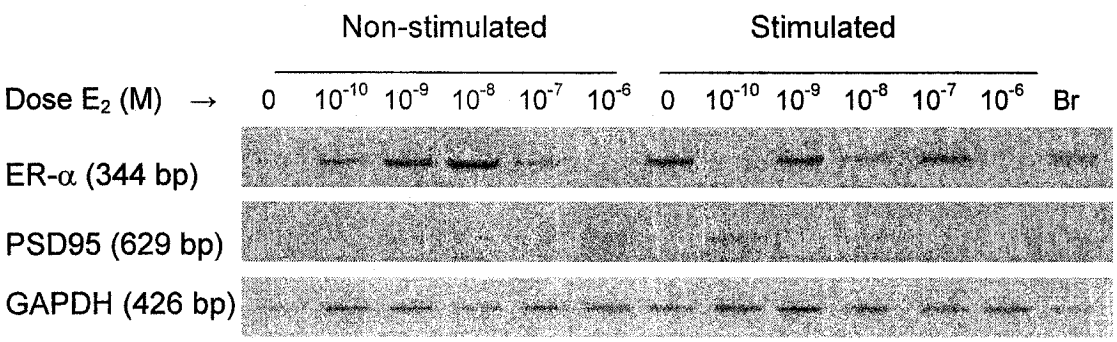

Chapter 4: Discussion

4.1 Validation of our osteoclast culture model: agonist and antagonist studies

Osteoclasts used for *in vitro* research are often derived from the established macrophage/monocyte cell line, RAW 264.7. The advantage of this approach is that the entire population of cultured cells can be differentiated to generate a uniform population of osteoclasts, many of which are multinucleated, therefore facilitating downstream molecular analyses. For the assessment of glutamate receptor subtype expression, osteoclast cell lines are not ideal since they often do not express the same receptor subtypes as those expressed by osteoclasts *in vivo* (154). For this reason, a primary culture system in which osteoclasts were differentiated from hematopoietic progenitor cells derived from mouse bone marrow was chosen. This culture system contained cells of both the hematopoietic (osteoclast) and mesenchymal (osteoblast, fibroblast, stromal cell) lineages, since osteoclasts depend on intercellular signals from osteoblasts/osteocytes to survive, differentiate, and function (33). There is recent evidence that supplementing the culture medium with M-CSF and RANKL will support osteoclast differentiation in the absence of osteoblast-lineage cells, and some groups now choose this route to obtain mature multinucleated osteoclasts (172-174). However, we chose a mixed culture system so that the diversity of cell types and differentiation stages present *in vivo* could be approximated in an *in vitro* environment. The cultures were grown under

conditions which favour osteoclast differentiation (20% fetal bovine serum, 10^{-8} M vitamin D_3). Cultures were harvested after 8 days, which is sufficient time to produce mature multinucleated osteoclasts, but short enough in duration that the osteoclasts possessed glutamate receptor expression profiles similar to those found *in vivo* (64). Finally, enriched populations of mature multinucleated osteoclasts were obtained from the mixed cultures for molecular analyses using the immunomagnetic bead isolation method outlined in section 2.7.

To assess whether our mixed cultures were an appropriate model for examining glutamate receptor subtype expression, we first needed to confirm that these cultures exhibited a phenotypic response to glutamate receptor agonists or antagonists. Observation of the effects of modulating glutamate signalling on the differentiation and bone resorptive ability of cultured osteoclasts allows the presence of functional glutamate receptors to be inferred and also shed some light on what role these receptors may play in osteoclasts.

Previously, our group and others have shown that NMDA receptor antagonists inhibit osteoclast function (138,158,175) and osteoclast differentiation (152,175). In the mixed cultures, 50 or 100 μM concentrations of the NMDA receptor antagonist MK801 reduced osteoclastic bone resorption (function) to approximately one-third of control levels (Figure 3.4A); as had been previously observed (138,175). MK801 concentrations of 10-100 μM inhibited osteoclast differentiation in the mixed cultures in a concentration-dependent manner (Figure

3.3A), an effect which had previously only been observed by ourselves and one other group (152,175). We have also shown that the AMPA receptor antagonist, NBQX, inhibited osteoclast differentiation and bone resorptive ability in the same concentration range as MK801 (Figures 3.3B and 3.4B). These results strongly suggest that the mature multinucleated osteoclasts in our mixed cultures expressed functional ionotropic glutamate receptors of both the NMDA and AMPA varieties and that these receptors play a role both in the differentiation and function of osteoclasts.

4.2 Identification of glutamate receptors on murine osteoclasts grown in mixed primary cultures

Since the culture system used to derive mature multinucleated osteoclasts for these experiments was somewhat different than those described by others, we needed to compare the glutamate receptor subtypes expressed in our osteoclast system with previously published results. Using immunocytochemistry, we identified the expression of NMDA receptor subunits 1, 2A, 2B, and 2C on osteoclasts cultured in our system. With the exception of NMDAR2C, these subunits have been previously found to be expressed by osteoclasts *in vitro* (138,141,152); additionally, the NMDAR1 subunit was previously identified *in vivo* (138). The AMPA receptor subunits 1, 2/3, and 4 were also expressed by osteoclasts; subunits 2/3 and 4 had been identified previously in our laboratory

through *in vivo* experiments (64), but AMPA receptor expression had not been identified previously in cultured osteoclasts (154). Finally, we found that osteoclasts expressed two group I metabotropic glutamate receptors, mGluR1α and mGluR5: other groups had not observed these receptors on osteoclasts (154,175).

During the initial characterization of our model system, we determined that a variety of glutamate receptor subtypes were expressed by osteoclasts when mixed cultures were immunostained. The presence of these receptors showed that our method of culturing osteoclasts produced cells with glutamate receptor subtype expression profiles similar to those observed previously *in vitro* and *in vivo* for several rodent species (64,138,141,143,152,175). Using the immunomagnetic bead-based method described in section 3.6, we produced osteoclast-enriched cell fractions from murine marrow-derived mixed cultures. RNA and protein were isolated from these osteoclast-enriched cell fractions for glutamate receptor subtype expression analysis. RT-PCR observations of high levels of TRAP1C expression and low levels of OCN expression indicated that the fractions consisted of many mature osteoclasts and few mature osteoblasts. Thus, osteoclasts contributed the majority of the molecular signal in these cell fractions.

When osteoclast-enriched cell fractions were examined by western blot analysis for glutamate receptor protein expression and by RT-PCR and northern analysis

for glutamate receptor mRNA expression, the initial immunocytochemical results were in most, but not all, cases confirmed. In particular, we used molecular analyses to examine the expression of the ionotropic receptor subunits. Western blot analysis showed that osteoclasts expressed NMDAR1, NMDAR2A, NMDAR2B, and AMPAR1 protein, but not NMDAR2C protein (Figure 3.13). Analysis of the mRNA expression of the glutamate receptor subunits by RT-PCR showed that NMDAR1, NMDAR2A, NMDAR2B, AMPAR1, and AMPAR3 mRNAs were expressed, but mRNA for NMDAR2C and AMPAR2 were not detected (Figure 3.14). Finally, northern analysis to confirm the RT-PCR data showed that mRNA for NMDAR1, NMDAR2B, AMPAR1, and AMPAR3 was expressed by osteoclasts, but mRNA for NMDAR2A was not detected (Figure 3.17). These are the first data to demonstrate glutamate receptor subtype mRNA expression in bone by northern analysis. In summary, our experiments show that both protein and mRNA for the NMDAR1, NMDAR2B, AMPAR1 and AMPAR3 subunits are expressed, that the NMDAR2A protein may be expressed, and that NMDAR2C and AMPAR2 were not detected. The expression of AMPA receptor subunits 1 and 3 on our osteoclasts is a novel finding and may represent a part of the glutamate signalling pathway previously overlooked in osteoclasts.

4.3 Association of glutamate receptors with actin and vinculin

We also wished to assess whether the glutamate receptor subunits we identified on osteoclasts colocalized with the cytoskeletal elements, actin and vinculin. Both actin and vinculin are important elements of the sealing zone formed when osteoclasts are actively resorbing bone; an actin ring surrounded by podosomal proteins forms to isolate the ruffled border membrane from the basal membrane and extracellular fluid (41). Association of glutamate receptors with actin and vinculin would place them at the cell surface that is in contact with the bone matrix; this would allow osteoclasts to receive glutamate signals from osteocytes buried within the bone matrix, and place glutamate receptors at the cell surface where mechanical stimulation is being sensed. Included in the podosomal proteins are integrins such as αVβ3 (vitronectin receptor) and the cytosolic adaptor proteins (vinculin, talin, etc.) that connect the integrins to the cytoskeleton. When osteoclasts cultured on glass coverslips were examined for glutamate receptor and cytoskeleton colocalization, NMDAR1 and NMDAR2B, but not AMPAR1, were found to colocalize with actin and vinculin (Figures 3.9-3.11). It is particularly interesting that the NMDA receptor subunits colocalized with actin and vinculin in the vicinity of the sealing zone. Localization on the surface of the cell, where the plasma membrane is in contact with bone places these receptors in an ideal location to sense mechanical stimulation, and raises the possibility that receptor activation may be regulated by interaction with focal adhesion proteins and/or integrins.

One possible means by which integrins may regulate osteoclast function is via the non-receptor tyrosine kinase c-Src. It has been recently shown in osteoclasts that, similar to endothelial cells, mechanical stimulation perceived by αVβ3 integrins activates RhoA, which in turn increases the activity of c-Src, a tyrosine kinase that can regulate receptors through phosphorylation (122,176,177). Within the integrin-rich podosomes, integrin activation also induces binding of c-Src to Pyk2 and Cbl; this complex allows c-Src to phosphorylate Pyk2 and Cbl, thus propagating the integrin signal to cause cell spreading, motility, and in the case of osteoclasts, sealing zone formation (Figure 4.1A) (176,177). Activity of c-Src has been shown to be essential to osteoclastic bone resorption, probably by inducing sealing zone formation, and possibly by limiting osteoclast apoptosis (176,177). The exact mechanism by which integrin-mediated c-Src activation induces osteoclast sealing zone formation is not known.

Interestingly, studies of mammalian central neurons have shown that NMDA receptors are also associated with c-Src and that c-Src-mediated tyrosine phosphorylation of these receptors increases the duration of channel opening in response to glutamate, therefore increasing cellular responses (Figure 4.1B) (178). NMDA receptors on osteoclasts were colocalized by confocal microscopy with the integrin adaptor protein vinculin, thus we speculate that the c-Src/Pyk2/Cbl complex is also in close proximity to these receptors. It is therefore possible that integrin-mediated responses to mechanical stimulation could

activate Src and allow it to phosphorylate local NMDA receptors, hence providing a transient and immediate mechanism to modulate the activity of these receptors in response to mechanical stimulation (Figure 4.1C). We expect that the cellular effect of moderately increasing calcium entry via NMDA receptors into osteoclasts would be to increase osteoclast function and differentiation based on the observed effects of the NMDA receptor antagonist MK801. MK801 decreased osteoclast function and differentiation in our cultures, and Itzstein et al have shown that MK801 inhibited the formation of actin rings in osteoclasts (158). Thus, mechanical stimulation could activate c-Src through an integrin-mediated pathway, allowing increased activity of local NMDA receptors by phosphorylation and therefore augment the increases in osteoclast function and/or differentiation produced by integrin signalling, resulting in increased bone remodelling (Figure 4.1C).

Repeated exposure to mechanical stimulation results in genomic effects; NMDAR1 expression appeared to decrease, which would result in fewer functional NMDA receptor channels being expressed (discussed in greater detail in section 4.5). Mechanical stimulation could increase the function of existing NMDA receptors through phosphorylation by c-Src, but the magnitude of the effect on osteoclast function and differentiation would be lower because of the decreased number of NMDA receptor channels (Figure 4.1D). To summarize, integrin-mediated c-Src activation in response to mechanical stimulation may transiently increase osteoclast activity and differentiation through NMDA receptor

modulation so as to "kick-start" bone remodelling, but the decreased number of NMDA receptor channels observed under chronic mechanical stimulation conditions would limit this effect and therefore keep osteoclast activity in check during periods of mechanical loading at the upper end of physiological levels where resorption would be inappropriate.

Figure 4.1: Proposed mechanism by which osteoclast NMDA receptor function is regulated in response to mechanical stimulation via integrin-mediated activation of c-Src.

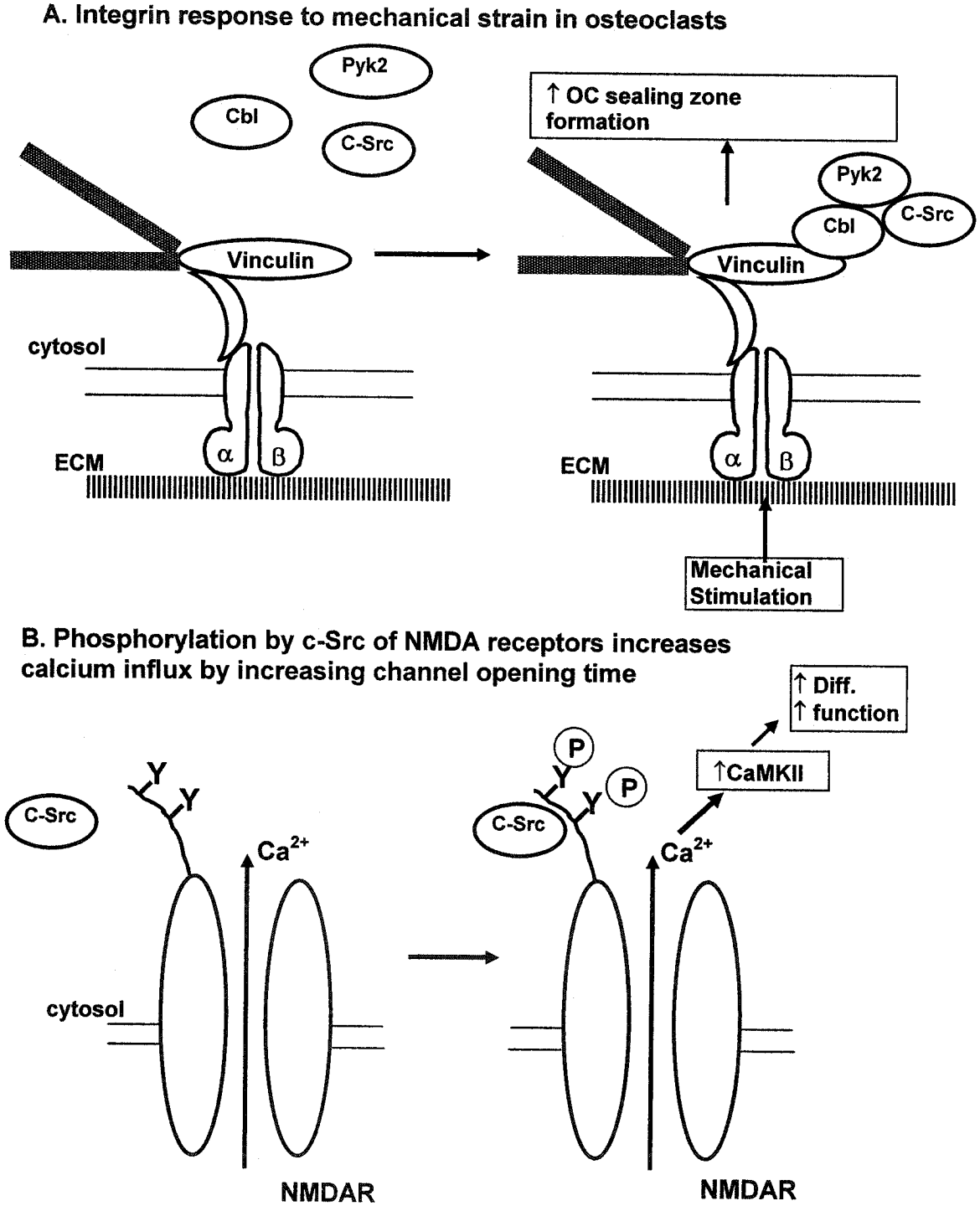

Figure 4.1 (continued): Proposed mechanism by which osteoclast NMDA receptor function is regulated in response to mechanical stimulation via integrin-mediated activation of c-Src.

C. c-Src activated by integrin responses to mechanical stimulation may modulate NMDA receptor function

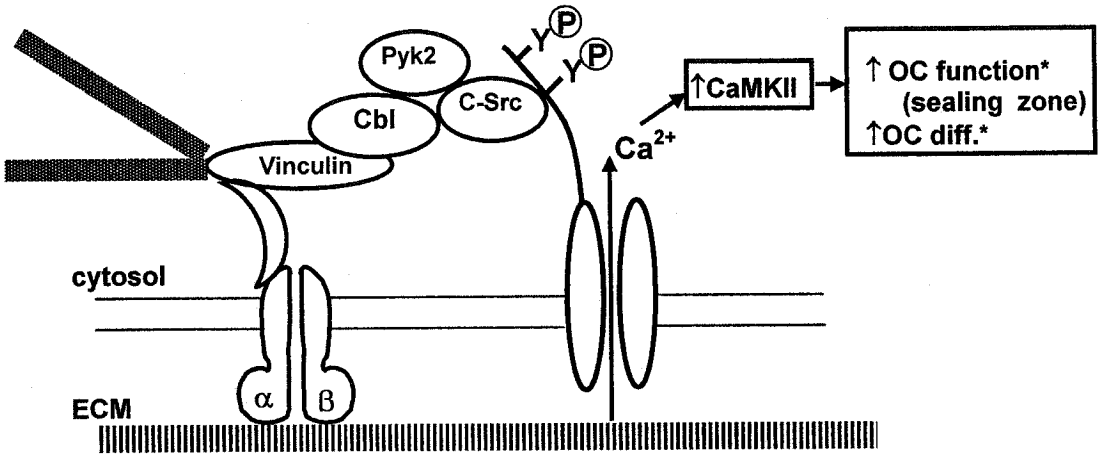

*Transient immediate response to Mech. Stimulation;
↑ OC activity and ↑ remodelling

D. Long term (genomic) effects of mechanical stimulation diminish the effect of integrin-mediated Src activation on osteoclasts

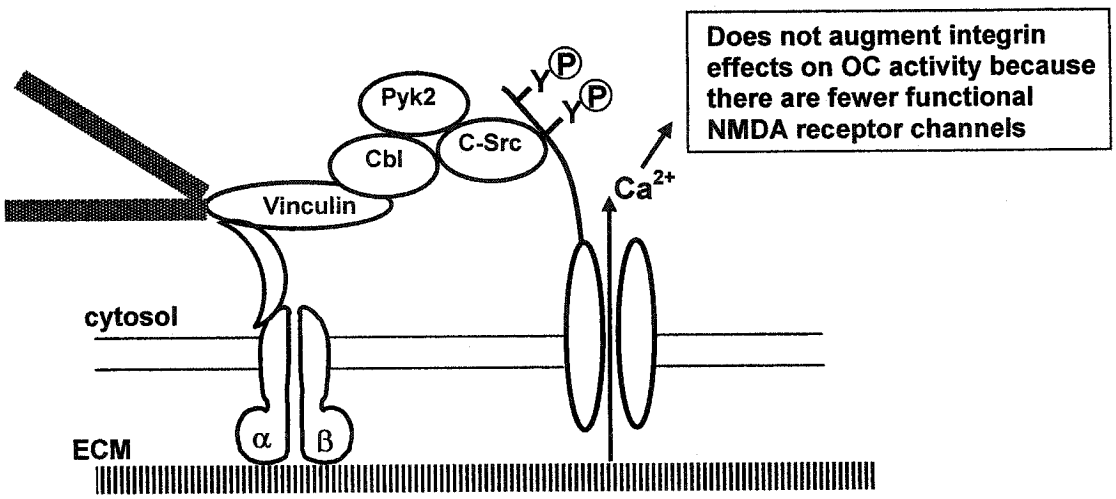

4.4 Glutamate receptor subtype expression profiles change in response to mechanical stimulation

Mechanical stimulation is known to be a major driving force for bone remodelling that leads to increased bone density and therefore decreased fracture risk. The expression of components of the glutamate signalling pathway (transporters, receptors, exocytosis machinery) have been shown to change in response to mechanical stimulation in bone cells (144,145). We demonstrated previously that mechanical stimulation appeared to decrease the expression of most of the glutamate receptor subtypes expressed on osteoclasts *in vivo* (64). In this project, we used RT-PCR and northern analysis along with immunocytochemistry to assess changes in osteoclast glutamate receptor subtype mRNA and protein expression induced by mechanical stimulation.

Using RT-PCR to assess the effects of mechanical stimulation on glutamate receptor subtype mRNA expression, we observed that mechanical stimulation decreased the expression of NMDAR1 and NMDAR2B, and increased mRNA expression of NMDAR2A, AMPAR1, and AMPAR3 (Figures 3.14 and 3.15). Northern analyses, however, showed somewhat different changes in glutamate receptor subtype expression: no statistically significant mechanical stimulation-induced changes in mRNA expression were observed for NMDAR1, NMDAR2B, AMPAR1, or AMPAR3, and NMDAR2A was not detected (Figure 3.17). The differences between RT-PCR and northern analysis are most likely due to RT-

PCR being a more sensitive method; if more repetitions of the northern analyses were performed, possibly using larger quantities of RNA, the results might more closely resemble those of the RT-PCR. Indeed, non-significant changes to glutamate receptor subtype mRNA expression, corroborating the observations of RT-PCR, were observed for NMDAR1 (decrease), and AMPAR1 and AMPAR3 (increases). The northern analysis of NMDAR2B mRNA showed a non-significant trend toward an increase in expression with mechanical stimulation while RT-PCR showed a decrease.

Western blot analyses showed that our osteoclasts expressed NMDAR1, NMDAR2A, NMDAR2B, and AMPAR1 proteins (AMPAR3 expression was not assessed, Figure 3.13). Unfortunately, the low abundance of the glutamate receptor subunits in osteoclast protein preparations produced faint signals and thus the assessment of receptor expression changes caused by mechanical stimulation was not considered feasible. The immunocytochemical experiments showed that protein expression of NMDAR1 and NMDAR2A appeared to decrease with mechanical stimulation and NMDAR2B expression did not change, while expression of the AMPA receptor subunits appeared to decrease only slightly, if at all (Table 3.1).

Both mRNA and protein studies suggest that mechanical stimulation decreases the number of functional NMDA receptors expressed at the cell surface (increases to NMDAR2B mRNA expression have little functional effect since

NMDAR1 is required to produce a functional ion channel). AMPA receptor expression, however, was observed to decrease or not change at the protein level, while increases were observed at the mRNA level. Since mRNA expression changes occur prior to protein expression changes, perhaps the effect on AMPA receptor expression caused by mechanical stimulation is delayed relative to the effect on NMDA receptor expression. It is, however, possible that increases to AMPA receptor expression were underway when cultures were harvested. Thus, experiments with endpoints later than those described in these experiments may reveal protein alterations consistent with the mRNA data.

The actions of NMDA appear to be mediated through calmodulin, calmodulin-dependent protein kinase II (CaMKII), and mitogen-activated protein kinase (MAPK) (127). The role of calmodulin is a feedback mechanism that is responsible for the calcium-dependent inactivation of NMDA receptors. For optimal function in the CNS, NMDA receptors are clustered together in post-synaptic densities with linkages to the actin cytoskeleton, mediated by molecules such as PSD-95 and α-actinin (127). When intracellular calcium levels are high, calmodulin binds to the NMDAR1 subunit and weakens its association with α-actinin, disrupting the NMDA receptor clusters and thus decreasing calcium influx (179,180). CaMKII appears to be closely associated with the NMDAR2B subunit: one of the roles of activated CaMKII is to phosphorylate AMPA receptors and thus increase the intracellular effects of glutamate (181). Calcium entry caused

by NMDA receptor activation has been shown to activate MAPK through a Ras-mediated pathway, although the exact mechanism is not known (182). Mechanical stimulation of osteoclasts decreased the expression of NMDA receptor channels, thus presumably decreasing intracellular signals mediated by CaMKII.

The action of glutamate on AMPA receptors causes the influx of Na^+, K^+ and Ca^{2+} into osteoclasts. AMPA receptors in the CNS exist in complex rafts of signalling molecules. At such sites, they have been shown to be associated with adaptor proteins such as GRIP (glutamate receptor interacting protein) and AKAP (A-kinase anchoring protein), and signalling molecules such as protein kinases A and C and G-protein Gαi subunits. It is possible, but not known, whether these molecules elicit downstream signals in response to AMPA receptor activity. Although the mechanism is not completely understood, calcium influx through AMPA receptors has been shown to activate MAPK, likely through a Raf kinase/MEK1 pathway (183), and this is thought to represent the chief intracellular signal of AMPA receptors. Mechanical stimulation of osteoclasts does not appear to have changed AMPA receptor protein expression, but the mRNA expression increases observed may lead to an increase in protein expression and therefore increase AMPA receptor-induced MAPK signalling pathways.

Even if mechanical stimulation did not alter AMPA receptor expression, by decreasing NMDA receptor expression the balance of signalling between the pathways mediated by these receptors would be shifted. Although their intracellular signalling mechanisms are not completely understood, it is clear that NMDA and AMPA receptors elicit their actions through different pathways. Under conditions of low or no mechanical stimulation, osteoclast glutamate signalling is mediated by a balance of NMDA and AMPA receptors. When osteoclasts are mechanically-stimulated, the signalling through AMPA receptors (MAPK) would play an increased role due to the decreased signalling via NMDA receptors (CaMKII). This shift from NMDA- to AMPA-mediated pathways may be vital to osteoclast responses to repeated mechanical stimulation, the endpoint of which is decreased osteoclast activity and differentiation.

4.5 The effects of estrogen on the mechanosensitivity of glutamate receptor subtype expression

We assessed the effects of estrogen on osteoclast differentiation and bone resorptive ability in our cultures by administering concentrations of 17β-estradiol ranging from 0.0001 μM to 1 μM during media changes. The upper range of concentrations is certainly higher than physiological estrogen levels, but administration of drugs *in vitro* likely does not resemble the same pulsatile regimen that occurs *in vivo*. Furthermore, the sustained levels of estrogen may

be lower than the actual doses due to metabolism by the cultures. Estrogen increased osteoclast differentiation at the lowest concentration tested of 0.0001 μM when compared with estrogen-free control cultures, suggesting that some level of estrogen is required for osteoclast function (Figure 3.6). At estrogen concentrations of 0.01 μM and higher, osteoclast differentiation was decreased to below control levels (Figure 3.6), representing the typical effect of estrogen on osteoclasts. When we examined the effects of estrogen on osteoclastic bone resorption, however, no statistically significant changes were noted for the range of 17β-estradiol concentrations tested (Figure 3.7). This was surprising as inhibition of osteoclast function by estrogen was anticipated. Finally, we demonstrated by RT-PCR that estrogen receptor ERα mRNA was expressed in our osteoclasts and that its expression was highest in cultures given concentrations of 17β-estradiol ranging from 0.001μM to 0.1 μM (Figure 3.18). The presence of the ERα receptor in our cultured osteoclasts demonstrates that these osteoclasts possess the means by which direct estrogen effects can occur in addition to indirect effects through local mediators secreted by osteoblasts.

In the brain, estrogen has been shown to impact upon glutamate signalling to produce increases in long-term potentiation (184). Studies showed that ovariectomy in rats produced decreases in the expression of NMDA receptor subunits NMDAR1 and NMDAR2B in the hippocampus, where much of long-term potentiation (memory) is mediated, while having no effect on AMPA receptor expression (184). Administration of 17β-estradiol to these animals, however,

returned NMDA receptor levels in the hippocampus to those of hormonally-intact animals and decreased AMPA receptor levels in both the frontal cortex and the nucleus accumbens (184). The direct mechanism of estrogen effects on glutamate receptor expression is not known, but NMDA receptors do possess SP1 sites in their promoter regions (185,186) which could be activated by binding of estrogen receptors with other coactivators (187) to elicit the observed increases in NMDA receptor expression with estrogen administration.

Knowing that estrogen changes glutamate receptor subtype expression in the brain, we looked for similar changes in osteoclasts using RT-PCR (Figure 3.16) and northern analysis (Figure 3.17). In non-stimulated osteoclasts, estrogen appeared to increase the mRNA expression of the NMDA receptor subunits 1, 2A, and 2B; such increases could produce increased NMDA receptor activity and therefore increased osteoclast differentiation and function. In mechanically-stimulated osteoclasts, estrogen appeared to have little effect on NMDAR1 mRNA expression (which was reduced to low levels compared to non-stimulated osteoclasts), had a non-concentration-dependent effect on NMDAR2A mRNA expression, and appeared to increase NMDAR2B mRNA expression. Estrogen appears to have very different effects on osteoclast NMDA receptor subtype expression, depending on whether or not cultures were mechanically-stimulated. The estrogen-induced increases in expression of NMDAR1 and NMDAR2A mRNA observed in non-stimulated osteoclasts were abrogated by mechanical stimulation; their expression appeared to be reduced by mechanical stimulation,

and estrogen no longer produced the concentration-dependent increases observed in the absence of mechanical stimulation. The estrogen-mediated increase in NMDAR2B mRNA expression observed in non-stimulated cultures appeared to be augmented in the presence of mechanical stimulation. However, mechanical stimulation decreased mRNA expression of the required NMDAR1 subunit and thus likely the number of functional NMDA channels would be fewer in mechanically-stimulated osteoclasts. It is unlikely that estrogen modulation of expression of the other NMDA receptor subunits would have appreciable functional effects in the presence of mechanical stimulation.

The effect of estrogen on AMPA receptor mRNA expression was quite different from the effects observed on NMDA receptor mRNA expression. In non-stimulated osteoclasts, estrogen appeared to produce a biphasic effect on AMPAR1 expression, where its expression was greatest at the extremes of the estrogen concentration range but decreased at the mid-range concentrations of 0.001 μM to 0.1 μM. In contrast, when mechanically-stimulated osteoclasts were examined, the biphasic effect of estrogen on AMPAR1 expression was reversed, with AMPAR1 expression being lowest at the extremes of the estrogen concentration range but elevated at mid-range concentrations of 0.0001 μM to 0.01 μM. In non-stimulated osteoclasts, AMPAR3 mRNA was expressed at high levels throughout the estrogen concentration range, but only at very low levels in the estrogen-free sample, suggesting that at least low levels of estrogen are required for AMPAR3 expression. Mechanical stimulation did not alter osteoclast

mRNA expression of AMPAR3, but estrogen concentrations of 0.01 μM and greater decreased AMPAR3 expression in the presence of mechanical stimulation.

From the clear differences in the effects of estrogen and mechanical stimulation on osteoclast NMDA and AMPA receptor expression, it is obvious that the intracellular pathways mediated by these receptors have different, and possibly opposing, effects on osteoclast differentiation and function. In the absence of mechanical stimulation, increases in NMDA receptor subtype expression would likely result in increased osteoclast differentiation and function. These increased NMDA receptor levels may be why osteoclast activity can be disinhibited under conditions of low mechanical strain (sedentary lifestyle, space flight) even in hormonally-intact individuals, leading to decreased bone density. The decrease in NMDAR1 expression caused by upper-end physiological mechanical stimulation would serve to limit osteoclast activity and differentiation. It is interesting to note that estrogen did not alter NMDAR1 expression in the presence of mechanical stimulation; this implies that when appropriate levels of mechanical stimulation are present, estrogen-mediated pathways become less important to the control of osteoclast differentiation and function. Finally, the mRNA expression of the AMPA receptor subunits was sensitive to estrogen levels both in the presence and absence of mechanical stimulation; an effect not observed with the NMDA receptors. The AMPA receptor expression profiles we observed demonstrated that the both the extent of AMPA receptor-mediated

signalling and the ratio of AMPAR1 versus AMPAR3 subtype expression were dependent on both mechanical stimulation and estrogen level.

4.6 Conclusions

The evidence these experiments provide about the expression of glutamate receptor subunits on osteoclasts demonstrates that glutamate signalling is an important pathway by which mechanical stimulation and hormonal levels can be sensed by osteoclasts. The body of evidence supporting the importance of glutamate signalling in bone is growing. All the necessary components of the glutamate signalling machinery as it is known in the CNS have been identified in bone cells, and modulation of glutamate signalling pathways have been shown to produce phenotypic effects (64,138,141-145,175). We demonstrated that osteoclasts grown in our murine marrow-derived mixed culture system express functional glutamate receptors of both NMDA and AMPA subgroups and thus are active participants in glutamate signalling pathways.

We hypothesize that the expression and activity of glutamate receptors on osteoclasts is regulated by mechanical stimulation and represents a way in which osteoclasts can modulate their intracellular responses to incoming glutamate signals from osteoblasts and/or osteocytes. Glutamate signalling in bone involves the release, via regulated exocytosis, of glutamate from osteoblasts

and/or osteocytes, which then binds to glutamate receptors on other osteoblasts and osteocytes as well as osteoclasts to elicit intracellular signals that produce phenotypic effects.

We colocalized NMDA receptors with the integrin adaptor protein vinculin, which suggests that some of these receptors are located on the plasma membrane in contact with bone matrix, where they would be in prime position to sense mechanical strain and receive glutamate signals from osteocytes. The close association of NMDA receptors with integrin signalling complexes also suggests that the integrin-mediated activation of the tyrosine phosphatase c-Src in response to mechanical stimulation may be able to increase NMDA channel function by phosphorylation and therefore transiently increase osteoclast activity as a means of initiating bone turnover under conditions of low mechanical stimulation.

When osteoclasts were mechanically stimulated, we observed that NMDA receptor expression decreased and AMPA receptor expression increased. We speculate that this shift from NMDA to AMPA receptor-mediated intracellular signalling forms part of the mechanism by which osteoclast function and differentiation are inhibited by repeated cyclic application of mechanical stimulation. The effects of estrogen on osteoclast glutamate receptor subtype expression further pointed out that NMDA and AMPA receptor-mediated pathways must elicit different phenotypic effects in osteoclasts. NMDA receptor

expression was responsive to estrogen only in the absence of mechanical stimulation, while AMPA receptor expression responded to estrogen both in the presence and absence of mechanical stimulation.

Glutamate signalling pathways within bone are speculated to be involved in the mediation of mechanical stimulation. Here, we have presented evidence that mechanical stimulation and estrogen levels modulate glutamate receptor subtype expression and thus affect the glutamate-mediated intracellular signalling pathways elicited in these cells. Understanding the mechanisms by which mechanical stimulation and estrogen affect glutamate signalling in bone will provide a more complete picture of how the pathways that control bone remodelling might be manipulated in the absence of normal influences, be they mechanical (sedentary lifestyle, bed rest, space flight) or hormonal (menopause), to provide therapeutic targets to achieve the restoration of normal bone balance.

References

1. The Arthritis Society of Canada website, 2003. http://www.arthritis.ca

2. Rubin C, Lanyon L 1985 Regulation of bone mass by mechanical strain magnitude. Calcified Tissue International **37:**411-417.

3. Rubin C, Lanyon L 1987 Osteoregulatory nature of mechanical stimuli - function as a determinant for adaptive remodelling in bone. Journal of Orthopaedic Research **5:**300-310.

4. Pead M, Skerry TM, Lanyon L 1988 Direct transformation from quiescence to bone formation in the adult periosteum following a single period of bone loading. Journal of Bone and Mineral Research **3:**647-656.

5. Lee K, Lanyon L 2004 Mechanical loading influences bone mass through estrogen receptor alpha. Exercise and Sport Sciences Reviews **32:**64-68.

6. Kerr D, Morton A, Dick I, Prince R 1996 Exercise effects on bone mass in postmenopausal women are site specific and load-dependent. Journal of Bone and Mineral Research **11:**218-225.

7. Hynes R 1987 Integrins: a family of cell surface receptors. Cell **48:**549-554.

8. Hynes R 1992 Integrins: versatility, modulation, and signaling in cell adhesion. Cell **69:**11-25.

9. Ruoslahti E, Pierschbacher M 1987 New perspectives in cell adhesion: RGD and integrins. Science **238:**491-497.

10. Marks S, Hermey D 1996 The structure and development of bone. In: Bilezikian J, Raisz L, Rodan G (eds.) Principles of Bone Biology. Academic Press Inc., San Diego. p. 3-14.

11. Marks S, Popoff S 1988 Bone cell biology: the regulation of development, structure, and function in the skeleton. American Journal of Anatomy **183:**1-44.

12. Serre C, Farley D, Delmas P, Chenu C 1999 Evidence for a dense and intimate innervation of the bone tissue, including glutamate-containing fibers. Bone **25:**623-629.

13. Imai S, Matsusue Y 2002 Neuronal regulation of bone metabolism and anabolism: calcitonin gene-related peptide-, substance P-, and tyrosine

hydroxlyase-containing nerves and the bone. Microcsopy Research and Technique **58:**61-69.

14. Irie K, Hara-Irie F, Ozawa H, Yajima T 2002 Calcitonin gene-related peptide (CGRP)-containing nerve fibers in bone tissue and their involvement in bone remodeling. Microcsopy Research and Technique **58:**85-90.

15. Goto T, Tanaka T 2002 Tachykinins and tachykinin receptors in bone. Microscopy Research and Technique **58:**91-97.

16. Lundberg P, Lerner UH 2002 Expression and regulatory role of receptors for vasoactive intestinal peptide in bone cells. Microscopy Research and Technique **58:**98-103.

17. Togari A 2002 Adrenergic regulation of bone metabolism: possible involvement of sympathetic innervation of osteoblastic and osteoclastic cells. Microscopy Research and Technique **58:**77-84.

18. Chenu C 2002 Glutamatergic innvervation in bone. Microscopy Research and Technique **58:**70-76.

19. Owen M 1980 The origin of bone cells in the postnatal organism. Arthritis and Rheumatism **23:**1073-1078.

20. Otto F, Thornell A, Crompton T, Denzel A, Gilmour K, Rosewell I, Stamp G, Beddington R, Mundlos S, Olsen B, Selby P, Owen M 1997 Cbfa1, a candidate gene for cleidocranial dysplasia syndrome, is essential for osteoblast differentiation and bone development. Cell **89:**765-771.

21. Komori T, Yagi H, Nomura S, Yamaguchi A, Sasaki T, Deguchi K, Shimizu Y, Bronson H, Gao R, Inada M, Sato M, Okamoto R, Kitamura Y, Yoshiki S, Kishimoto T 1998 Targeted disruption of Cbfa1 results in a complete lack of bone formation owing to maturational arrest of osteoblasts. Cell **89:**755-764.

22. Compston JE 2001 Sex steriods and bone. Physiological Reviews **81:**419-447.

23. Cameron D 1968 The Golgi apparatus in bone and cartilage cells. Clinical Orthopaedics **58:**191-211.

24. Steinberg T, Civitelli R, Geist S, Robertson A, Hick E, Veenstra R, Wang H-Z, Warlow P, Westphale E, Liang J, Beyer E 1994 Connexin 43 and connexin 45 form gap junctions with different molecular permeabilities in osteoblastic cells. EMBO Journal **13:**744-750.

25. Yanmaguchi D, Ma D, Lee A, Huang J, Gruber H 1994 Isolation and characterization of gap junctions in the osteoblastic MC3T3-E1 cell line. Journal of Bone and Mineral Research **9:**791-803.

26. Aubin J, Liu F 1996 The Osteoblast Lineage. In: Bilezikian J, Raisz L, Rodan G (eds.) Principles of Bone Biology. Academic Press Inc., San Diego. pp. 51-68.

27. Bord S, Horner A, Hembry R, Reynolds J, Compston JE 1996 Production of collagenase by human osteoblasts and osteoclasts in vivo. Bone **19:**35-40.

28. Aarden E, Burger E, Nijweide P 1994 Function of osteocytes in bone. Journal of Cellular Biochemistry **55:**287-299.

29. Doty S 1981 Morphological evidence of gap junctions between bone cells. Calcified Tissue International **33:**509-512.

30. Rawlinson S, Mosley J, Suswillo R, Pitsillides A, Lanyon L 1995 Calvarial and limb bone cells in organ and monolayer culture do not show the same early responses to dynamic mechanical strain. Journal of Bone and Mineral Research **10:**1225-1232.

31. Walker D 1975 Bone resorption restored in osteopetrotic mice by transplants of normal bone marrow and spleen cells. Science **190:**784-785.

32. Suda T, Nakamura I, Jimi E, Takahashi N 1997 Regulation of osteoclast function. Journal of Bone and Mineral Research **12:**869-879.

33. Suda T, Udagawa N, Takahashi N 1996 Cells of bone: osteoclast differentation. In: Bilezikian J, Raisz L, Rodan G (eds.) Principles of Bone Biology. Academic Press, San Diego. p. 87-103.

34. Berger U, Wilson P, McClelland R, Colston M, Haussler M, Pike J, Coomber R 1988 Immunocytochemical detection of 1-alpha,25-dihydroxyvitamin D receptors in normal human tissues. Journal of Clinical Endocrinology and Metabolism **67:**607-613.

35. Yasuda H, Shima N, Nakagawa N, Yamaguchi K, Kinosaki M, Goto M, Mochizuki S-I, Tsuda E, Morinaga T, Udagawa N, Takahashi N, Suda T, Higashio K 1999 A novel molecular mechanism modulating osteoclast differentiation and function. Bone **25:**109-113.

36. Yasuda H, Shima N, Nakagawa N, Yamaguchi K, Kinosaki M, Mochizuki S-I, Tomoyasu A, Yano K, Goto M, Murakami A, Tsuda E, Morinaga T, Higashio K, Udagawa N, Takahashi N, Suda T 1998 Osteoclast differentiation factor is a ligand for osteoprotegerin/osteoclastogenesis-inhibitory factor and is identical to TRANCE/RANKL. Proceedings of the National Academy of Sciences USA **95:**3597-3602.

37. Takahashi H, Udagawa N, Suda T 1999 A new member of tumor necrosis factor ligand family, ODF/OPGL/TRANCE/RANKL, regulates osteoclast differentiation and function. Biochemical and Biophysical Research Communications **256:**449-455.

38. Yasuda H, Shima N, Nakagawa N, Mochizuki S-I, Yano K, Fujise N, Sato Y, Goto M, Yamaguchi K, Kuriyama M, Kanno T, Murakami A, Tsuda E, Morinaga T, Higashio K 1998 Identity of osteoclastogenesis inhibitory factor (OCIF) and osteoprotegerin (OPG): a mechanism by which OPG/OCIF inhibits osteoclastogenesis in vitro. Endocrinology **139:**1329-1337.

39. Felix R, Cecchini M, Fleisch H 1990 Macrophage colony stimulating factor restores in vivo bone resorption in the op/op osteopetrotic mouse. Endocrinology **127:**2592-2594.

40. Takahashi N, Udagawa N, Akatsu T, Tanaka H, Shionome M, Suda T 1991 Role of colony-stimulating factors in osteoclast development. Journal of Bone and Mineral Research **6:**977-985.

41. Suda T, Nakamura I, Jimi E, Takahashi N 1997 Regulation of osteoclast function. Journal of Bone and Mineral Research **12:**869-879.

42. Udagawa N, Takahashi N, Jimi E, Matsuzaki K, Tsurukai T, Itoh K, Nakagawa N, Yasuda H, Goto M, Tsuda E, Higashio K, Gillespie M, Martin TJ, Suda T 1999 Osteoblasts/stromal cells stimulate osteoclast activation through expression of osteoclast differentiation factor/RANKL but not macrophage colony-stimulating factor. Bone **25:**517-523.

43. Nesbitt S, Nesbit A, Helfrich M, Horton M 1993 Biochemical characterization of human osteoclast integrins. Osteoclasts express alpha V beta 3, alpha 2 beta 1, and alpha V beta 1 integrins. Journal of Biological Chemistry **268:**16737-16745.

44. Horton M, Taylor M, Arnett T, Helfrich M 1991 Arg-gly-asp (RGD) peptides and the anti-vitronectin receptor antibody 23C6 inhibit dentine resorption and cell spreading by osteoclasts. Experimental Cell Research **195:**368-375.

45. Vaananen K, Karhukkorpi E, Sundquist K, Wallmark B, Roininen I, Hentunen T, Tuukkanen J, Lakkakorpi P 1990 Evidence for the presence of a proton pump of the vacuolar H(+)-ATPase type found in the ruffled borders of osteoclasts. Journal of Cell Biology **111:**1305-1311.

46. Salo J, Lehenkari P, Mulari M, Metsikko K, Vaananen K 1997 Removal of osteoclast bone resorption products by transcytosis. Science **276:**219-220.

47. Blair H 1998 How osteoclasts degrade bone. BioEssays **20:**837-846.

48. Mundy G 1996 Bone-resorbing cells. In: Primer on the Metabolic Bone Diseases and Disorders of Mineral Metabolism. Lippincott-Raven Publishers, Philadelphia, p. 16-24.

49. Frost H 1969 Tetracycline-based histological analysis of bone remodelling. Calcified Tissue Research **3:**211-237.

50. Dallas S, Rosser J, Mundy G, Bonewald L 2002 Proteolysis of latent transforming growth factor-beta (TGF-b)-binding protein-1 by osteoclasts. Journal of Biological Chemistry **277:**21352-21360.

51. Nijweide P, Burger E, Nulend J, van der Plas A 1996 The Osteocyte. In: Bilezikian J, Raisz L, Rodan G (eds.) Principles of Bone Biology. Academic Press, San Diego. p. 115-126.

52. Pfeilschifter J, Chenu C, Bird A, Mundy G, Roodman G 1989 Interleukin-1 and tunor necrosis factor stimulate the formation of human osteoclast-like cells in vitro. Journal of Bone and Mineral Research **4:**113-118.

53. Vaananen K 1996 Osteoclast function: biology and mechanisms. In: Bilezikian J, Raisz L, Rodan G (eds.) Principles of Bone Biology. Academic Press, San Diego. p. 103-114.

54. Wolff J 1892 Das Gesetz der Transformation der Knochen. Hirschwald, Berlin.

55. Wheldon G 1984 Disuse osteoporosis: physiological aspects. Calcified Tissue International **36:**S146-S150.

56. Carmeliet G, Vico L, Bouillon R 2001 Space flight: a challenge for normal bone homeostasis. Critical Reviews in Eukaryotic Gene Expression **11:**131-144.

57. Prince R, Smith M, Dick I, Webb P, Henderson N, Harris M 1991 Prevention of postmenopausal osteoporosis: A comparative study of

exercise, calcium supplementation and hormone replacement therapy. New England Journal of Medicine **325:**1189-1195.

58. Simkin A, Ayalon J, Leichter I 1987 Increased trabecular bone density due to bone-loading exercises in postmenopausal osteoporotic women. Calcified Tissue International **40:**59-63.

59. Einhorn T 1996 Biomechanics of Bone. In: Bilezikian J, Raisz L, Rodan G (eds.) Principles of Bone Biology. Academic Press, San Diego. p. 25-38.

60. Duncan R, Turner C 1995 Mechanotransduction and the functional response of bone to mechanical strain. Calcified Tissue International **57:**344-358.

61. Rubin C, Lanyon L 1984 Regulation of bone formation by applied dynamic loads. Journal of Bone and Joint Surgery **66A:**397-402.

62. Skerry TM, Lanyon L 1993 Immobilization induced bone loss in the sheep is not modulated by calcitonin treatment. Bone **14:**511-516.

63. Mosley J, March B, Lynch J, Lanyon L 1997 Strain magnitude related changes in whole bone architecture in growing rats. Bone **20:**191-198.

64. Szczesniak A 2000 The expression of glutamate receptor subunits in rat skeletal tissue: effect of mechanical loading on receptor subunit and subtype expression MSc Thesis, Department of Pharmacology. Dalhousie University, Halifax, pp 117.

65. O'Connor J, Lanyon L, McFie H 1982 The influence of strain rate on adaptive bone remodelling. Journal of Biomechanics **15:**767-781.

66. Turner C, Owan I, Takano Y 1995 Mechanotransduction in bone - role of strain-rate. American Journal of Physiology: Endocrinology and Metabolism **32:**E438-E442.

67. Frost H 1997 Why do marathon runners have less bone than weight lifters? A vital-biomehcanical view and explanation. Bone **20:**183-189.

68. Reilly D, Burstein A 1974 The mechanical properties of cortical bone. Journal of Bone and Joint Surgery **56A:**1001-1022.

69. McAllister T, Du T, Frangos J 2000 Fluid shear stress stimulates prostaglandin and nitric oxide release in bone marrow-derived preosteoclast-like cells. Biochemical and Biophysical Research Communications **270:**643-648.

70. Sims J, Karp S, Ingber D 1992 Altering the cellular mechanical force balance results in integrated changes in cell, cytoskeletal and nuclear shape. Journal of Cell Science **103:**1215-1222.

71. McNamee H, Ingber D, Schwartz M 1993 Adhesion of fibronectin stimulates inositol lipid synthesis and enhance PDGF-induced inositol lipid breakdown. Journal of Cell Biology **121:**673-678.

72. Zimolo Z, Wesolowski G, Tanaka H, Hyman J, Hoyer J, Rodan G 1994 Soluble alphaV-beta3 integrin ligands raise [Ca2+]i in rat osteoclasts and mouse-derived osteoclast-like cells. American Journal of Physiology **266:**C376-C381.

73. Schwartz M 1993 Spreading of human endothelial cells on fibronectin or vitronectin triggers elevation of intracellular free calcium. Journal of Cell Biology **120:**1003-1010.

74. Duncan R, Harter L, Levin D, Hruska K 1992 Regulation of stretch activated cation channel activity via the cytoskeleton is similar to hormone modulation. Molecular Biology of the Cell **3:**389.

75. Duncan R, Hruska K 1994 Chronic, intermittent loading alters mechanosensitive channel characteristics in osteoblast-like cells. American Journal of Physiology **267:**F909-F916.

76. Sandy J, Meghij S, Farndale R, Meikle M 1989 Dual elevation of cyclic AMP and inositol phosphates in response to the mechanical deformation of murine osteoblasts. Biochimica et Biophysica Acta **1010:**265-269.

77. Lean J, Jagger C, Chambers T, Chow J 1995 Increased insulin-like growth factor I mRNA expression in rat osteocytes in response to mechanical stimulation. American Journal of Physiology: Endocrinology and Metabolism **268:**E318-E327.

78. Chyun J, Raisz L 1984 Stimulation of bone formation by prostaglandin E2. Prostaglandins **27:**97-103.

79. Murray D, Rushton N 1990 The effect of strain on bone cell prostaglandin E2 release: a new experimental method. Calcified Tissue International **47:**35-39.

80. Ozawa H, Imamura K, Abe E, Takahashi H, Hiraide T, Shibaski Y, Fukufura T, Suda T 1990 Effect of continuous applied compressive pressure on mouse osteoblast-like cells (MC3T3-E1) in vitro. Journal of Cellular Physiology **142:**177-185.

81. Pitsillides A, Rawlinson S, Suswillo R, Bourrin S, Zaman G, Lanyon L 1995 Mechanical strain-induced NO production by bone cells: a possible role in adaptive bone (re)modelling? FASEB Journal **9:**1614-1622.

82. Turner C 1998 Three rules for bone adaptation to mechanical stimuli. Bone **23**(5)**:**399-407.

83. Rickard D, Subramaniam M, Spelsberg T 1999 Molecular and cellular mechanisms of estrogen action on the skeleton. Journal of Cellular Biochemistry Supplements **32/33:**123-132.

84. Eriksen E, Colvard D, Berg N, Graham M, Mann K, Spelsberg T, Riggs BL 1988 Evidence of estrogen receptors in normal human osteoblast-like cells. Science **241:**84-86.

85. Braidman I, Davenport L, Carter D, Selby P, Mawer E, AJ F 1995 Preliminary in situ identification of estrogen target cells in bone. Journal of Bone and Mineral Research **10:**74-80.

86. Pennsler J, Langman C, Radosevitch J, Maminta M, Mangkornkanok M, Higbee R, Molteni A 1990 Sex steroid hormone receptors in normal and dysplastic bone disorders in children. Journal of Bone and Mineral Research **5:**493-498.

87. Vidal O, Kindblom L-G, Ohlsson C 1999 Expression and localization of estrogen receptor-beta in murine and human bone. Journal of Bone and Mineral Research **14:**923-929.

88. Wronski T, Walsh C, Ignaszewski L 1986 Histologic evidence for osteopenia and increased bone turnover in ovariectomized rats. Bone **7:**119-123.

89. Wronski T, Dann L, Horner S 1986 Time-course of vertebral osteopenia in ovariectomized rats. Bone **10:**295-301.

90. Dempster D, Birchman R, Xu R, Lindsay R, Shen U 1995 Temporal changes in cancellous bone structure immediately after ovariectomy. Bone **16:**157-161.

91. Kalu D, Liu C, Hardin R, Hollis B 1989 The aged rat model of ovarian hormone deficiency bone loss. Endocrinology **124:**7-16.

92. Brockstedt H, Kassem M, Eriksen E, Mosekilde L, Melsen F 1993 Age- and sex-related changes in iliac cortical bone mass and remodelling. Bone **14:**681-691.

93. Eastell R, Delmas P, Hodgson S, Eriksen E, Mann K 1988 Bone formation rate in older normal women: concurrent assessment with bone histomorphometry, calcium kinetics and biochemical markers. Journal of Clinical Endocrinology and Metabolism **67**:741-748.

94. Riggs BL, Jowsey J, Goldsmith R, Kelly P, Hoffman D, Arnaud C 1972 Short- and long-term effects of estrogen and synthetic anabolic hormone in postmenopausal osteoporosis. Journal of Clinical Investigation **51**:1659-1663.

95. Vedi S, Skingle S, Compston JE 1996 The effects of long-term hormone replacement therapy on bone remodelling in postmenopausal women. Bone **19**:535-539.

96. Vedi S, Croucher P, Garrahan N, Compston JE 1996 Effects of hormone replacement therapy on cancellous bone microstructure in postmenopausal women. Bone **19**:69-72.

97. Eichner S, Lloyd K, Timpe E 2003 Comparing therapies for postmenopausal osteoporosis prevention and treatment. Annals of Pharmacotherapy **37**:711-724.

98. Donahue H 2000 Gap junctions and biophysical regulation of bone cell differentiation. Bone **26**:417-422.

99. Ko K, McCulloch C 2001 Intercellular mechanotransduction: cellular circuits that coordinate tissue responses to mechanical loading. Biochemical and Biophysical Research Communications **285**:1077-1083.

100. Burger E, Klein-Nulend J 1999 Mechanotransduction in bone - role of the lacuno-canalicular network. FASEB Journal **13**:S101-S112.

101. Mosley J, Lanyon L 1998 Strain rate as a controlling influence on adaptive modeling in response to dynamic loading of the ulna in growing male rats. Bone **23**:313-318.

102. Brown T 2000 Techniques for mechanical stimulation of cells in vitro: a review. Journal of Biomechanics **33**:3-14.

103. Glucksmann A 1939 Studies on bone mechanics in vitro II: the role of tension and pressure in chondrogenesis. Anatomical Record **73**:39-56.

104. Bassett C, Hermann L 1961 Influence of oxygen concentration and mechanical factors on differentiation of connective tissue in vitro. Nature **193**:460-461.

105. Rodan G, Bourret L, Harvey A, Mensi T 1975 3',5'-cyclic AMP and 3',5'-cyclic GMP mediators of the mechanical effects on bone remodelling. Science **189**:467-469.

106. Yeh C, Rodan G 1984 Tensile forces enhance PGE synthesis in osteoblasts grown on collagen ribbon. Calcified Tissue International **36**(S):67-71.

107. Bourret L, Rodan G 1976 The role of calcium in the inhibition of cAMP acculuation in epiphyseal cartilage cells exposed to physiological pressure. Journal of Cell Physiology **88**:353-361.

108. Burger E, Klein-Nulend J, Veldhuizen J 1992 Mechanical stress and osteogenesis in vitro. Journal of Bone and Mineral Research **7**(S2):S397-S401.

109. Klein-Nulend J, Veldhuizen J, Burger E 1986 Increased calcification of growth plate cartilage as a result of compressive force in vitro. Arthritis and Rheumatism **29**:1002-1009.

110. Davies P 1995 Flow mediated endothelial mechanotransduction. Physiology Review **75**:519-560.

111. Topper J, Cai J, Qiu Y, Anderson K, Xu Y, Deeds J, Feeley R, Gimeno C, Woolf E, Tayber O, Mays G, Sampson B, Schoen F, Gimbrone M, Falb D 1997 Vacular MADs: two novel MAD-related genes selectively inducible by flow in human vascular endothelium. Proceedings of the National Academy of Sciences USA **94**:9314-9319.

112. Levesque M, Nerem R 1985 The elongation and orientation of cultured endothelial cells in response to shear stress. Journal of Biomechanical Engineering **107**:341-347.

113. Leung D, Glagof S, Matthews M 1977 A new in vitro system for studying cell response to mechanical stimulation. Experimental Cell Research **109**:285-298.

114. Ives C, Eskin S, McIntyre L 1986 Mechanical effects on endothelial cell morphology: in vitro assessment. In Vitro Cellular and Developmental Biology **22**:500-507.

115. Jones D, Nolte H, Scholubbers J, Turner E, Veltel D 1991 Biochemical signal transduction of mechanical strain in osteoblast-like cells. Biomaterials **12**:101-110.

116. Hasegawa S, Sata S, Suzuki Y, Brunette D 1985 Mechanical stretching increases the number of cultured bone cells synthesizing DNA and alters their pattern of protein synthesis. Calcified Tissue International **37**:431-436.

117. Banes A, Gilbert J, Taylor T, Monbureau O 1985 A new vacuum-operated stress-providing instrument that applies static or variable duration cyclic tension or compression to cells in vitro. Journal of Cell Science **75**:35-42.

118. Gilbert J, Banes A, Weinhold P, Link G, Jones G 1994 Strain profiles for circular plates and membranes employed to mechanically deform cell in vitro. Journal of Biomechanics **27**:1169-1178.

119. Jahangir A, Lee JM, Waldman S, Anderson GI 2002 Mechanical characterization of a novel cell stimulating system (CSS) to apply dynamic, uniform and isotropic biaxial strains to cells in vivo. Biomedical Science Instrumentation **38**:215-220.

120. Carmeliat G, Bouillon R 1999 The effect of microgravity on morphology and gene expression of osteoblasts in vitro. FASEB Journal **13**(S129-S134).

121. Ingber D 1999 How cells (might) sense microgravity. FASEB Journal **13**:S3-S15.

122. Shyy J, Chien S 2002 Role of integrins in endothelial mechanosensing of shear stress. Circulation research **91**:769-775.

123. Karp G 1999 Cell and Molecular Biology, 2nd Edition ed. John Wiley and Sons, New York.

124. Choi D, Rothman S 1990 The role of glutamate neurotoxicity in hypoxic-ischemic neuronal death. Annual Reviews in Neuroscience **13**:171-182.

125. Aarts M, Tymianski M 2003 Novel treatment of excitotoxicity: targeted disruption of intracellular signalling from glutamate receptors. Biochemical Pharmacology **66**:877-886.

126. Hollman M, Heinemann S 1994 Cloned glutamate receptors. Annual Reviews in Neuroscience **17**:31-108.

127. Dingledine R, Borges K, Bowie D, Traynelis S 1999 The glutamate receptor ion channels. Pharmacological Reviews **51**:8-51.

128. Nakanishi S 1992 Molecular diversity of glutamate receptors and implications for brain function. Science **258**:597-603.

129. Monyer H, Sprengel R, Schoepfer R, Herb A, Higuchi M, Lomeli H, Burnashev N, Sakmann B, Seeburg P 1992 Heteromeric NMDA receptors: molecular and functional distinction of subtypes. Science **256:**1217-1221.

130. Clements J, Westbrook G 1991 Activation kinetics reveal the number of glutamate and glycine binding sites on the N-methyl-D-aspartate receptor. Neuron **7:**605-613.

131. Ozawa S, Kamiya H, Tsuzuki K 1998 Glutamate receptors in the mammalian central nervous system. Progress in Neurobiology **54:**581-618.

132. Mosbacher J, Schoepfer R, Monyer H, Burnashev N, Seeburg P 1994 A molecular determinant for submilliseconds desensitization in glutamate receptors. Science **266:**1059-1062.

133. Sommer B, Burnashev N, Verdoorn T, Keinanen K, Sakmann B, Seeburg P 1992 A glutamate receptor channel with high affinity for domoate and kainate. EMBO Journal **11:**1651-1656.

134. Lomeli H, Wisden W, Kohler M, Keinanen K, Sommer B, Seeburg P 1992 High-affinity kainate and domoate receptors in rat brain. FEBS Letters **307:**139-143.

135. Pin J, Duvoisin R 1995 Review: Neurotransmitters I: The metabotropic glutamate receptors, structure and functions. Neuropharmacology **34:**1-26.

136. Okamoto R, Hori S, Akazawa C, Hayashi Y, Shigemoto R, Mizuno N, Nakanishi S 1994 Molecular characterization of a new metabotropic glutamate receptor mGluR7 coupled to the inhibitory cyclic AMP signal transduction. Journal of Biological Chemistry **269**(1231-1236).

137. Pin J, Bockaert J 1995 Get receptive to metabotropic glutamate receptors. Current Opinion in Neurobiology **5:**342-349.

138. Chenu C, Serre C, Raynal C, Burt-Pichat B, Delmas P 1998 Glutamate receptors are expressed by bone cells and are involved in bone resorption. Bone **22:**295-299.

139. Espinosa L, Itzstein C, Cheynel H, Delmas P, Chenu C 1999 Active NMDA glutamate receptors are expressed by mammalian osteoclasts. Journal of Physiology **518.1:**47-53.

140. Genever P, Skerry TM 2001 Regulation of spontaneous glutamate release activity in osteoblastic cells and its role in differentiation and survival: evidence for intrinsic glutamatergic signalling in bone. FASEB Journal 15:1586-1588.

141. Itzstein C, Cheynel H, Burt-Pichat B, Merle B, Espinosa L, Delmas P, Chenu C 2001 Molecular identification of NMDA glutamate receptors expressed in bone cells. Journal of Cellular Biochemistry **82:**134-144.

142. Patton A, Genever P, Birch M, Peet N, Grabowski P, Rands R, Williamson D, Howarth S, Suva L, Skerry TM 1997 Glutamate signalling in human and rat bone cells. Bone **20:**225.

143. Patton A, Genever P, Birch M, Suva L, Skerry TM 1998 Expression of an N-methyl-D-aspartate-type receptor by human and rat osteoblasts and osteoclasts suggests a novel glutamate signalling pathway in bone. Bone **22:**645-649.

144. Skerry TM 1999 Identification of novel signalling pathways during functional adaptation of the skeleton to mechanical loading: the role of glutamate as a paracrine signalling agent in the skeleton. Journal of Bone and Mineral Metabolism **17:**66-70.

145. Mason D, Suva L, Genever P, Patton A, Steuckle S, Hillam R, Skerry TM 1997 Mechanically regulated expression of a neural glutamate transporter in bone: a role for excitatory amino acids as osteotropic agents? Bone **20:**199-205.

146. Laketic-Ljubojevic I, Suva L, Maathuis F, Sanders D, Skerry TM 1999 Functional characterization of N-methyl-D-aspartic acid-gated channels in bone cells. Bone **25:**631-637.

147. Gu Y, Publicover S 2000 Expression of functional metabotropic glutamate receptors in primary cultured rat osteoblasts. Journal of Biological Chemistry **275:**9684-9689.

148. Martin TJ, Ng KW 1994 Mechanisms by which cells of the osteoblast lineage control osteoclast formation and activity. Journal of Cellular Biochemistry **56:**357-366.

149. Hinoi E, Fujimori S, Takemori A, Kurabayashi H, Nakamura I, Yoneda Y 2002 Demonstration of mRNA for particular AMPA and kainate receptor subunits in immature and mature cultured rat calvarial osteoblasts. Brain Research **943:**112-116.

150. Hinoi E, Fujimori S, Nakamura Y, Balcar V, Kubo K, Ogita K, Yoneda Y 2002 Constitutive expression of heterologous N-methyl-D-aspartate receptor subunits in rat adrenal medulla. Journal of Neuroscience Research **68:**36-45.

151. Hinoi E, Fujimori S, Nakamura Y, Yoneda Y 2001 Group III metabotropic glutamate receptors in rat cultured calvarial osteoblasts. Biochemical and Biophysical Research Communications **281:**341-346.

152. Merle B, Itzstein C, Delmas P, Chenu C 2003 NMDA glutamate receptors are expressed by osteoclast precursors and are involved in the regulation of osteoclastogenesis. Journal of Cellular Biochemistry **90:**424-436.

153. Hinoi E, Fujimori S, Takarada T, Taniura H, Yoneda Y 2002 Facilitation of glutamate release by ionotropic glutamate receptors in osteoblasts. Biochemical and Biophysical Research Communications **297:**452-458.

154. Mason D 2004 Glutamate signalling and its potential application to tissue engineering of bone. European Cells and Materials **7:**12-26.

155. Taylor A 2002 Functional osteoblastic ionotropic glutamate receptors are a prerequisite for bone formation. Journal of Musculoskeletal Neuron Interactions **2:**415-422.

156. Skerry TM, Genever P 2001 Glutamate signalling in non-neuronal tissues. Trends in Pharmacological Sciences **22:**174-181.

157. Hinoi E, Fujimori S, Yoneda Y 2003 Modulation of cellular differentiation by N-methyl-D-aspartate receptors in osteoblasts. FASEB Journal **17:**1532-1534.

158. Itzstein C, Espinosa L, Delmas P, Chenu C 2000 Specific antagonists of NMDA receptor prevent osteoclast sealing zone formation required for bone resorption. Biochemical and Biophysical Research Communications **268:**201-209.

159. Gray C, Marie H, Arora M, Tanaka K, Boyde A, Jones S, Attwell D 2001 Glutamate does not play a major role in controlling bone growth. Journal of Bone and Mineral Research **16:**742-749.

160. Peet N, Grabowski P, Laketic-ljubojevic I, Skerry TM 1999 The glutamate receptor antagonist MK801 modulates bone resorption in vitro by a mechanism predominantly involving osteoclast differentiation. FASEB Journal **13:**2179-2185.

161. Minkin C 1982 Bone acid phosphatase: tartrate-resistant acid phosphatase as a marker of osteoclast function. Calcified Tissue International **34:**285-290.

162. Anderson G, MacQuarrie R, Osinga C, Chen Y, Langman M, Gilbert R 2001 Inhibition of leukotriene function can modulate particulate-induced changes in bone cell differentiation and activity. Journal of Biomedical Materials Research **58:**406-414.

163. Bradford MM 1976 A rapid and sensitive method for the quantitation of microgram quantities of protein utilizing the principle of protein-dye binding. Analytical Biochemistry **72:**248-254.

164. Ausubel FM, Brent R, Kingston RE, Moore DD, Seidman JG, Smith JA, Struhl S 2001 Current Protocols in Molecular Biology, vol. 2. John Wiley and Sons.

165. Laemmli UK 1970 Cleavage of structural proteins during the assembly of the head of bacteriophage T4. Nature **227:**680-685.

166. Birnboim HC, Doly J 1979 A rapid alkaline lysis procedure for screening recombinant plasmid DNA. Nucleic Acids Research **7:**1513-1522.

167. Birnboim HC 1983 A rapid alkaline extraction method for the isolation of plasmid DNA. Methods in Enzymology **100:**243-255.

168. Goldmann W 2002 Mechanical aspects of cell shape regulation and signalling. Cell Biology International **26:**313-317.

169. Zambonin-Zallone A, Teti A, Carano A, Marchisio P 1988 The distribution of podosomes in osteoclasts cultured on bone laminae: effect of retinol. Journal of Bone and Mineral Research **35:**517-523.

170. Tang W, Wesley M, Freeman W, Liang B, Hemby S 2004 Alterations in ionotropic glutamate receptor subunits during binge cocaine self-administration and withdrawal in rats. Journal of Neurochemistry **89:**1021-1033.

171. Gomperts S 1996 Clustering membrane proteins: it's all coming together with the PSD-95/SAP90 protein family. Cell **84:**659-662.

172. Zauli G, Rimondi E, Nicolin V, Melloni E, Celeghini C, Secchiero P 2004 TNF-related apoptosis inducing ligand (TRAIL) blocks osteoclastic differentiation induced by RANKL and M-CSF. Blood **104:**2044-2050.

173. Muzylak M, Flanagan A, Ingham K, Gunn N, Price J 2002 A feline assay using osteoclasts generated in vitro from peripheral blood for screening anti-resorptive agents. Research in Veterinary Science **73:**283-290.

174. Hoebertz A, Arnett T 2003 Isolated osteoclast cultures. Methods in Molecular Medicine **80:**53-64.

175. Mukhida M 2001 Honours thesis, Department of Biology. Dalhousie University, Halifax.

176. Miyazaki T, Sanjay A, Neff J, Tanaka S, Horne W, Baron R 2004 Src kinase activity is essential for osteoclast function. Journal of Biological Chemistry **279:**17660-17666.

177. Sanjay A, Houghton A, Neff J, Didomenico E, Bardelay C, Antoine E, Levy J, Gailit J, Bowtell D, Horne W, Baron R 2001 Cbl associates with Pyk2 and Src to regulate Src kinase activity, alpha(v)beta(3) integrin-mediated signaling, cell adhesion, and osteoclast motility. Journal of Cell Biology **152:**181-195.

178. Yu X, Askalan R, Kiel GI, Salter M 1997 NMDA channel regulation by channel-associated protein tyrosine kinase Src. Science **275:**674-678.

179. Hisatune C, Umemori H, Inoue T, Michikawa T, Kohda K, Mikoshiba K, Yamamoto T 1997 Phosphorylation-dependent regulation of N-methyl-D-aspartate receptors by calmodulin. Journal of Biological Chemistry **272:**20805-20810.

180. Zhang S, Ehlers M, Bernhardt J, Su C, Huganir R 1998 Calmodulin mediates calcium-dependent inactivation of N-methyl-D-aspartate receptors. Neuron **21:**443-453.

181. Strack S, Colbran R 1998 Autophosphorylation-dependent targeting of calcium/calmodulin-dependent protein kinase II by the NR2B subunit of the N-methyl-D-aspartate receptor. Journal of Biological Chemistry **273:**20689-20692.

182. Chen H, Rojasj-Soto M, Oguni A, Kennedy M 1998 A synaptic Ras-GTPase activating protein (p135 SynGAP) inhibited by CaM kinase II. Neuron **20:**895-904.

183. Wang Y, Durkin J 1995 Alpha-amino-3-hydroxy-5-methyl-4-isoxazolepropionic acid, but not N-methyl-D-aspartate, activates mitogen-activated protein kinase through G-protein beta-gamma subunits in rat cortical neurons. Journal of Biological Chemistry **270:**22783-22787.

184. Cyr M, Ghribi O, Thibault C, Morissette M, Landry M, Di Paolo T 2001 Ovarian steroids and selective estrogen receptor modulators activity on rat brain NMDA and AMPA receptors. Brain Research Reviews **37:**153-161.

185. Bai G, Kusiak J 1995 Functional analysis of the proximal 5'-flanking region of the N-methyl-D-aspartate receptor subunit gene. Journal of Biological Chemistry **270:**7737-7744.

186. Suchanek B, Seeburg P, Sprengel R 1995 Gene structure of the murine N-methyl-D-aspartate receptor subunit NR2C. Journal of Biological Chemistry **270:**41-44.

187. Katzenellenbogen J, O'Malley B, Katzenellenbogen B 1996 Tripartite steroid hormone receptor pharmacology: interaction with multiple effector sites as a basis for the cell-and promoter-specific action of these hormones. Molecular Endocrinology **10:**119-131.